

2001

Mechanistic studies and synthetic applications of oxygen atom transfer reactions catalyzed by rhenium(V) dithiolato complexes and methyltrioxorhenium (MTO)

Ying, 1974 Wang
Iowa State University

Follow this and additional works at: <https://lib.dr.iastate.edu/rtd>

 Part of the [Organic Chemistry Commons](#)

Recommended Citation

Wang, Ying, 1974, "Mechanistic studies and synthetic applications of oxygen atom transfer reactions catalyzed by rhenium(V) dithiolato complexes and methyltrioxorhenium (MTO)" (2001). *Retrospective Theses and Dissertations*. 1088.
<https://lib.dr.iastate.edu/rtd/1088>

This Dissertation is brought to you for free and open access by the Iowa State University Capstones, Theses and Dissertations at Iowa State University Digital Repository. It has been accepted for inclusion in Retrospective Theses and Dissertations by an authorized administrator of Iowa State University Digital Repository. For more information, please contact digirep@iastate.edu.

INFORMATION TO USERS

This manuscript has been reproduced from the microfilm master. UMI films the text directly from the original or copy submitted. Thus, some thesis and dissertation copies are in typewriter face, while others may be from any type of computer printer.

The quality of this reproduction is dependent upon the quality of the copy submitted. Broken or indistinct print, colored or poor quality illustrations and photographs, print bleedthrough, substandard margins, and improper alignment can adversely affect reproduction.

In the unlikely event that the author did not send UMI a complete manuscript and there are missing pages, these will be noted. Also, if unauthorized copyright material had to be removed, a note will indicate the deletion.

Oversize materials (e.g., maps, drawings, charts) are reproduced by sectioning the original, beginning at the upper left-hand corner and continuing from left to right in equal sections with small overlaps.

Photographs included in the original manuscript have been reproduced xerographically in this copy. Higher quality 6" x 9" black and white photographic prints are available for any photographs or illustrations appearing in this copy for an additional charge. Contact UMI directly to order.

ProQuest Information and Learning
300 North Zeeb Road, Ann Arbor, MI 48106-1346 USA
800-521-0600

UMI[®]

Mechanistic studies and synthetic applications of oxygen atom transfer reactions catalyzed
by rhenium(V) dithiolato complexes and methyltrioxorhenium (MTO)

by

Ying Wang

A dissertation submitted to the graduate faculty
in partial fulfillment of the requirements for the degree of
DOCTOR OF PHILOSOPHY

Major: Organic Chemistry

Major Professor: James H. Espenson

Iowa State University

Ames, Iowa

2001

UMI Number: 3016754

UMI[®]

UMI Microform 3016754

Copyright 2001 by Bell & Howell Information and Learning Company.

All rights reserved. This microform edition is protected against
unauthorized copying under Title 17, United States Code.

Bell & Howell Information and Learning Company
300 North Zeeb Road
P.O. Box 1346
Ann Arbor, MI 48106-1346

Graduate College
Iowa State University

This is to certify that the Doctoral dissertation of
Ying Wang
has met the dissertation requirements of Iowa State University

Signature was redacted for privacy.

Major Professor

Signature was redacted for privacy.

For the Major Program

Signature was redacted for privacy.

For the Graduate College

TABLE OF CONTENTS

GENERAL INTRODUCTION	1
Introduction	1
Dissertation Organization	5
References	6
CHAPTER I. KINETICS AND MECHANISM OF OXYGEN ATOM TRANSFER BETWEEN PHOSPHINES AND PYRIDINE N-OXIDES CATALYZED BY AN OXORHENIUM(V) DITHIOLATO PHOSPHINE COMPOUNDS	7
Abstract	7
Introduction	8
Experimental Section	10
Results	12
Interpretation and Discussion	43
References	53
CHAPTER II. EFFICIENT CATALYTIC CONVERSION OF PYRIDINE N-OXIDES TO PYRIDINES WITH AN OXORHENIUM(V) CATALYST	55
Abstract	55
Results and Discussion	55
References	61
CHAPTER III. OXIDATION OF SULFIDES BY <i>TERT</i>-BUTYL HYDROPEROXIDE CATALYZED BY AN OXORHENIUM(V) DITHIOLATO COMPLEX – A GENERAL AND EFFICIENT SYNTHESIS OF SULFOXIDES AND SULFONES.	62
Abstract	62

Introduction	63
Results and Discussion	65
Conclusion	87
Experimental Section	87
References	90
CHAPTER IV. OXIDATION OF SYMMETRIC DISULFIDES WITH HYDROGEN PEROXIDE CATALYZED BY METHYLTRIOXORHENIUM	96
Abstract	96
Introduction	97
Experimental Section	98
Results	101
Discussion	104
References	106
GENERAL CONCLUSIONS	113
ACKNOWLEDGMENTS	115

Mechanistic studies and synthetic application of oxygen transfer reactions catalyzed by methyltrioxorhenium (MTO) and rhenium(V) dithiolato complexes

Ying Wang

Major Professor: James H. Espenson

Iowa State University

A series of Re(V) dithiolato complexes catalyze the rapid and efficient transfer of an oxygen atom from a wide range of ring-substituted pyridine N-oxides to triphenylphosphine, yielding the pyridines in high yield. Some of these complexes can also catalyze the oxidation of a variety of sulfides to sulfoxides and sulfones with *tert*-butyl hydroperoxide in excellent yield with high selectivity and generality. Heavily substituted thiophenes can also be converted to the corresponding S-oxides with moderate to excellent yields using this catalytic system.

The kinetics and mechanism of these two oxygen transfer reactions were also studied. The mechanisms feature a common aspect in that phosphines and sulfides, being the substrates, inhibit the reaction. Rate constants were obtained for the oxygen atom transfer reactions between pyridine N-oxides and phosphines catalyzed by Re(V) dithiolato complexes. In the case of oxygen atom transfer reaction between *tert*-butyl hydroperoxide and sulfide catalyzed by Re(V) dithiolato compounds, an induction period is observed due to the slow ligand exchange step. Reaction schemes are proposed to interpret the kinetic data. In both cases, the active intermediates are Re(VII) dioxo species, which were detected at the low temperature.

Organic disulfides with both alkyl and aryl substituents are oxidized by hydrogen peroxide when CH_3ReO_3 (MTO) is used as a catalyst. Thiosulfinate is formed in the first

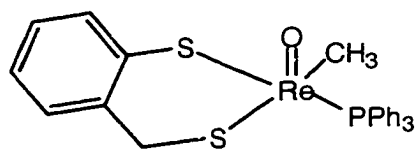
step in about an hour with nearly quantitative yield. Kinetics studies of the first oxidation reaction established that two peroxorhenium compounds are the active forms of the catalyst. Rate constants were obtained and a mechanism was proposed in which the electron-rich sulfur attacks the peroxy oxygen of intermediates.

GENERAL INTRODUCTION

Introduction

Oxygen atom transfer reactions catalyzed by transition-metal compounds continue to attract great interest due to their fundamental role in chemistry and biology.¹ One major category of oxygen transfer catalysts is high-valent transition metal-oxo complexes, with metals such as molybdenum, tungsten and rhenium. In comparison with Mo(VI)/Mo(IV) and W(VI)/W(IV) catalytic systems, one can envisage a parallel rhenium chemistry with a pair of Re(VII)/Re(V) species that can transfer an oxygen atom to the substrate by going through a Re(VII)/Re(V) loop. Indeed, some Re(V) compounds reported are good oxygen transfer catalysts.²⁻⁵

Recently, a series of Re(V) compounds was synthesized in our group and among them is the Re(V) dithiolato complex MeReO(mtp)(PPh₃) **1** where mtpH₂ is 2-(mercaptomethyl)thiophenol (*o*-HSC₆H₄CH₂SH). This compound has been found to catalyze oxygen atom transfer reactions. The deprotection of pyridine N-oxides by phosphines and the syntheses of sulfoxide and sulfones from sulfides by *tert*-butyl hydroperoxide have been investigated.



MeReO(mtp)PPh₃

Chapters I and II deal with the synthesis, kinetics and mechanism of the catalytic conversion of pyridine N-oxides to pyridines by phosphines catalyzed by **1** and related Re(V) dithiolato complexes. From the synthetic point, selective deoxygenation of heteroaromatic N-oxides is an important step in the synthesis of heterocycles in many procedures. Many known methods are limited by the side reactions or reduction of a ring substituent; others require tedious procedures. The synthesis reported in Chapter II offers a convenient and efficient method for this transformation that can easily be carried out on the gram scale. The literature reports mechanistic studies of the biologically related oxomolybdenum complexes as catalysts for the deoxygenation of pyridine N-oxides by phosphines, partly motivated by the fact that some pyridine N-oxides are enzymatic substrates. Chapter I reports studies of the kinetics and mechanism of oxygen transfer from pyridine N-oxides to phosphines catalyzed by **1**. Several methods were used to explore the mechanisms, including the initial rate and time course methods, competition reaction design, and detection of the intermediates by means of low temperature NMR spectroscopy.

These studies aid in the design of new catalysts and provide a better understanding of the chemistry of rhenium centered oxygen atom transfer reactions.

In search for other oxygen atom transfer reactions that can be catalyzed by this series of Re(V) dithiolato complexes, we also found that **1** can efficiently catalyze the oxidation of sulfides to sulfoxides when *tert*-butyl hydroperoxide is used as the stoichiometric oxidizing reagent. These results are discussed in Chapter III. Oxidation of sulfides is the most widely used method for synthesizing sulfoxides. Oxidation of thiophenes is particularly interesting due to its potential use in the industrial desulfurization process. Oxidation of the heavily substituted thiophenes present the biggest challenge among the

thiophene series. In this chapter, oxidation of thiophenes by our catalytic system is also discussed. In the course of this research, concurrently, mechanistic studies were carried out to help us understand the catalytic cycle and in turn to assist us in optimizing catalysis and, especially, selectivity. KinSim, a kinetics simulation program, was used to help us understand the unique features of this catalytic transformation.

The synthesis developed in this chapter has many advantages. Over-oxidation of sulfoxides is avoided by the choice of appropriate reaction conditions. In many reported sulfoxide syntheses, over-oxidation is unavoidable and a mixture of oxidation products is obtained. This method offers further advantage in that functional groups presented in the substrates are not affected. In the presence of an excess of one equiv. of *tert*-butyl hydroperoxide and **1** at 50 °C, sulfones were obtained quantitatively.

We also attempted to synthesize chiral sulfoxides by exploring chiral Re(V) dithiolato catalysts since chiral sulfoxides are useful building blocks in organic synthesis and asymmetric sulfoxidation using chiral catalysts has drawn much attention. In contrast to the symmetry of MTO, Re(V) dithiolato complexes seem to be much better candidates for asymmetric catalysis. Although the initial experiments were not successful, one could imagine the success of making chiral Re(V) catalysts for asymmetric oxidation with more studies.

The most widely used and also well-known rhenium catalyst for oxygen atom transfer reactions is methyltrioxorhenium CH_3ReO_3 , abbreviated as MTO.^{6,7} The essence of the MTO chemistry is its ability to activate hydrogen peroxide to form two active rhenium peroxo-species, both of which are able to transfer an oxygen atom to various substrates as

demonstrated in the past decade.⁸⁻¹³ The reaction mechanisms are also well studied and understood. MTO is best activated by hydrogen peroxide. In the MTO chemistry, the rhenium stays at Re(VII) in the catalytic cycle by forming the peroxy-species.

Chapter IV reports the oxidation of the symmetric disulfide by hydrogen peroxide catalyzed by MTO. Disulfide functional groups have been studied quite extensively because of their important role in metabolism, via a variety of mechanistic paths. Various intermediate compounds can be obtained from the disulfide functional group using different oxidants under well-controlled condition. Some of these intermediate compounds are useful in organic synthesis. Peracids are the reagents most commonly used to oxidize disulfides. Molybdate and tungstates are effective catalysts under the phase transfer conditions, too. Hydrogen peroxide can oxidize the disulfide although without a catalyst, a large excess and high reaction temperature are needed. When MTO was used as the catalyst, the first oxidation product is thiosulfinate that in the presence of excess hydrogen peroxide is further oxidized to thiosulfonate and eventually to sulfonic acid. Kinetic studies were carried out for the first oxidation since it is much faster than the subsequent oxidation steps. Both rhenium peroxy-species, $\text{MeReO}_2(\kappa^2\text{-O}_2)$ and $\text{MeReO}_2(\kappa^2\text{-O}_2)_2(\text{H}_2\text{O})$, are able to transfer an oxygen atom to the disulfide. Their reactivities are quite similar in this case. The rate constants obtained were compared with those from earlier kinetic studies for the sulfides to gain a more global understanding about the kinetics and mechanisms of MTO catalyzed reactions.

Dissertation Organization

The dissertation consists of four chapters. Chapter II has been published in *Organic Letters*. Chapter IV has been published in *Journal of Organic Chemistry*. On the basis of Chapters I and III, two papers are now being prepared for submission for publication. Each chapter is self-contained with its own equations, figures, tables and references. Following the last chapter is the general conclusions. All the work in this dissertation was performed by the author.

References

- (1) Murahashi, S.; Davies, S. G. *Transition Metal Catalysed Reaction*; Blackwell Science: Oxford; Malden, MA, 1999.
- (2) Gunaratne, H. D.; McKervey, M. A.; Feutren, S.; Finlay, J.; Boyd, J. *Tetrahedron Lett.* **1998**, *39*, 5655.
- (3) Abu-Omar, M. M.; McPherson, L. D.; Arias, J.; Bereau, V. M. *Angew. Chem. Int. Ed. Engl.* **2000**, *39*, 4310.
- (4) Arias, J.; Newlands, C. R.; Abu-Omar, M. *Inorg. Chem.* **2001**, *40*, 2185.
- (5) Huang, R.; Espenson, J. H. *Inorg. Chem.* **2001**, *40*, 994.
- (6) Espenson, J. H. *J. Chem. Soc. Chem. Commun.* **1999**, 479.
- (7) Hermann, W. A.; Kratzer, R. M.; Fischer, R. W. *Angew. Chem. Int. Ed. Engl.* **1997**, *36*, 2652.
- (8) Hermann, W. A.; Fischer, R. W.; Rauch, M. U. *Angew. Chem. Int. Ed. Engl.* **1993**, 1157.
- (9) Zhu, Z.; Espenson, J. H. *J. Org. Chem.* **1995**, 7728.

- (10) Vassell, K. A.; Espenson, J. H. *Inorg. Chem.* **1994**, 5491.
- (11) Zhu, Z.; Espenson, J. H. *J. Org. Chem.* **1995**, 1326.
- (12) Murray, R. W.; Lyanar, K. *Tetrahedron Lett.* **1997**, 335.
- (13) Abu-Omar, M.; Espenson, J. H. *J. Am. Chem. Soc.* **1995**, 272.

**CHAPTER I. KINETICS AND MECHANISM OF THE OXYGEN
TRANSFER REACTION BETWEEN PHOSPHINES AND PYRIDINE
N-OXIDES CATALYZED BY AN OXORHENIUM(V) DITHIOLATO
PHOSPHINE COMPOUND**

A paper being prepared for submission to the *Journal of the American Chemical Society*

Ying Wang and James H. Espenson

Abstract

The kinetics and mechanism of the oxygen atom transfer reaction between the pyridine N-oxides and phosphines catalyzed by $(o\text{-SC}_6\text{H}_4\text{CH}_2\text{S})(\text{PPh}_3)\text{Re}(\text{O})\text{CH}_3$, abbreviated as $\text{MeReO}(\text{mtp})\text{PPh}_3$, were studied. Phosphines inhibit the reaction while pyridine N-oxides accelerate it. A reaction scheme is proposed to interpret the kinetic data. The scheme features a fast ligand substitution reaction between the parent phosphine catalyst and pyridine N-oxide to form the analogous dithiolato methyl(oxo) rhenium(V) complex $\text{MeReO}(\text{mtp})\text{OPy}$ with the liberation of free phosphine. This compound will then pick up another pyridine N-oxide in a second rapid and unfavorable equilibrium to form a six-coordinated compound $\text{MeReO}(\text{mtp})(\text{OPy})_2$. This intermediate generates the rhenium(VII) dioxo intermediate $\text{MeReO}_2(\text{mtp})(\text{OPy})$ in the rate-controlling step. The dioxo rhenium(VII) species is able to transfer an oxygen atom to phosphine in a fast step to generate phosphine oxide. Rate constants were obtained and the rhenium(VII) dioxo species was detected at low temperature in the ^1H NMR spectrum.

Introduction

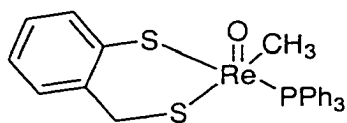
Oxygen atom transfer reactions involving transition metals have been studied quite extensively but still hold great interest because of their importance in biological systems, in organic synthesis and in industrial process.¹⁻⁴ Of all the elements, the oxygen atom transfer reactions of molybdenum have been extensively investigated and well understood.⁵⁻⁷ In the biological systems, the molybdenum oxotransferases are able to catalyze oxygen atom transfer reactions through a catalytic cycle between Mo(VI) and Mo(IV). In comparison to the Mo^{VI}/Mo^{IV} pair, we can construct a pair of Re^{VII}/Re^V species such that a catalytic cycle can be obtained through the oxidation of rhenium(V) compound by the oxygen donor and the reduction of the resulting rhenium(VII) compound by the oxygen acceptors.

Recently, a series Re(V) compounds with dithiolato ligands were synthesized and characterized.⁸⁻¹⁰ Some of these Re(V) compounds showed good activities as oxygen atom transfer catalysts.^{11,12} Among them is MeReO(mtp)PPh₃ (mtp = "*o*-SC₆H₄CH₂S") **1** whose structure is given in Chart 1. It has been found to rapidly and efficiently catalyze the oxygen atom transfer reaction between pyridine N-oxides and phosphines (eq 1).¹¹

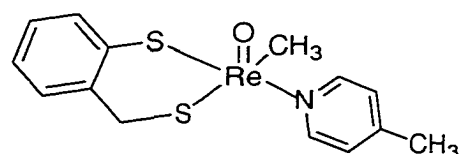
Our primary interest in this work lies in that deoxygenation of heteroaromatic N-oxides is an important step in the synthesis of heterocycles in many procedures.^{13,14} Since many methods developed are limited by side reactions or reduction of the ring substituents and may require tedious procedures, this method offers a good alternative approach.^{15,16} In addition, biologically related oxomolybdenum complexes are also able to catalyze deoxygenation of pyridine N-oxides with phosphines. Mechanistic studies have been done

for these reactions partly due to the fact that some of the pyridine N-oxides are enzymatic substrates.^{1,2,17} So it would be interesting to learn the catalytic role of $\text{MeReO}(\text{mtp})\text{PPh}_3$ in this deoxygenation reaction as part of our goal to gain understanding of rhenium compounds catalyzed oxygen atom transfer reactions. In this paper, the kinetics and mechanism of the oxygen transfer reaction between pyridine N-oxides and phosphines catalyzed by **1** were studied by several methods, such as the initial rate and time course methods, competition reaction design and detection of the intermediates by means of low temperature NMR techniques.

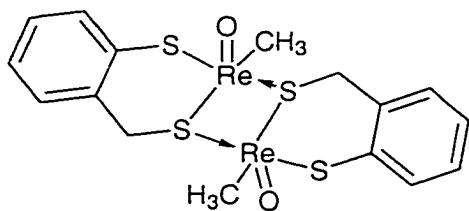
Chart 1



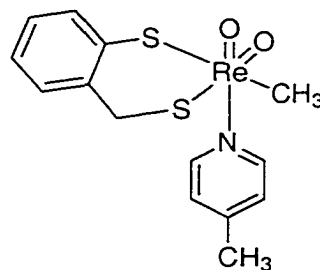
$\text{MeReO}(\text{mtp})\text{PPh}_3$, **1**



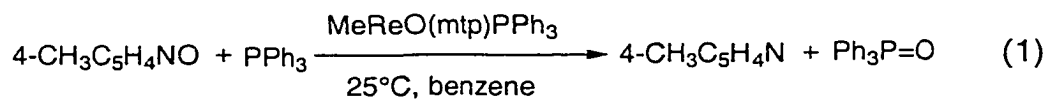
$\text{MeReO}(\text{mtp})(4\text{-CH}_3\text{C}_5\text{H}_4\text{N})$, **2**



$\{\text{MeReO}(\text{mtp})\}_2$, **3**



$\text{MeReO}_2(\text{mtp})(4\text{-CH}_3\text{C}_5\text{H}_4\text{N})$, **4**



Experimental Section

Materials. methyltrioxorhenium CH_3ReO_3 , abbreviated as MTO, was synthesized from sodium perrhenate and tetramethyltin (Strem).¹⁸ It is the precursor for compound **1-4**. The dimeric complex $\{\text{MeReO}(\text{mtp})\}_2$ **3** was prepared from MTO and mtpH_2 as reported earlier.¹⁹ The monomeric phosphine complexes, $\text{MeReO}(\text{mtp})\text{PAr}_3$, were prepared by reacting 2.1 equiv. of phosphines with compound **3**.¹¹ These rhenium(V) phosphine complexes used in this paper have been characterized by NMR spectroscopy, elemental analysis and crystallography.^{8,20} All of them have similar UV-vis, ^1H NMR and ^{31}P NMR spectra. The ^{31}P chemical shifts for the monomeric phosphine complexes used in this study are summarized in Table 1. $\text{MeReO}(\text{SCH}_2\text{CH}_2\text{S})\text{PPh}_3$ **9**, another catalyst, closely related to **1**, was synthesized by the published procedure.²¹ Other reagents were purchased from commercial sources and used without further purification. Benzene (Fisher Spectranalyzed) was used as the solvent for the kinetic studies. Deuterated toluene was used in the low temperature NMR experiments. The rate constants reported herein were determined at 25°C.

Table 1. The ^{31}P NMR chemical shifts for $\text{MeReO}(\text{mtp})[(4\text{-RC}_6\text{H}_4)_3\text{P}]$ in C_6D_6

$\text{MeReO}(\text{mtp})[(4\text{-RC}_6\text{H}_4)_3\text{P}]$,						
R=	MeO	Me	H	F	Cl	CF_3
δ (ppm)	24.7	26.5	27.8	25.5	26.5	27.3

Instrumentation. Shimadzu scanning spectrophotometers were used to record UV-vis spectra and kinetic curves. Optical cells of 1 cm path length were used throughout the study. Reactions were followed by monitoring the disappearance of pyridine N-oxides in the UV region at 330-360 nm. The reaction in eq 1 was monitored at 330 nm where the ϵ of 4-picoline N-oxide was determined to be $807 \text{ L mol}^{-1} \text{ cm}^{-1}$. ^1H and ^{31}P NMR spectra were recorded with Bruker DRX 400 MHz spectrometers. The ^1H chemical shifts reported here were measured relative to the residual ^1H resonance of the deuterated solvent benzene and toluene. Chemical shifts for ^{31}P were referenced to 85% H_3PO_4 . Low temperature experiments at 240 K were performed using $\text{CD}_3\text{C}_6\text{D}_5$ as solvent. A solution of compound 2 was prepared by adding 24 mM 4- $\text{CH}_3\text{C}_5\text{H}_4\text{N}$ into 2.0 mM compound 3 solution *in situ*.²² The initial rate method was used first to determine the rate as a function of the concentration of each of the species on which it depends. When this method was used, the absorbance readings were first converted to concentrations using eq 2. The concentration-time data thus obtained were fitted by a polynomial function, typically fifth-order, by means of the program KaleidaGraph. The initial rate v_i , in units $\text{mol L}^{-1} \text{ s}^{-1}$, is then seen from eq 3 to be given by the coefficient m_1 .

$$C_t = C_0 \times \frac{\text{Abs}_t - \text{Abs}_\infty}{\text{Abs}_0 - \text{Abs}_\infty} \quad (2)$$

$$C_t = C_0 - m_1t - m_2t^2 - m_3t^3 - m_4t^4 - m_5t^5 \dots \quad (3)$$

When phosphines were used in large excess over pyridine N-oxides, the absorbance-time data showed that the reaction followed pseudo-second order kinetics. The absorbance-time data from each such experiment were analyzed according to eq 4, from which a pseudo-second order rate constant k_{ψ} was obtained by nonlinear least-squares fitting.²³

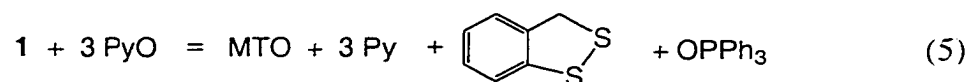
$$\text{Abs}_t = \text{Abs}_{\infty} + \frac{\text{Abs}_0 - \text{Abs}_{\infty}}{1 + [\text{PyO}]_0 k_{\psi} t} \quad (4)$$

Results

Preliminary Considerations. The oxygen atom transfer reaction (eq 1) between 4-picoline N-oxide and triphenylphosphine catalyzed by **1** was first studied as a model reaction to obtain the rate law. A ¹H NMR experiment in 0.7 mL of C₆D₆ was carried out at these concentrations: 42 μM catalyst, 14 mM PPh₃ and 14 mM 4-picoline N-oxide. The reaction went to completion within one min as monitored by ¹H and ³¹P NMR spectroscopy. In the absence of the catalyst, no observable reaction was detected in at least 10 h. The efficiency of the catalyst was demonstrated by kinetic traces in UV-vis experiments as shown in Figures 1a and 1b. Oxygen involvement could be excluded since the control reactions performed under argon showed virtually the same kinetic traces as ones performed in air.

In the absence of PPh₃, compound **1** reacts with 4-picoline N-oxide to form MTO, O=PPh₃ and the disulfide oxidation product of the dithiolate ligand (eq 5) on a much slower time scale compared to the catalytic reaction in eq 1. Neither the disulfide oxidation product

nor MTO was detected during and after the catalytic reaction in eq 1. One can conclude, therefore, that the recycling of **1** between resting and active states prevents its decomposition. On the other hand, without PPh₃, or when it has been exhausted, reaction in eq 5 will occur.



Determination of the Rate Law. The initial rate method was first used to learn the dependence of the rate on the concentrations of the species in the rate law. The data are summarized in Table 2. When triphenylphosphine was used in excess over 4-picoline N-oxide, the initial rate is first-order with respect to [**1**] and inversely dependent on [PPh₃]. These dependencies are illustrated in Figures 2 and 3 by plots of v_i vs. one concentration, the others being held constant. The slope of each line gives the order of the reaction with respect to that concentration variable. Increasing [4-CH₃C₅H₄NO] increased the initial rate more strongly and it was found that v_i has a second-order dependence on [4-CH₃C₅H₄NO](Figure 4). From these three independent observations, the initial rate expressed in terms of the concentrations of PPh₃, 4-picoline N-oxide and **1**, can be described by eq 6.

$$v = k \left(\frac{[4 - \text{CH}_3\text{C}_5\text{H}_4\text{NO}]^2 [\mathbf{1}]}{[\text{PPh}_3]} \right) \quad (6)$$

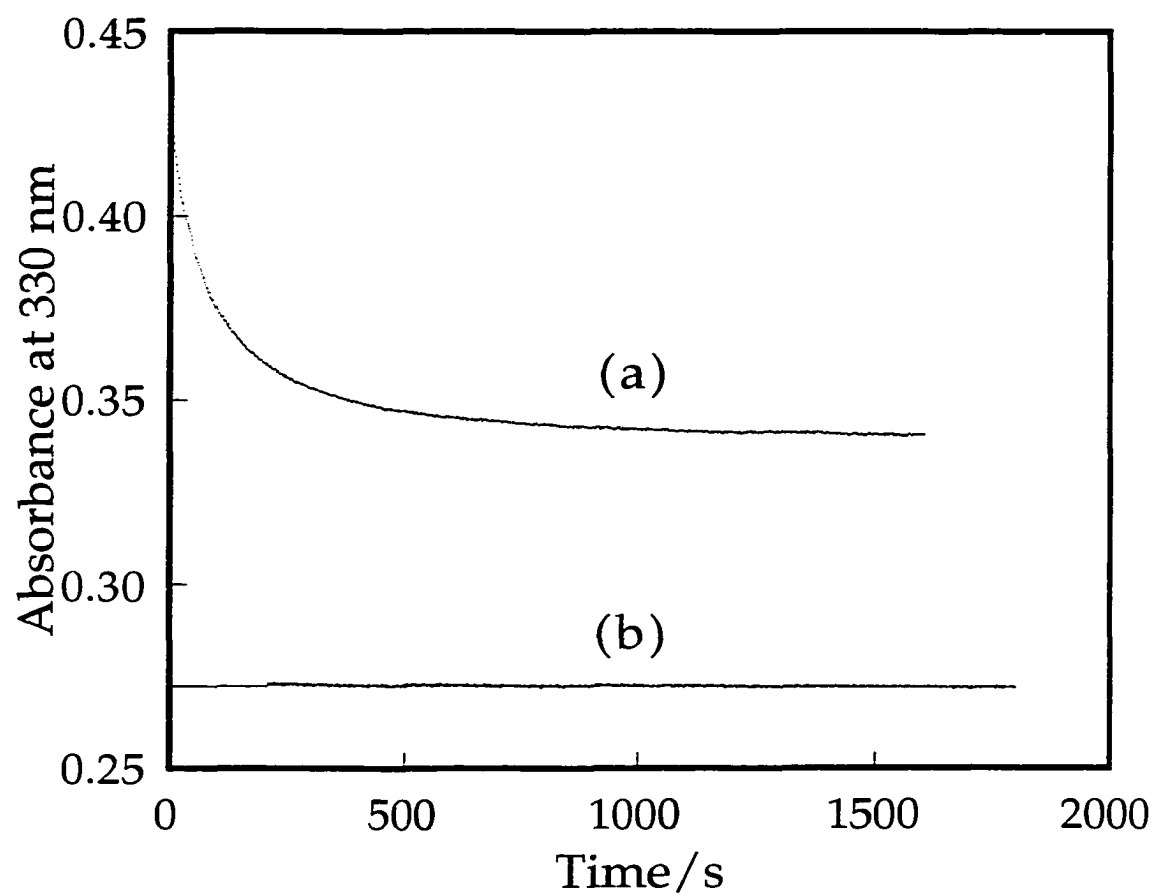


Figure 1a. Experiments showing the efficiency of catalyst **1** were monitored at 330 nm in benzene at 25°C (1 cm optical path length cell). Line (a) represents the reaction between 5 mM triphenylphosphine and 0.1 mM 4-picoline N-oxide with 0.05 mM of **1**. Line (b) represents the control experiment without **1**.

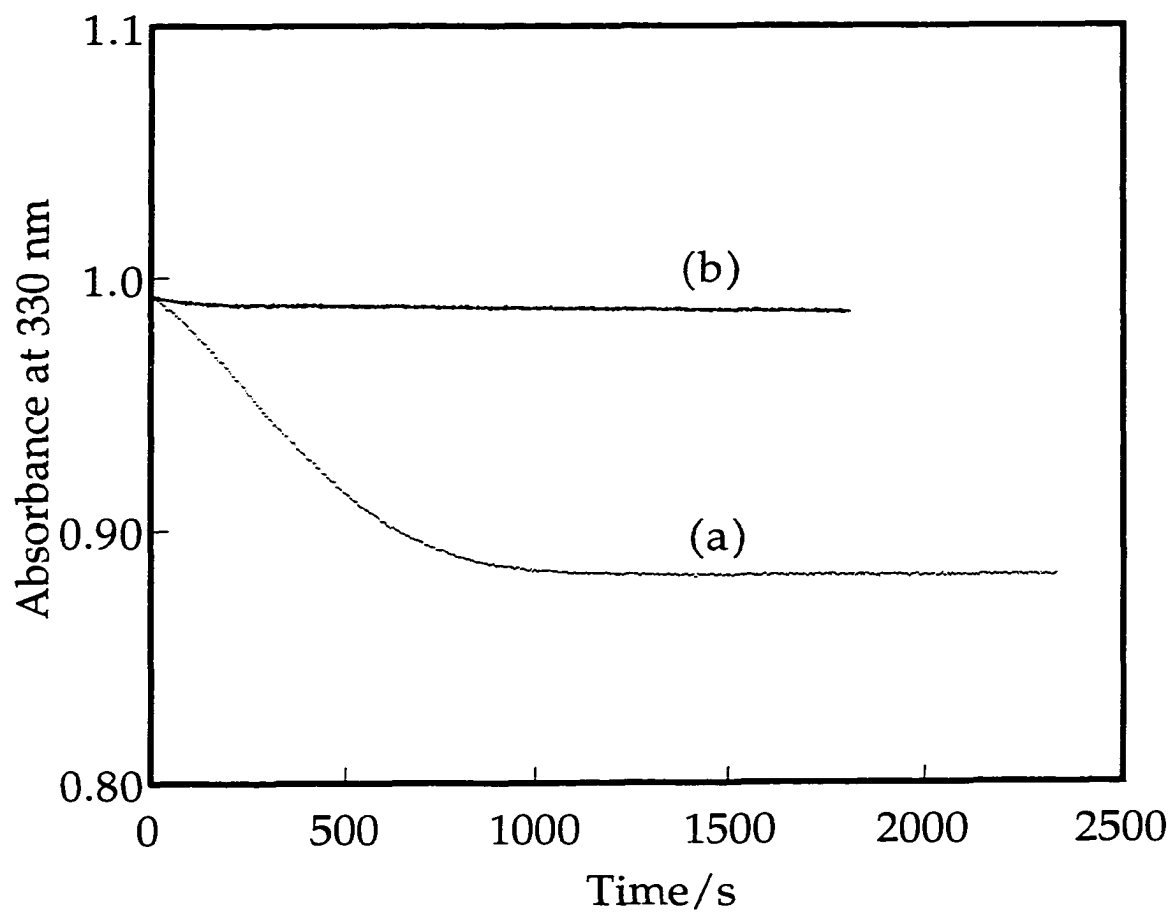


Figure 1b. Experiments showing the efficiency of catalyst **1** were monitored at 330 nm in benzene at 25°C (1 cm optical path length cells). Line (a) represents a solution containing 1 mM 4-picoline N-oxide and 0.1 mM triphenylphosphine with 0.1 μ M of **1**. Line (b) is the control experiment without **1**. The unusual shape of the kinetic profile for the catalyzed pathway arises when excess 4-picoline N-oxide is used as explained in the text.

Table 2. Kinetic data (initial reaction rates) for the oxidation of PPh₃ by 4-CH₃C₅H₄NO catalyzed by **1**.

[PPh ₃] / 10 ⁻³ M	4-CH ₃ C ₅ H ₄ NO / 10 ⁻⁴ M	[1] / 10 ⁻⁵ M	v _i / 10 ⁻⁶ mol L ⁻¹ s ⁻¹
40.0	1.00	5.00	0.169
30.0	1.00	5.00	0.254
20.0	1.00	5.00	0.348
20.0	2.00	10.0	2.43
20.0	3.00	1.00	0.623
20.0	1.00	6.00	3.81
20.0	4.00	1.00	1.04
10.0	1.00	5.00	0.644
7.00	2.00	2.00	1.48
5.00	1.00	5.00	1.51
5.00	3.00	5.00	13.2
5.00	1.00	6.06	1.58
5.00	5.00	5.00	26.1
5.00	1.00	4.85	1.39
5.00	1.00	3.00	0.749
5.00	1.00	4.00	1.23
5.00	1.00	1.00	0.308
5.00	2.00	5.00	4.69

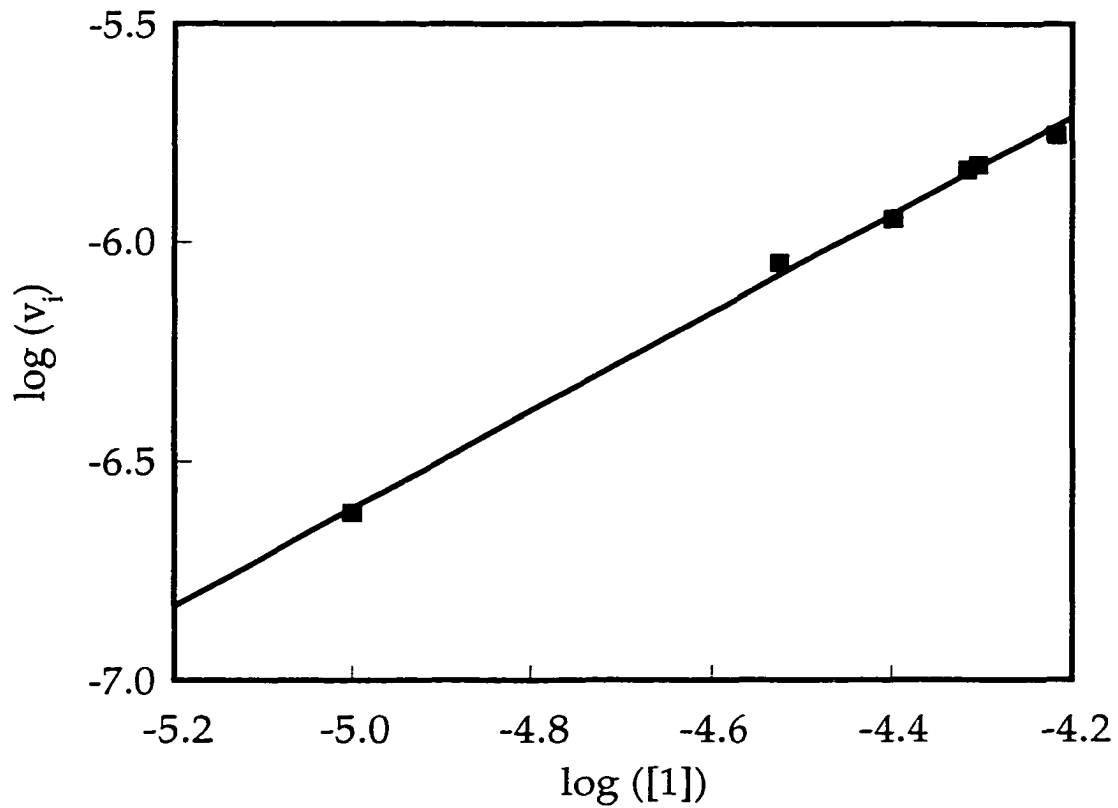


Figure 2. A plot on a log-log scale of the initial rate against the initial concentration of **1** when $[\text{PPh}_3]$ was kept at 5 mM and $[\text{4-CH}_3\text{C}_5\text{H}_4\text{NO}]$ at 0.1 mM at 25°C in benzene. The slope of the line equals one, showing that v_i has a first-order dependence on $[1]$.

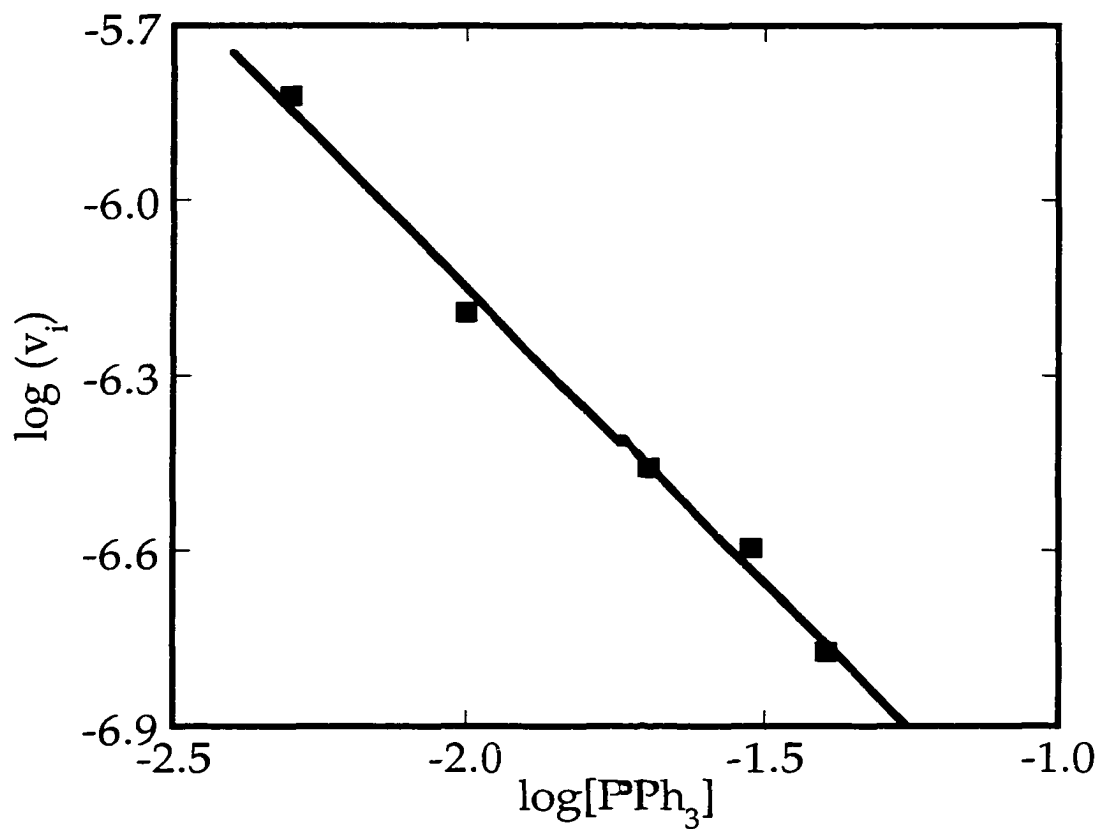


Figure 3. A plot on a log-log scale of the initial rate against the initial concentration of PPh_3 . when **[1]** was kept at 5×10^{-5} M and $[\text{4-CH}_3\text{C}_5\text{H}_4\text{NO}]$ at 1×10^{-4} M at 25°C in benzene. The slope of the line equals -1 , showing that v_i has an inverse dependence on $[\text{PPh}_3]$.

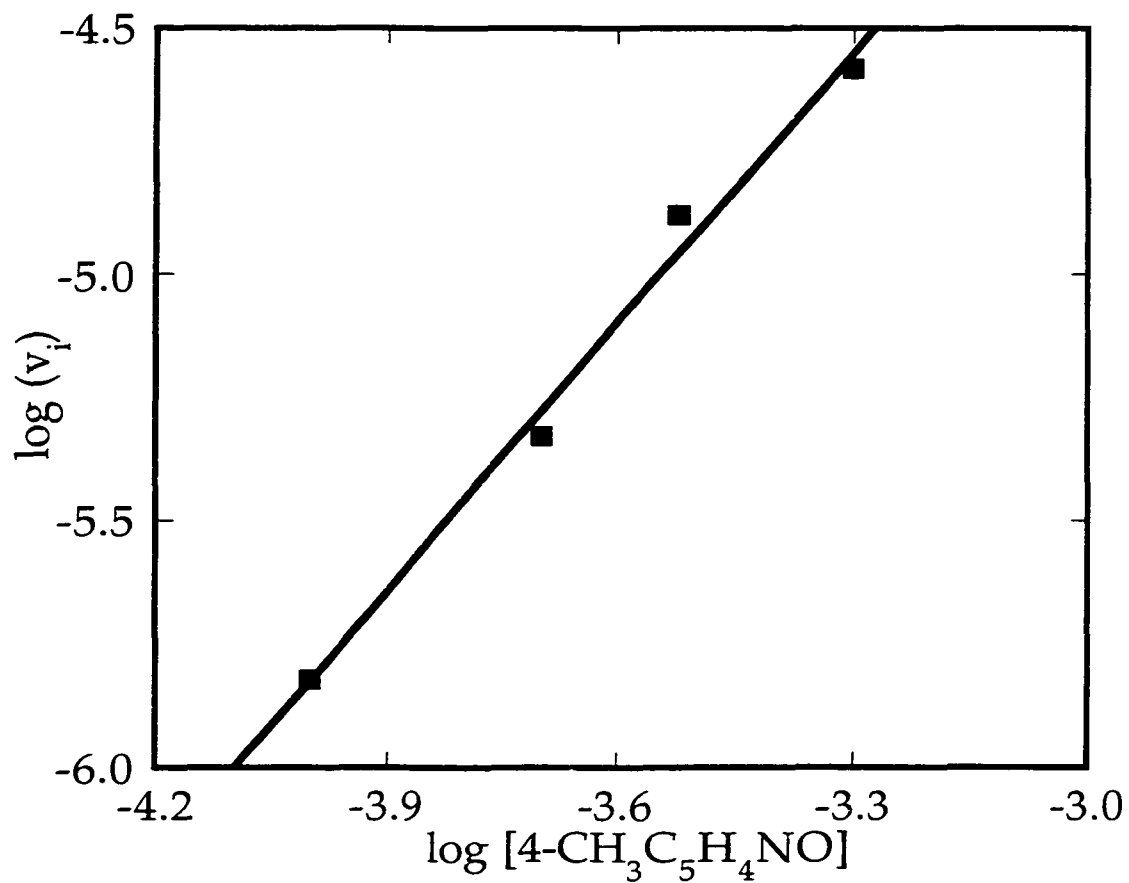


Figure 4. A plot on a log-log scale of the initial rate against the initial concentration of 4- $\text{CH}_3\text{C}_5\text{H}_4\text{NO}$ when $[\text{PPh}_3]$ was kept at 5 mM and $[1]$ at 0.05 mM at 25°C in benzene. The slope of the line equals 2, showing that v_i has a second-order dependence on $[4\text{-CH}_3\text{C}_5\text{H}_4\text{NO}]$.

To demonstrate that eq 6 has the correct form, one evaluates k by plotting v_i against the composite initial concentration term in the bracket in eq 6. Figure 5 shows that plot. The slope of the line gives $k = (1.24 \pm 0.03) \times 10^4 \text{ M}^{-1} \text{ s}^{-1}$.

Eq 6 was obtained by the initial rate method when excess PPh_3 was used over 4-picoline N-oxide. Under these conditions, no decomposition of the catalyst was observed. Thus, if eq 6 can be applied to the whole kinetic course, it predicts a second-order dependence with respect to the concentration of 4-picoline N-oxide when PPh_3 was used in large excess. Indeed, with PPh_3 varied from 5-40 mM and **1** from $(1-6) \times 10^{-5} \text{ M}$, second-order kinetic curves were obtained. The data could be fitted by eq 4 typically when 0.1 mM 4- $\text{CH}_3\text{C}_5\text{H}_4\text{NO}$ was used (Figure 6a). Pseudo-second order rate constant k_ψ can be obtained from the fittings. From eq 6, the expression of k_ψ can be written in eq 7.

$$k_\psi = \frac{[\mathbf{1}]}{[\text{PPh}_3]} k \quad (7)$$

Figure 7 shows the dependence of k_ψ on $[\text{PPh}_3]$ in a series of experiments with 0.1 mM 4- $\text{CH}_3\text{C}_5\text{H}_4\text{NO}$ and 0.05 mM **1**. As one can see, the reaction rate slows down with increasing PPh_3 concentration. A k value of $(1.53 \pm 0.05) \times 10^4 \text{ M}^{-1} \text{ s}^{-1}$ was obtained by fitting the data to eq 7. As a check on this data treatment, the absorbance-time data in Figure 6a were also fitted to eq 8 which is rearranged form of eq 4 (Figure 6b). The intercepts of these lines are the same, which is $1/(\text{Abs}_0 - \text{Abs}_\infty)$ as seen from eq 8. The value of k_ψ was obtained from the

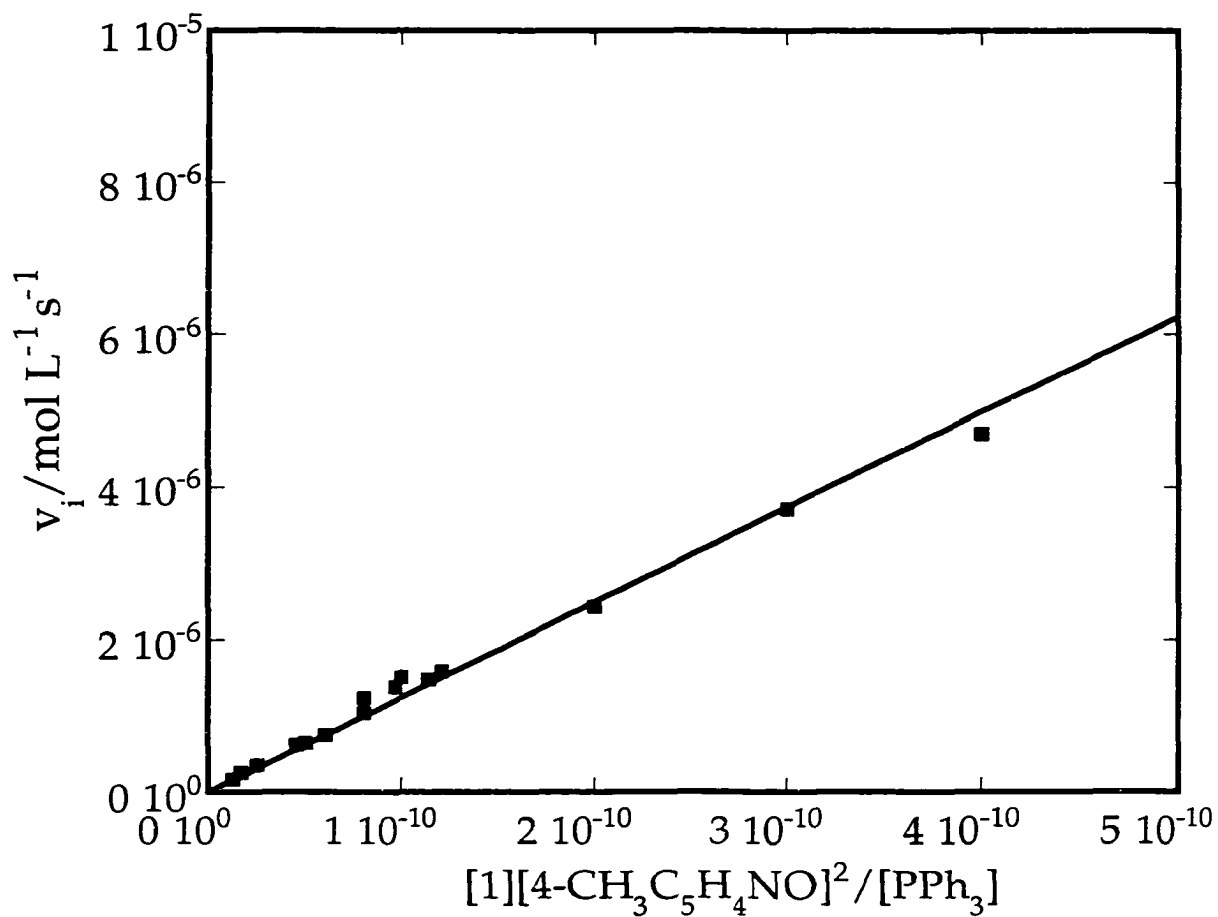


Figure 5. A plot of the initial rate against the composite term $[1][4\text{-CH}_3\text{C}_5\text{H}_4\text{NO}]/[\text{PPh}_3]$ at 25°C in benzene. The plot was fitted to eq 6 from which a k value of $(1.24 \pm 0.03) \times 10^4 \text{ M}^{-1} \text{ s}^{-1}$ was obtained from the slope.

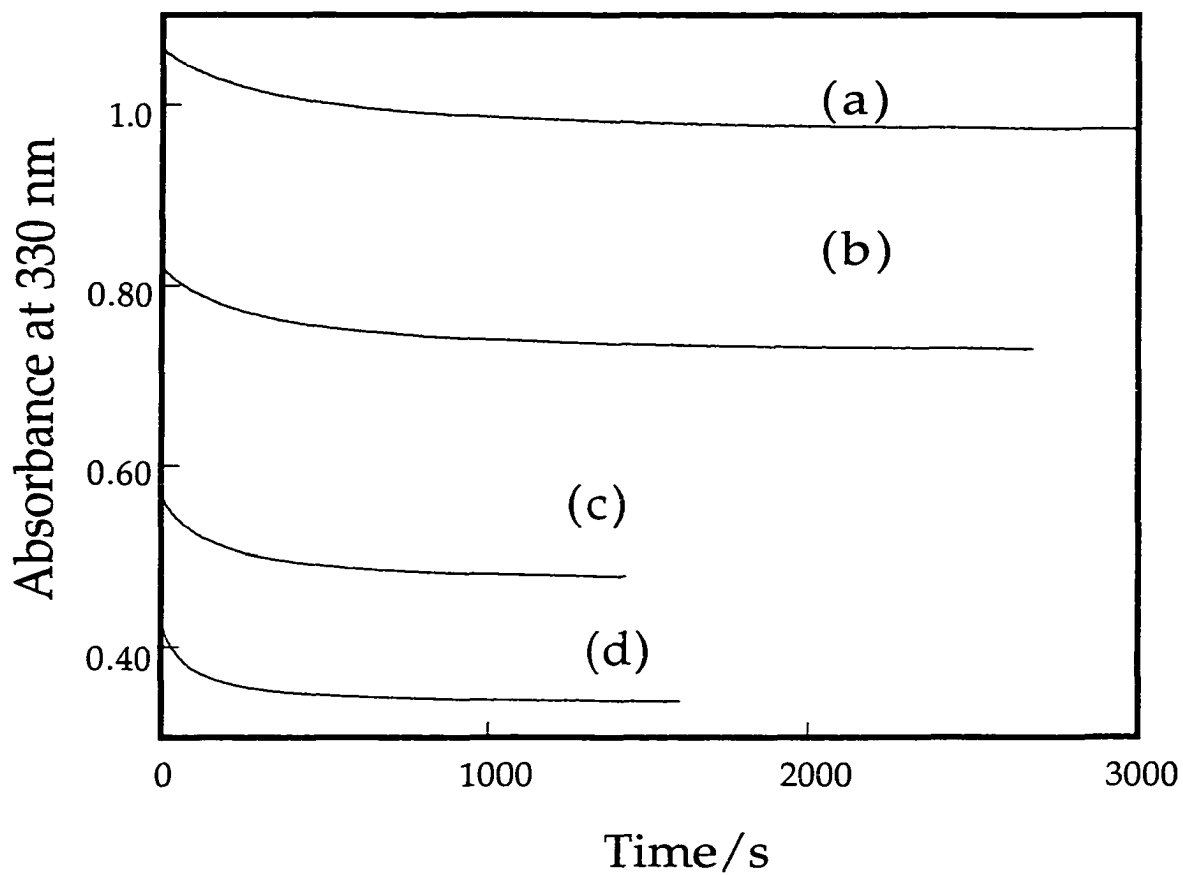


Figure 6a. Absorbance-time recordings were obtained for the reaction between 4-picoline N-oxide and triphenylphosphine catalyzed by **1** in benzene at 25°C . [4-CH₃C₅H₄NO] was kept at 0.1 mM and [1] = 0.05 mM for curves (a) to (d). [PPh₃]: (a) 30 mM, (b) 20 mM, (c) 10 mM, (d), 5 mM. The rate in each case follows pseudo-second order kinetics.

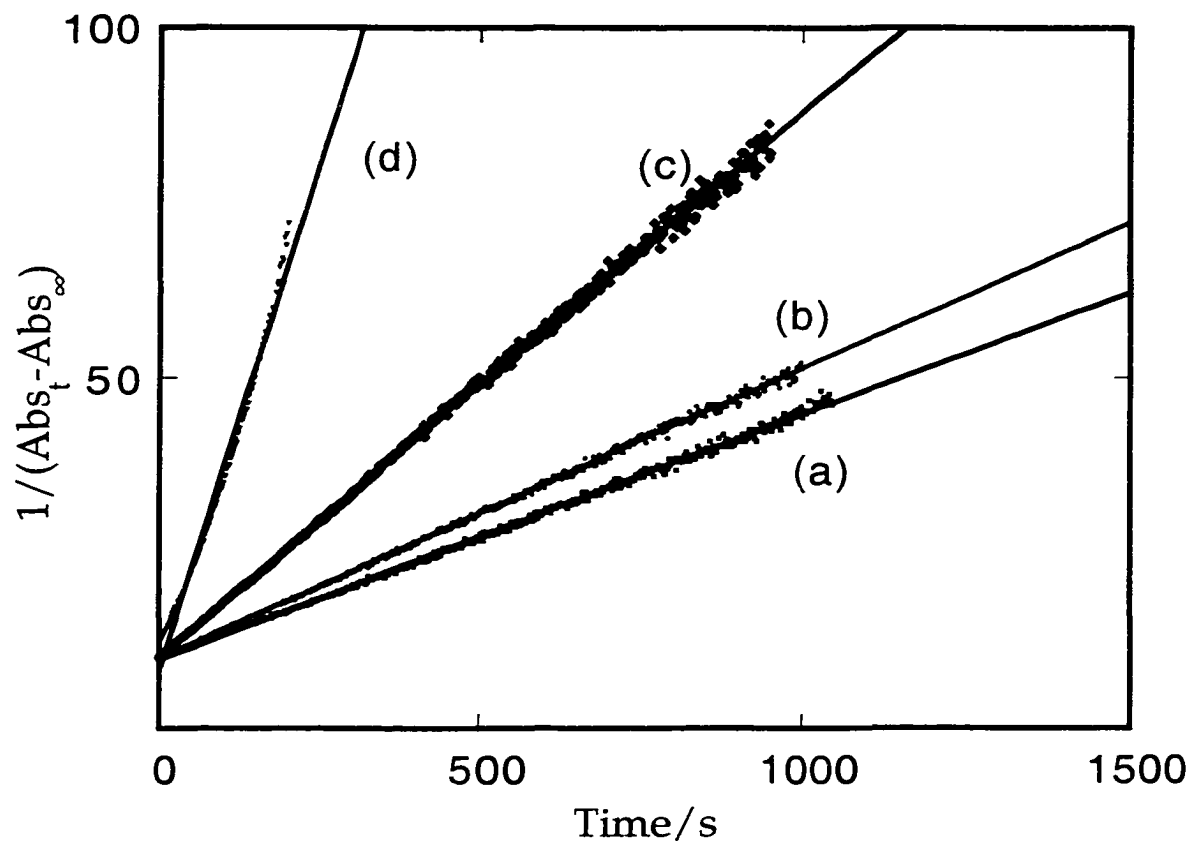


Figure 6b. An analysis of the kinetic data for the reaction between 4-picoline N-oxide and triphenylphosphine catalyzed by **1** monitored at 330 nm in benzene at 25°C. The absorbance-time readings were fitted to eq 8 for data taken to 78-88% completion. In four experiments shown, $[4\text{-CH}_3\text{C}_5\text{H}_4\text{NO}]$ was kept at 0.1 mM and $[1] = 0.05$ mM for curves (a) to (d). $[\text{PPh}_3]$: (a) 30 mM, (b) 20 mM, (c) 10 mM, (d), 5 mM.

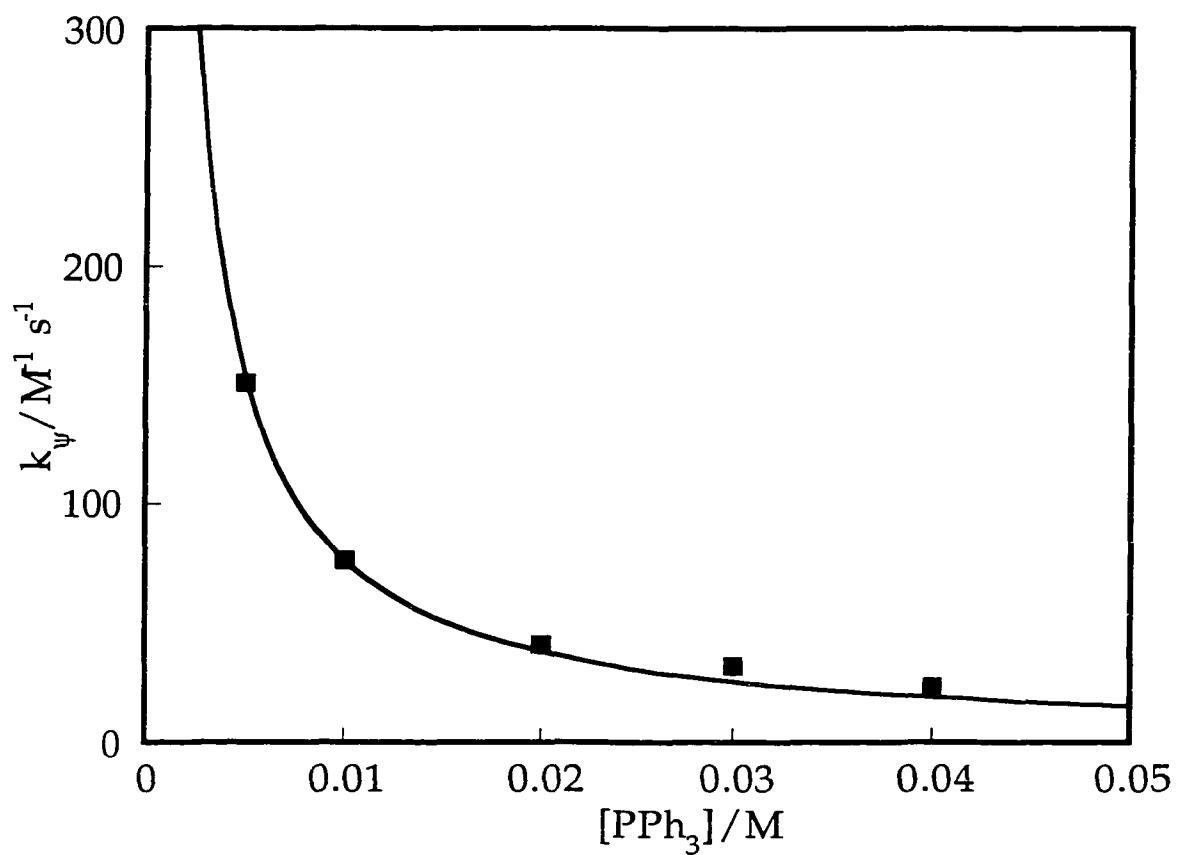


Figure 7. Plot of k_{ψ} against the concentration of PPh_3 for the reaction in eq 1. The curve is fitted by eq 7 and gave k of eq 1 $1.53 \times 10^4 M^{-1} s^{-1}$ at $25^{\circ}C$ in benzene. The concentration of 4-picoline N-oxide was kept at 0.1 mM and [1] at 0.05 mM.

slope of the lines under the same treatment. The two treatments in eq 4 and eq 8 gave similar results although all the rate constants reported in the tables are those obtained from the non-linear squares fitting to eq 4.

$$\frac{1}{\text{Abs}_t - \text{Abs}_\infty} = \frac{1}{\text{Abs}_0 - \text{Abs}_\infty} + \frac{[\text{PyO}]_0 k_\psi t}{\text{Abs}_0 - \text{Abs}_\infty} \quad (8)$$

From eq 7, k_ψ should not have any dependence on the concentration of 4-picoline N-oxide. Indeed, results obtained for varying [4-CH₃C₅H₄NO] from 0.1 to 0.5 mM gave virtually the same k_ψ value when [PPh₃] and [1] were fixed at constant values. One then can put all the data together to construct one plot which shows the linear dependence of k_ψ on 1/[PPh₃] (Figure 8) giving $k = (1.55 \pm 0.05) \times 10^4 \text{ M}^{-1} \text{ s}^{-1}$. The linear dependence on catalyst 1 is depicted in Figure 9. All the data are summarized in Table 3. Thus, the rate law shown in eq 6 is verified by these experiments.

To gain more information about the reaction mechanism, a series of experiments was carried out by using different Substrates (pyridine N-oxides, Ar₃P and CH₃ReO(mtp)(Ar₃P) compounds as the catalysts). Eq 6 still applies under these variations. Thus, all these experiments used phosphines in excess over pyridine N-oxides. The kinetic curves again were fitted to eq 6 to obtain the values of k. The first set of kinetics experiments refers to reactions between 4-picoline N-oxide and different phosphines, mostly (4-RC₆H₄)₃P with 1 as the catalyst. The data are summarized in Table 4. The identities of the free phosphine and the coordinated phosphine can either be the same or different in the above set of

experiments, as we synthesized a series of $\text{MeReO(mtp)}[(4\text{-RC}_5\text{H}_4)_3\text{P}]$ compounds. All these compounds effectively catalyze the reaction in eq 1 on the basis of NMR and UV-vis evidence. Thus another series of experiments was performed using 4-picoline N-oxide while varying the free phosphine $(4\text{-RC}_5\text{H}_4)_3\text{P}$ and the corresponding $\text{MeReO(mtp)}[(4\text{-RC}_5\text{H}_4)_3\text{P}]$. The k values obtained were summarized in Table 5.

Table 6 shows the k values of different pyridine N-oxides reacting with PPh_3 catalyzed by **1**. The rate constants span for several orders of magnitude. Sterically hindered 2,6-lutidine N-oxide is also able to transfer an oxygen to triphenylphosphine although the reaction is several orders of magnitude slower with k of eq 6 (5.95 ± 0.15) $\text{M}^{-1} \text{s}^{-1}$.

Table 4. k values obtained for the reaction of different phosphines with 4-picoline N-oxide catalyzed by MeReO(mtp)PPh_3 at 25°C in benzene.

Phosphine	3σ	$k / 10^3$ ($\text{M}^{-1} \text{s}^{-1}$)
$(\text{MeOC}_6\text{H}_4)_3\text{P}$	-0.81	2.94 ± 0.03
$(\text{MeC}_6\text{H}_4)_3\text{P}$	-0.51	2.43 ± 0.01
$(\text{C}_6\text{H}_5)_3\text{P}$	0	15.5 ± 0.5
$(\text{FC}_6\text{H}_4)_3\text{P}$	0.18	24.5 ± 0.1
$(\text{ClC}_6\text{H}_4)_3\text{P}$	0.69	117 ± 1
$(\text{CF}_3\text{C}_6\text{H}_4)_3\text{P}$	1.62	276 ± 4
Cy_2PhP		0.40 ± 0.01

Table 3. Values of k_{ψ} obtained from the second-order kinetic fittings under different concentrations of PPh_3 , 4- $\text{CH}_3\text{C}_5\text{H}_4\text{NO}$ and catalyst **1**.

$[\text{PPh}_3]/10^{-3} \text{ M}$	$[4\text{-CH}_3\text{C}_5\text{H}_4\text{NO}]/10^{-4} \text{ M}$	$[1]/10^{-5} \text{ M}$	$k_{\psi} / \text{M}^{-1} \text{ s}^{-1}$
5.00	1.00	6.10	177
5.00	1.00	4.80	145
5.00	1.00	1.80	50.9
5.00	1.00	5.00	151
5.00	1.00	1.00	24.1
5.00	1.00	3.00	89.8
5.00	1.00	4.00	113
40.0	1.00	5.00	26.6
30.0	1.00	5.00	33.6
20.0	1.00	5.00	37.9
10.0	1.00	5.00	76.5
10.0	2.00	5.00	74.2
15.0	2.00	5.00	62.5
20.0	2.00	5.00	40.3
30.0	2.00	5.00	32.0
40.0	5.00	5.00	23.2

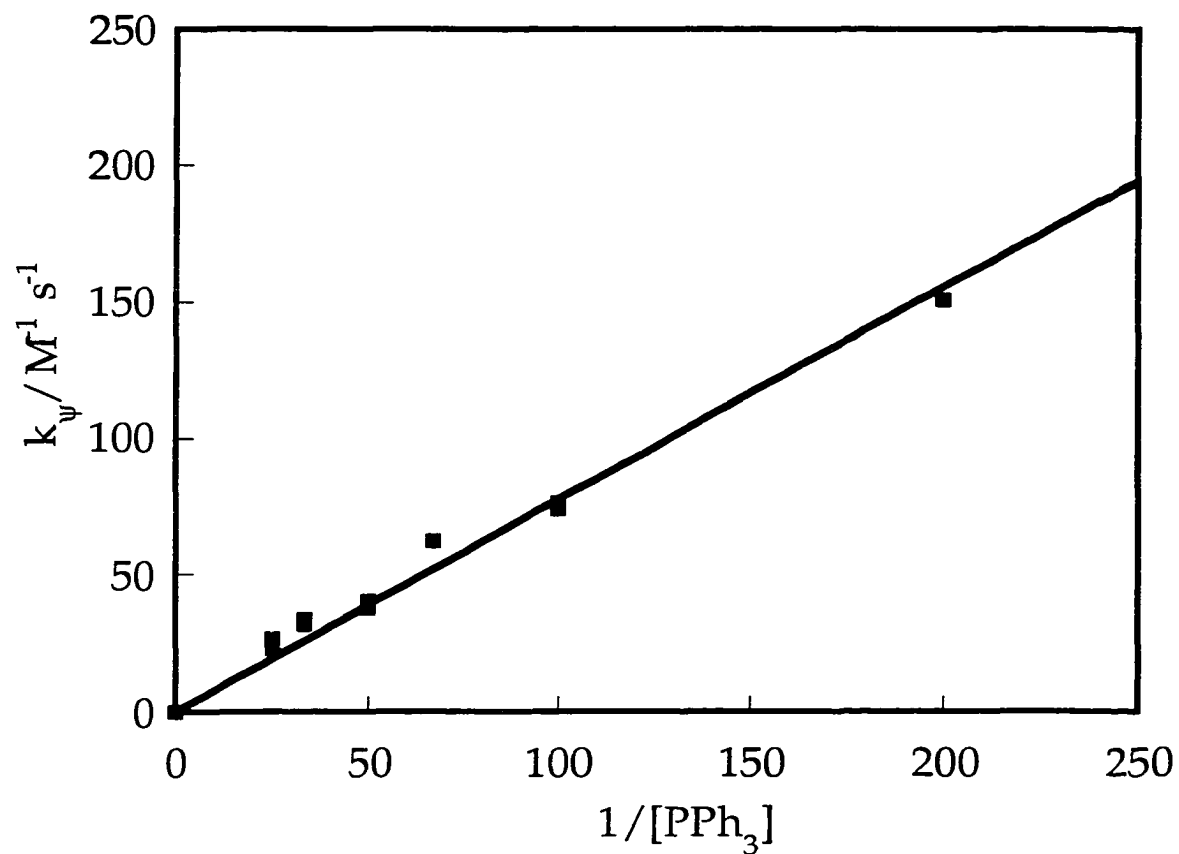


Figure 8. A plot of k_{ψ} against the inverse of the triphenylphosphine concentration varying from 5 to 40 mM for the reaction in eq 1. The concentration of 4-picoline N-oxide was varied from 0.1 to 0.5 mM and catalyst **1** was kept at 0.05 mM at 25°C in benzene. The fitting (eq 7) gave k of eq 6 $1.55 \times 10^4 \text{ M}^{-1} \text{ s}^{-1}$.

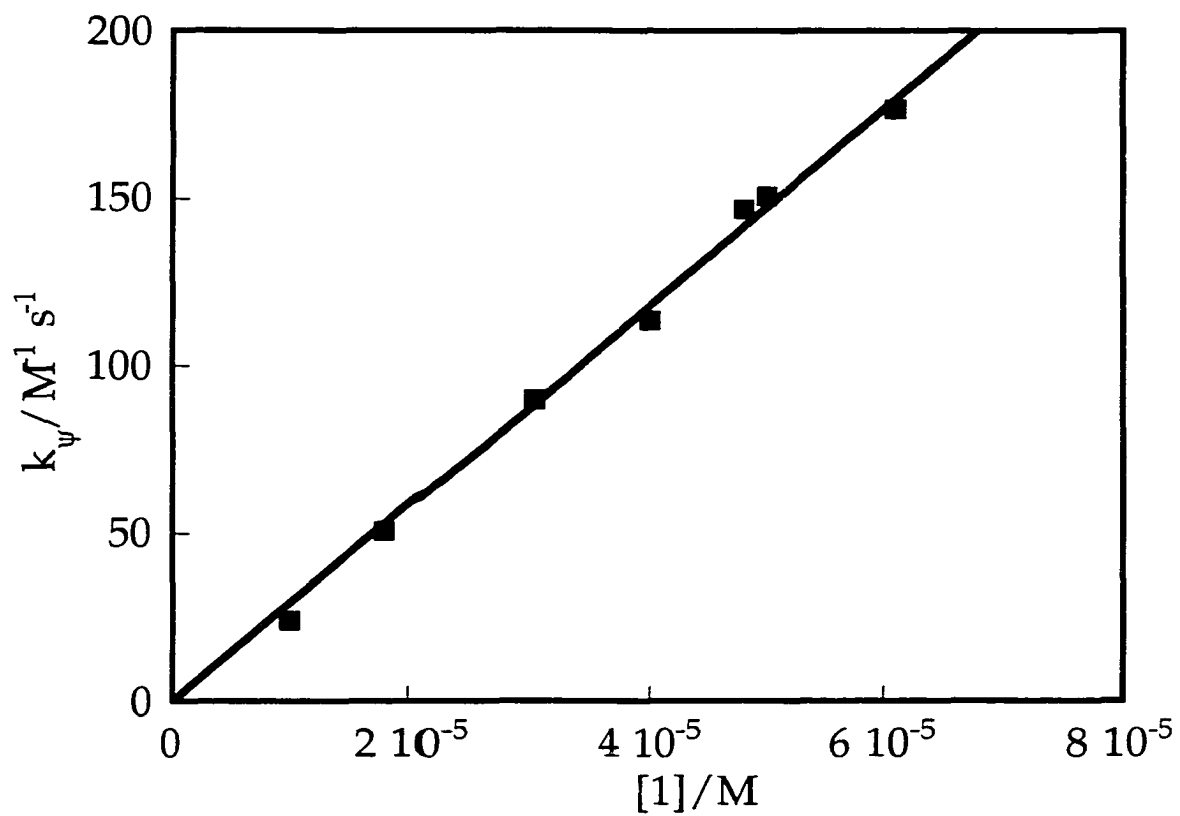


Figure 9. Plot of k_{ψ} against the concentration of 1 for the reaction in eq 1 while keeping 4-picoline N-oxide at 0.1 mM and triphenylphosphine at 5 mM at 25°C in benzene.

Table 5. k values obtained for the reaction between (4-R-C₆H₄)₃P and 4-picoline N-oxide catalyzed by MeReO(mtp)[(4-R-C₆H₄)₃P] at 25°C in benzene.

		3σ	k (M ⁻¹ s ⁻¹)/10 ³
R=	(4-R-C ₆ H ₄) ₃ P, M[(4-R-C ₆ H ₄) ₃ P], R=		
MeO	MeO	-0.81	1.93 ± 0.02
Me	Me	-0.51	2.92 ± 0.04
H	H	0	15.5 ± 0.5
F	F	0.18	58.8 ± 0.1
Cl	Cl	0.69	99.4 ± 0.3
CF ₃	CF ₃	1.62	477 ± 6

Table 6. k values obtained for the reaction of phosphines with different N-oxides catalyzed by MeReO(mtp)PPh₃ at 25°C in benzene.

Pyridine N-oxide	σ	k (M ⁻¹ s ⁻¹)/10 ³
4-MeOC ₅ H ₄ NO	-0.27	19.1 ± 0.2
4-MeC ₅ H ₄ NO	-0.17	15.5 ± 0.5
4-C ₅ H ₅ NO	0	1.22 ± 0.04
4-PhC ₅ H ₄ NO	-0.01	0.38 ± 0.03
4-NCC ₅ H ₄ NO	0.66	0.00404 ± 0.00002
4-NO ₂ C ₅ H ₄ NO	0.78	0.00178 ± 0.00005
2,6-lutidine N-oxide		0.00595 ± 0.000009

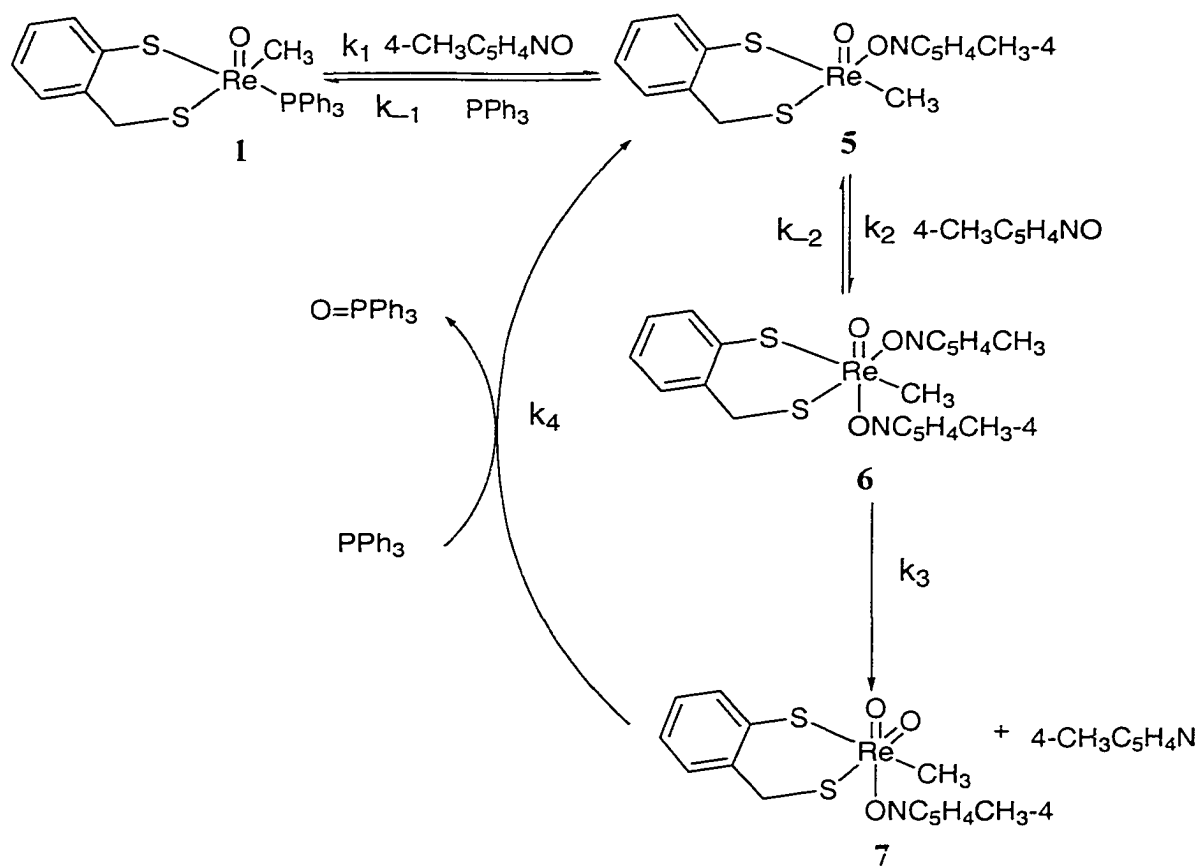
The full rate law, without any assumption as to a limiting form, may be even more complicated than this. It is disadvantageous to perform numerous experiments at variable concentrations of each substrates to reveal the full rate law. To assist us in kinetics design, a preliminary reaction scheme is proposed in Scheme 2, from which one can design falsifying tests that may lead to modification of the scheme. It is proposed that a fast ligand substitution reaction between **1** and 4-picoline N-oxide takes place first to form $\text{MeReO}(\text{mtp})(4\text{-CH}_3\text{C}_5\text{H}_4\text{NO})$ **5** and so liberates triphenylphosphine. This step accounts for the inverse dependence on the triphenylphosphine, for one power of the 4-picoline N-oxide dependence and for the first order dependence of the rate on the catalyst **1**. The catalytic intermediate **5**, in a second rapid but unfavorable equilibrium, then adds another 4- $\text{CH}_3\text{C}_5\text{H}_4\text{NO}$ to form the six-coordinate $\text{Re}(\text{V})$ compound **6**. That step would account for the second power of 4-picoline N-oxide in the rate law. According to the scheme proposed, a dioxo $\text{Re}(\text{VII})$ intermediate, $\text{MeRe}(\text{O})_2(\text{mtp})(4\text{-CH}_3\text{C}_5\text{H}_4\text{NO})$ **7**, is formed in the rate controlling step. Finally, that $\text{Re}(\text{VII})$ intermediate transfers an oxygen atom to phosphine in a much more rapid reaction that releases phosphine oxide, regenerating catalytic intermediate **5**, and continuing the cycle.

On the basis of Scheme 2, a rate law can be derived by making steady-state approximations for intermediate compounds **5** and **6**. The derived rate law is given by eq 9.

$$v = -\frac{d[4\text{-CH}_3\text{C}_5\text{H}_4\text{NO}]}{dt} = \frac{k_1 k_2 k_3 [\mathbf{1}] [4\text{-CH}_3\text{C}_5\text{H}_4\text{NO}]^2}{k_2 k_3 [4\text{-CH}_3\text{C}_5\text{H}_4\text{NO}] + (k_{-1} k_3 + k_{-1} k_{-2}) [\text{PPh}_3]} \quad (9)$$

When PPh_3 was used in excess over 4-picoline N-oxide, $k_3k_2[4\text{-CH}_3\text{C}_5\text{H}_4\text{NO}] \ll (k_{-1}k_3 + k_2k_{-1})[\text{PPh}_3]$ and the first term in the denominator can be dropped. Under this assumption, the rate law becomes eq 10.

Scheme 2



$$v = -\frac{d[4\text{-CH}_3\text{C}_5\text{H}_4\text{NO}]}{dt} = \frac{k_1k_2k_3[1][4\text{-CH}_3\text{C}_5\text{H}_4\text{NO}]^2}{(k_{-1}k_3 + k_{-1}k_2)[\text{PPh}_3]} \quad (10)$$

Rhenium(V) dithiolato complexes $\text{CH}_3\text{ReO}(\text{mtp})(\text{L})$ have been isolated when L is a monodentate ligand such as pyridine or phosphine.^{13,26} $\text{CH}_3\text{ReO}(\text{mtp})(\text{L})_2$, however, has never been isolated when L is a monodentate ligand, even with excess L. So it is reasonable to assume that k_{-2} is a large number. To the contrary, k_3 represents the cleavage of the N–O covalent bond, which Scheme 2 assigned as the rate-controlling step. Thus, the equation can be further simplified by assuming $k_3 \ll k_{-2}$. Under these assumptions, the rate law simplified to eq 11, which is exactly the form that we obtained from the kinetic studies with excess phosphine (eq 6). Thus the k in eq 7 represents the combination of the rate constants $K_1K_2k_3$.

$$v = \frac{K_1K_2k_3[\mathbf{1}]}{[\text{PPh}_3]} [4 - \text{CH}_3\text{C}_5\text{H}_4\text{NO}]^2 = k_{\psi} [4 - \text{CH}_3\text{C}_5\text{H}_4\text{NO}]^2 \quad (11)$$

Kinetics with excess Picoline N-oxide. Eq 11 depicts the rate law under conditions with a large excess of triphenylphosphine over 4-picoline N-oxide. From eq 9, with 4-picoline N-oxide used in excess over triphenylphosphine, $k_2k_3[4 - \text{CH}_3\text{C}_5\text{H}_4\text{NO}] \gg (k_{-1}k_3 + k_2k_{-1})[\text{PPh}_3]$ and the latter term can be dropped. Under these conditions, the rate law should become eq 12.

$$v = k_1[\mathbf{1}][4 - \text{CH}_3\text{C}_5\text{H}_4\text{NO}] \quad (12)$$

When excess of 4-picoline N-oxide is used, the reaction becomes very fast. To monitor the reaction in UV-vis spectroscopy conveniently, the concentration of the catalyst needed to be lowered dramatically. As mentioned previously, one also needs to consider the possible interference of the reaction between 4-picoline N-oxide and **1** when excess 4-picoline N-oxide is used. The decomposition reaction might come into play towards the end of the reaction whereas it is negligible when excess triphenylphosphine is used. Indeed, the peculiar shape of Figure 1b signals the interference of the decomposition reaction when excess 4-picoline N-oxide was used. As we mentioned before, the decomposition reaction happens at a longer time scale. Thus, the initial rate method can be used to avoid this problem in a series of experiments with excess 4-picoline N-oxide over triphenylphosphine. Catalyst **1** was kept at a particular low concentration, typically 1×10^{-7} M. The linear dependence of v_i on 4-picoline N-oxide is depicted in Figure 10 giving a value of k_1 of $(9.6 \pm 0.3) \times 10^2 \text{ M}^{-1} \text{ s}^{-1}$.

Competition Kinetics to Determine Relative Rate Constants for a Fast Step in Scheme 2. The last step in Scheme 2 features a fast oxygen transfer from $\text{MeRe}(\text{O})_2(\text{mtp})(4\text{-CH}_3\text{C}_5\text{H}_4\text{NO})$ to triphenylphosphine. No absolute kinetic data can be obtained for it since it occurs after the rate-controlling step. But the relative rates for this step can be obtained by employing a pair of phosphines in a single reaction. The reaction with 4-picoline N-oxide itself is too fast to be monitored conveniently by NMR spectroscopy even with a tiny amount of the catalyst. Thus 2-methyl-4-nitropyridine N-oxide was chosen in these competition reactions because of two rate-inhibition effects as seen from Scheme 2: its ortho methyl group provides the steric hindrance to slow down the

ligand exchange step and reduce the extent of the formation of catalytic intermediate 6. Its nitro group, being electron-withdrawing, dramatically slows down the reaction as one can see from Table 7. With the new substrate, the reaction was indeed quite low. In most cases, it needed more than 10 h to go to completion under the conditions used for the competition reactions. Thus the formation of the phosphine oxides and the disappearance of the phosphines could be monitored over a period of 2 to 4 h for the beginning part when 20-35 mM 2-methyl-4-nitropyridine N-oxide, 15-25 mM of each phosphine and 0.2-0.5 mM MeReO(mtp)PPh₃ were used. The concentration of each phosphine was determined by the integration of the ¹H or ³¹P NMR signals during the reaction.

Phosphine oxide forms at a rate given by eq 13 from Scheme 2.

$$v_4 = k_4[7][PPh_3] \quad (13)$$

Or, with phosphines in general, say (PY₃)^a, the rate (eq 14) is

$$v_4^a = \frac{d[(Y_3PO)^a]}{dt} = k_4^a[7][(PY_3)^a] \quad (14)$$

Two such equations for two phosphines, (PY₃)^a and (PY₃)^b in a single reaction were divided, giving eq 15 where k₄^a and k₄^b stand for the rate constant for the last step in Scheme 2.

$$\frac{d[(Y_3PO)^a]/dt}{d[(Y_3PO)^b]/dt} = \left(\frac{k_4^a}{k_4^b} \right) \frac{[(PY_3)^a]}{[(PY_3)^b]} \quad (15)$$

Integration of eq 15 between the limits $t = 0$ and t gives the expression in eq 16 where $[(PY_3)^a]_t$ and $[(PY_3)^b]_t$ stand for the remaining concentration of each of the free phosphine at various times during the beginning part of the reaction.

$$\ln[(PY_3)^a]_t = \frac{k_4^a}{k_4^b} \ln[(PY_3)^b]_t + \text{constant} \quad (16)$$

Each logarithmic term was evaluated and one plotted against the other. The slope of the line gives the rate constant ratios. Two sets of experimental data are shown in Figure 11, plotted as in eq 16. Various phosphine pairs were used and the rate constant ratios obtained were normalized relative to that for PPh_3 ($k_4^H = 1.0$). The values of k_4^Y/k_4^H are summarized in Table 7.

Detection of a Reaction Intermediate. Efforts to capture the intermediates by monitoring the reaction between 4-picoline N-oxide and compound **1** at room temperature failed due to the fast decomposition reaction that followed. Indeed, compound **1** and MTO, which is one of the final oxidized products, are the only observable rhenium species in the 1H -NMR spectrum for the reaction between 4-picoline N-oxide and compound **1**. Since phosphines are better ligands than pyridine N-oxides, K_1 should be less than unity. The intermediates remain at a very low concentration which are difficult to detect. From previous studies, pyridine ligands in $MeReO(mtp)(Py)$ are known to be very labile. Indeed,

at low temperature, when two equiv. of 4-CH₃C₅H₄NO was added into a solution of MeReO(mtp)(4-CH₃C₅H₄N) **2** containing excess 4-CH₃C₅H₄N at 240 K, a red species was formed immediately upon mixing in almost quantitative yield, tentatively assigned the structure of compound **4**, MeRe(O)₂(mtp)(4-CH₃C₅H₄N). it is a dioxorhenium(VII) compound. The ¹H NMR spectrum of **4** is displayed in Figure 12.

Table 7. Relative rate constants for oxidation of phosphines by 2-methyl-4-nitropyridine N-oxide catalyzed by MeReO(mtp)PPh₃.

Phosphine	3σ	k ₄ ^Y /k ₄ ^H
(MeOC ₆ H ₄) ₃ P	-0.81	6.30
(MeC ₆ H ₄) ₃ P	-0.51	2.84
(C ₆ H ₅) ₃ P	0	1
(FC ₆ H ₄) ₃ P	0.18	0.55
(ClC ₆ H ₄) ₃ P	0.69	0.40
(CF ₃ C ₆ H ₄) ₃ P	1.62	0.11
PPh ₂ Me		3.11

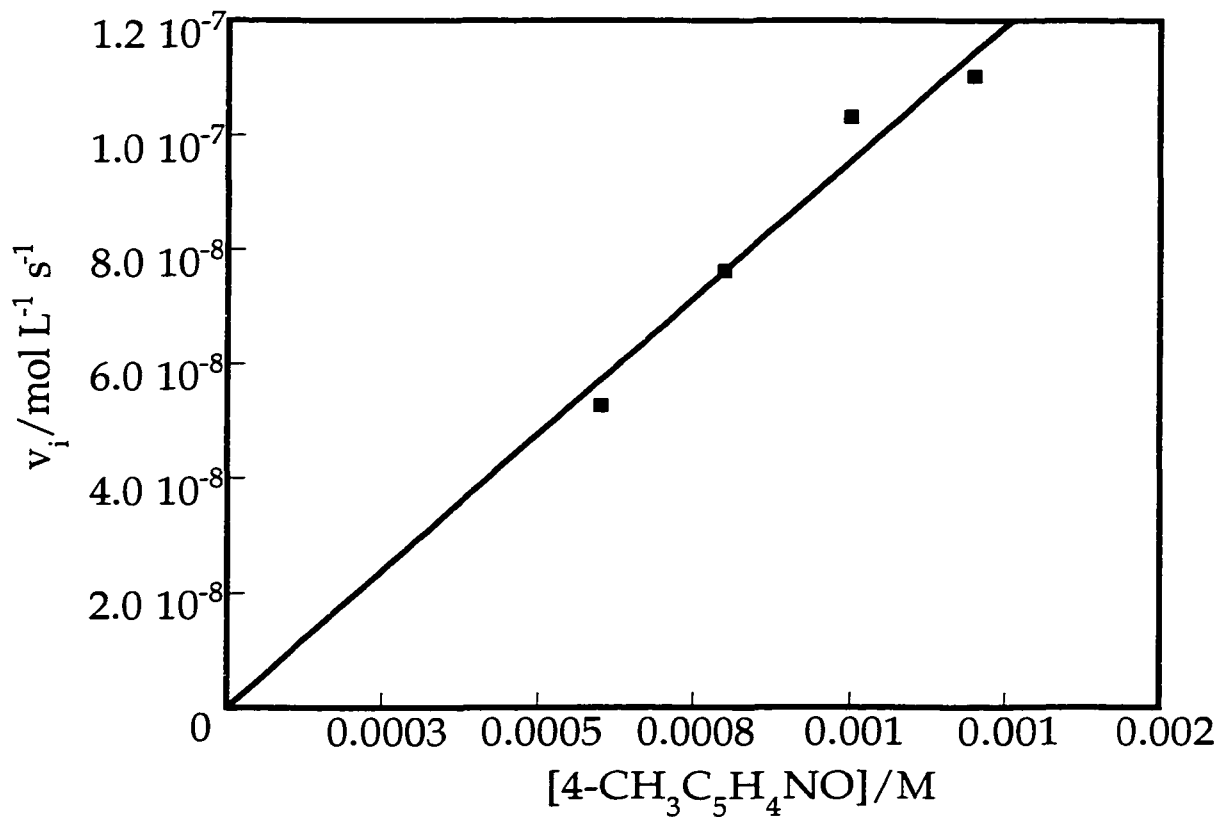


Figure 10. Plot of initial rate against the concentration of 4-picoline N-oxide for the reaction in eq 1 monitored at 330 nm. Triphenylphosphine is kept constant at 0.1 mM and **1** is kept at 1×10^{-7} M at 25°C in benzene. The curve is fitted to eq 12.

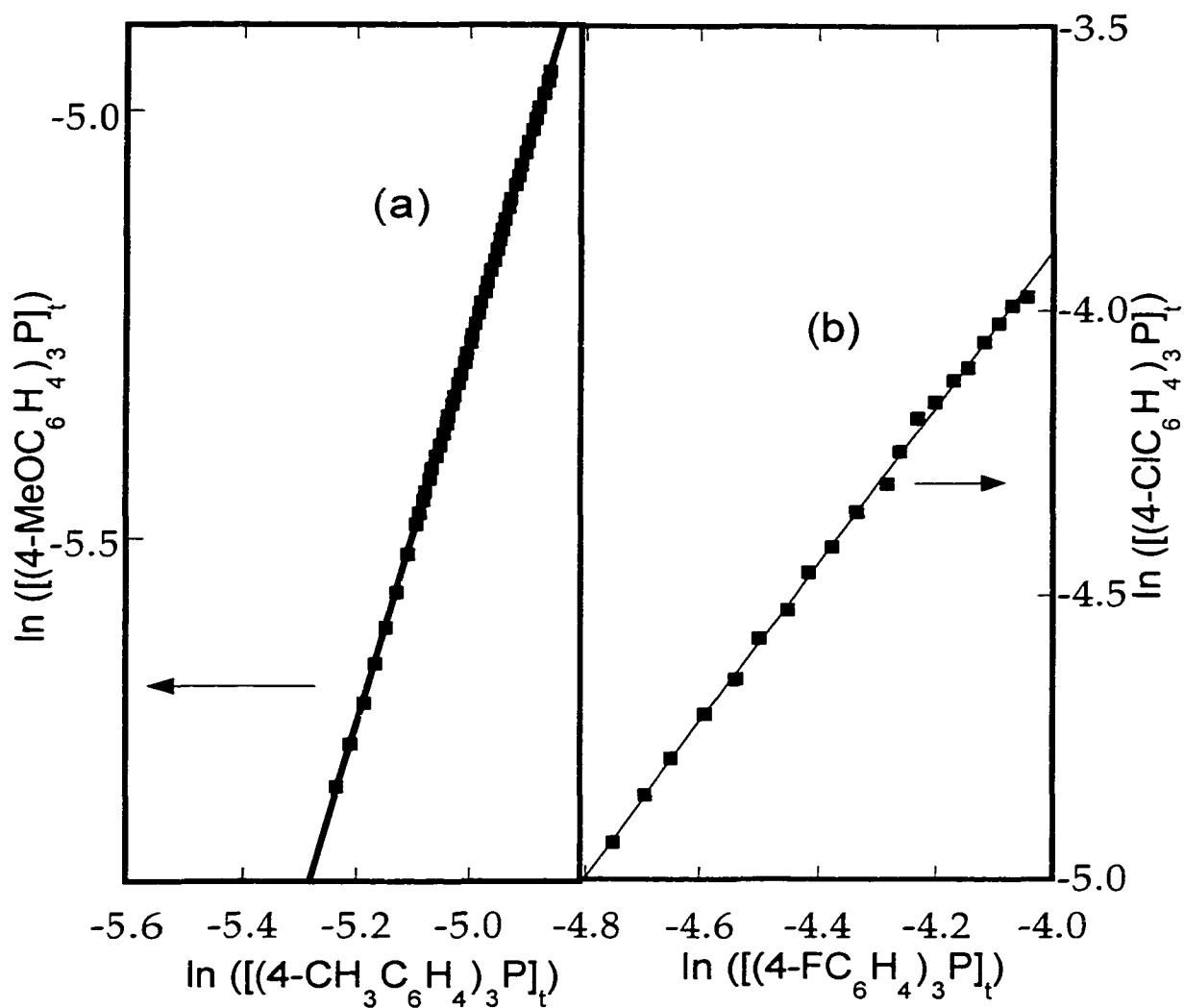


Figure 11. Kinetic data for the competition reaction between two different phosphines and 2-methyl-4-nitropyridine N-oxide catalyzed by **1** at 25°C monitored by ^1H or ^{31}P NMR. The rate constant ratios are given by the slope of these double logarithmic plots. Experiment (a) had 10 mM each of $(4\text{-MeOC}_6\text{H}_4)_3\text{P}$ and $(4\text{-MeC}_6\text{H}_4)_3\text{P}$ with 20 mM 2-methyl-4-nitropyridine N-oxide and 0.5 mM **1**. Experiment (b) contained 20 mM each of $(4\text{-ClC}_6\text{H}_4)_3\text{P}$ and $(4\text{-FC}_6\text{H}_4)_3\text{P}$ with 32 mM 2-methyl-4-nitropyridine N-oxide and 0.5 mM **1**.

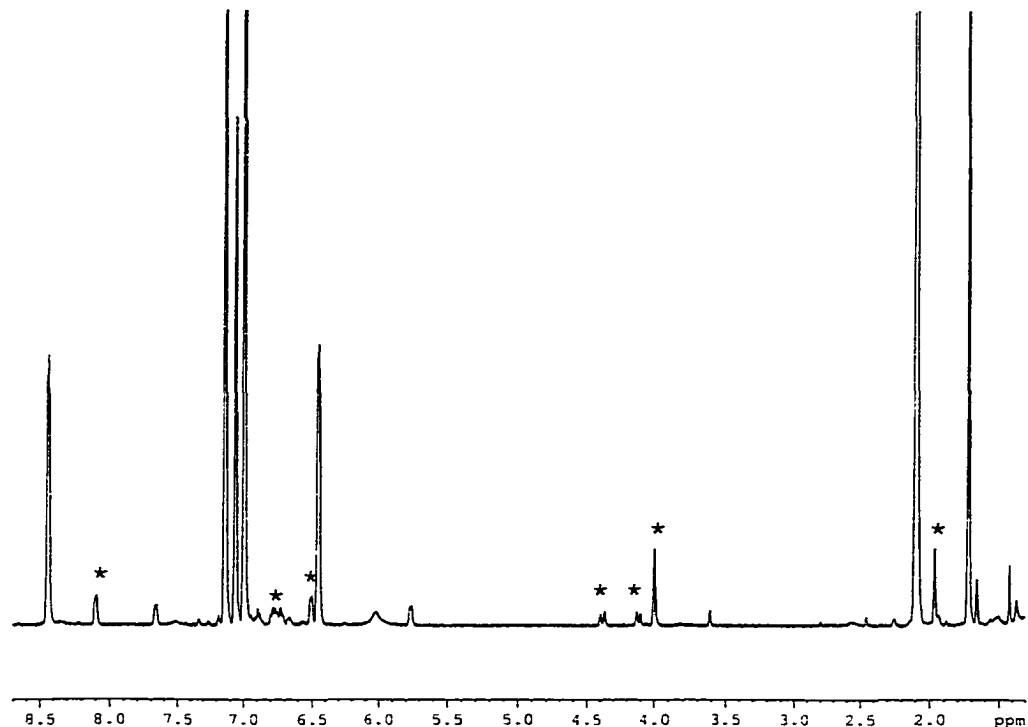


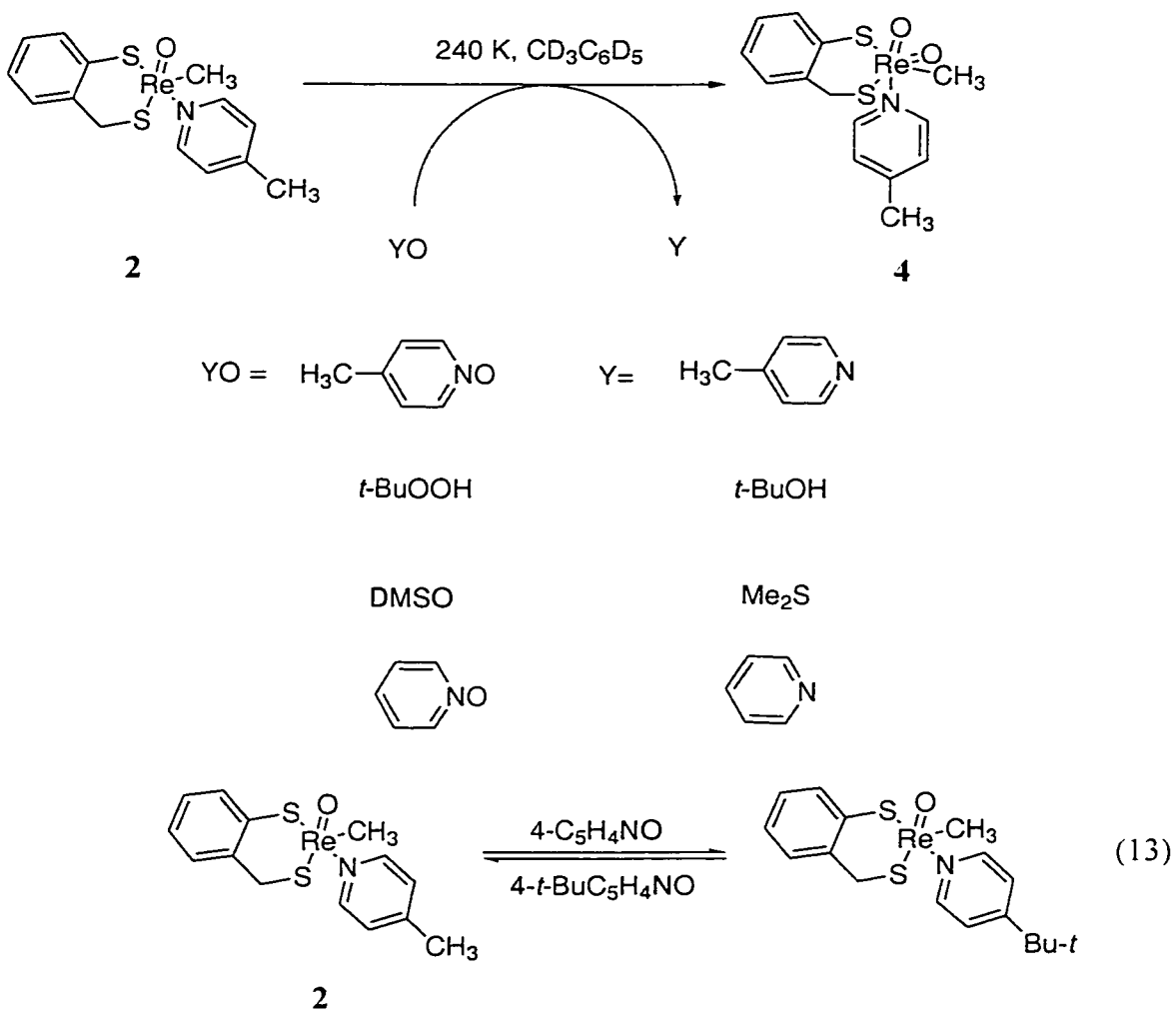
Figure 12. The ^1H NMR spectrum of a solution of compound **4** taken immediately after adding three equiv. of 4-picoline N-oxide into a solution containing 4 mM compound **2** and 20 mM free 4-picoline in $\text{CD}_3\text{C}_6\text{D}_5$ at 240 K. The following resonances belong to compound **4** (*): δ (ppm) 1.96 (s, 3H), 3.99 (s, 3H), 4.11 (d, 1H, $J = 12$ Hz), 4.38 (d, 1H, $J = 12$ Hz), 6.51(d, 2H, $J = 4$ Hz), 6.6-7.0 (m, 4H), 8.08 (d, 2H, $J = 4$ Hz). Other resonances in this spectra belong to 4-picoline: δ (ppm) 1.73 (s, 3H), 8.46 (d, 2H, $J = 4$ Hz), 6.47 (d, 2H, $J = 4$ Hz); 4-picoline N-oxide: δ (ppm) 1.42 (s, 3H), 5.75 (d, 2H, $J = 4$ Hz), 7.66 (d, 2H, $J = 4$ Hz); residual ^1H resonances of $\text{CD}_3\text{C}_6\text{D}_5$ δ (ppm) 2.09 (m), 6.98 (m), 7.00 (m), 7.09 (m).

The red species, which has a structure of **4** rather than **5** or **8**, is verified based on peak integration that shows free 4-picoline is formed. Further evidence was obtained by adding *tert*-butyl hydroperoxide, dimethyl sulfoxide and pyridine N-oxide to a solution containing the same concentration of **2** at 240 K. Compound **4** was formed in all these cases as shown in Scheme 3. This shows that the identity of the compound **4** does not depend on the identity of the oxidants. Furthermore, the pyridine ligand coordinated to the rhenium center is labile and another pyridine ligand in the system will compete to coordinate to it. Indeed, when 4-*tert*-butylpyridine was added to a solution containing compound **4**, ligand exchange was observed as shown in eq 13. Efforts to detect intermediate **7** by adding excess picoline N-oxide to a solution of **4** failed and only the final products, MTO and the disulfide oxidation product mtp, were observed. Attempts to isolate **4** failed. Over longer period time at 240 K, **4** decomposes to unidentified species. Addition of PPh₃ to a solution containing compound **4**, gave O=PPh₃ immediately at 240 K as seen from the ³¹P spectrum. This again indicates that Re(VII) is the active catalyst.

Catalysis by Compound 3. We reported previously that both bromide ion and pyridine further accelerated the reaction (eq 1).¹¹ Interestingly, the dimeric {MeReO(mtp)}₂ **3** is an even better catalyst than **1**. The catalytic effects of added nucleophiles and catalysis by **3** are depicted in Figure 13. Here 2-methyl-4-nitropyridine N-oxide was reacted with triphenylphosphine in the presence of different catalytic systems. Again, this pyridine N-oxide was chosen because that the nitro group on the pyridine N-oxide will allow the reaction to proceed more slowly for conveniently monitoring by ¹H NMR spectroscopy.

Also, its methyl group gives a convenient resonance signal to follow. The catalysis of **3** is roughly 45 times faster per rhenium atom than that of **1** under same condition.

Scheme 3



Some low temperature experiments were carried out trying to detect the active catalytic form in the compound **3** catalysis. At low temperature in deuterated toluene, when 0.8-15.2 mM 4-picoline N-oxide was added into a solution containing 2.0 mM **3**,

compounds $3(4\text{-CH}_3\text{C}_5\text{H}_4\text{NO})$, where one 4-picoline N-oxide is coordinated to **3** and $3(4\text{-CH}_3\text{C}_5\text{H}_4\text{NO})_2$ with two 4-picoline N-oxide coordinated, are formed. The reaction is exceptionally rapid. The $^1\text{H-NMR}$ signals of **3**, $3(4\text{-CH}_3\text{C}_5\text{H}_4\text{NO})$ and $3(4\text{-CH}_3\text{C}_5\text{H}_4\text{NO})_2$ could not be resolved even at 240 K as shown in Figure 14. From previous data,²⁵ the equilibrium constants for $3/3(4\text{-CH}_3\text{C}_5\text{H}_4\text{NO})$, $3(4\text{-CH}_3\text{C}_5\text{H}_4\text{NO})/3(4\text{-CH}_3\text{C}_5\text{H}_4\text{NO})_2$ are $K_1 = 4.1 \times 10^3 \text{ L mol}^{-1}$ and $K_2 = 1.7 \times 10^2 \text{ L mol}^{-1}$.²² On the basis of these data, under the concentrations used here for 4-picoline N-oxide, both $3(4\text{-CH}_3\text{C}_5\text{H}_4\text{NO})$ and $3(4\text{-CH}_3\text{C}_5\text{H}_4\text{NO})_2$ are the major species in the last 4 spectra in Figure 14. Increasing the concentration of 4-picoline N-oxide is not plausible due to the low solubility of the picoline N-oxides at 240 K in toluene. Thus, the chemical shifts for $3(4\text{-CH}_3\text{C}_5\text{H}_4\text{NO})_2$ could not be obtained by adding enough 4-picoline N-oxide to get the $3(4\text{-CH}_3\text{C}_5\text{H}_4\text{NO})_2$ as the major species. Over longer period of time at 240 K, no signals were detected except that of the final products, MTO and disulfide, No other species was built up in significant amount. Upon adding PPh_3 into any of the solutions in Figure 14, O=PPh_3 was formed immediately even at 240 K in deuterated toluene.

Interpretation and Discussion

Hammett correlation. The phosphine substrate inhibits the oxygen transfer reaction between 4-picoline N-oxide and PPh_3 catalyzed by **1**. This peculiar phenomenon can be explained by the ligand exchange step in Scheme 2 where the coordinated phosphine is released in the first step. From Table 5, the rate increases with electron-withdrawing group on the para position of the phenyl rings in triarylphosphine when the coordinated and free phosphines are identical. To illustrate this effect, a Hammett plot can be constructed for the

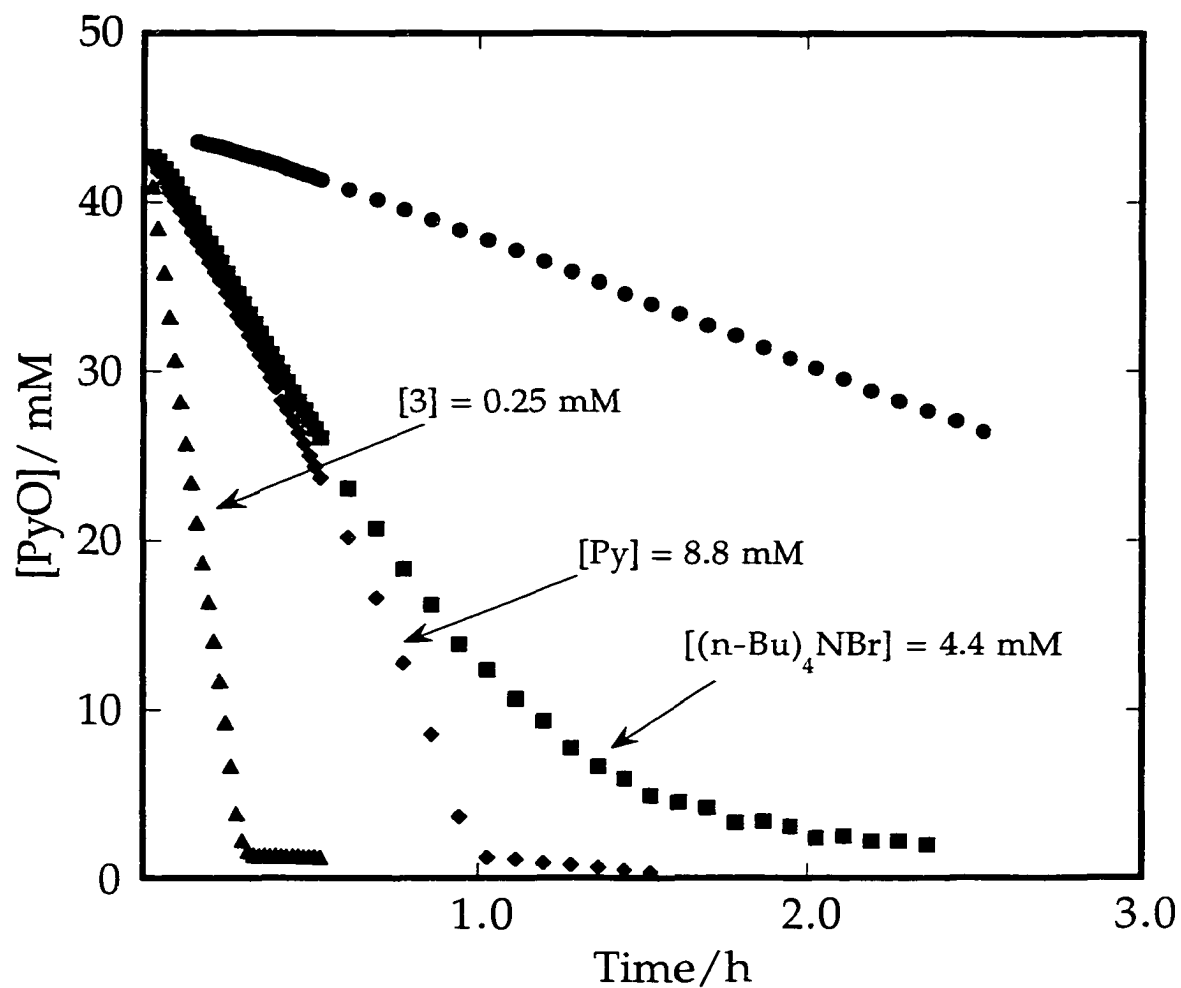


Figure 13. The catalytic effects of different systems illustrated by monitoring the disappearance of the starting material 44.4 mM 2-methyl-4-nitropyridine N-oxide in the reaction with 44.4 mM triphenylphosphine under different catalytic conditions using ¹H NMR kinetic program. From top to bottom: [1]=1 mM; [1]=1 mM, [(n-Bu)₄NBr]= 4.4 mM; [1]= 1mM, [Py]=8.8 mM; [3] = 0.25 mM

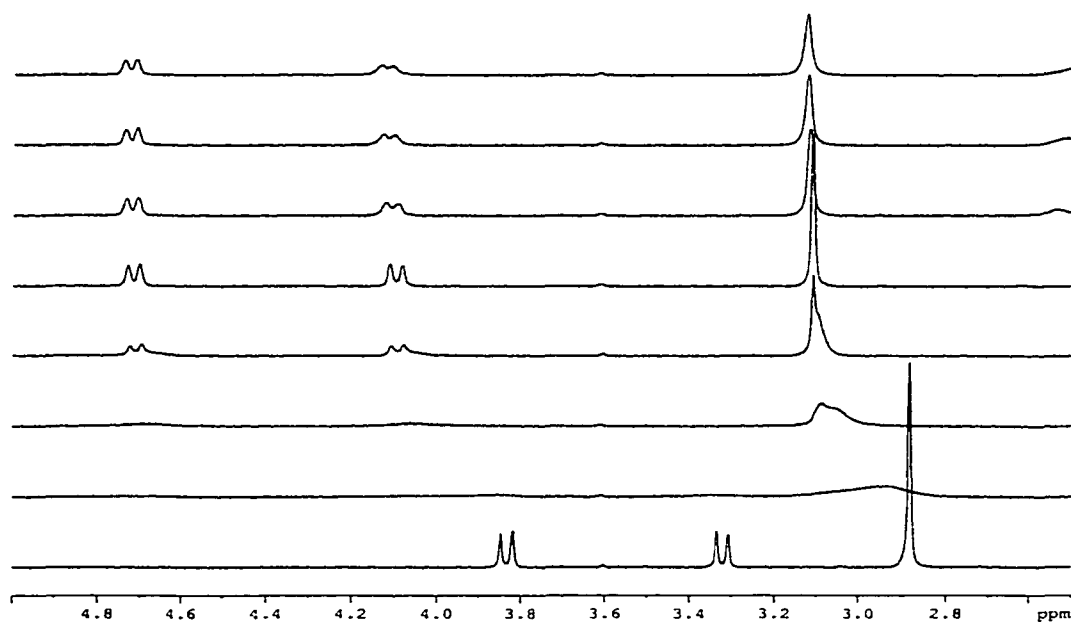


Figure 14. A series of stacked ^1H -NMR spectra recorded by adding different amount of 4-picoline N-oxide into a solution containing 2 mM compound 3 at 240 K in deuterated toluene. From bottom to top: $[\text{4-CH}_3\text{C}_5\text{H}_4\text{NO}]/\text{mM} = 0, 0.8, 1.6, 2.4, 3.2, 7.2, 11.2, 15.2$

reaction between $(4\text{-RC}_5\text{H}_4)_3\text{P}$ and 4-picoline N-oxide catalyzed by $\text{MeReO}(\text{mtp})[(4\text{-RC}_6\text{H}_5)_3\text{P}]$ which gave a ρ value of 1.03 ± 0.12 (Figure 15, line 2). This is in accordance with the mechanism. Lowering the Lewis basicity of the coordinated phosphine will facilitate the ligand exchange step thus accelerates the whole rate. These results also implying that k_4 is a fast oxygen transfer step. Was the k_4 term in the rate law, one would have expected the opposite electronic effect with a negative ρ value considering explicitly

that the electron-donating para substituents will react faster with the Re(VII) dioxo intermediate 7.

From Scheme 2, phosphine is also involved in the step where Re(VII) intermediate 7 will transfer an oxygen atom to phosphine and release phosphine oxide. Although this fast step occurs after the rate-controlling step, information can be obtained by competition kinetics design and the rate constant ratios thus can be determined. A Hammett plot for k_4 is shown in Figure 15, line 3 by plotting $\log(k_4^Y/k_4^H)$ for the para substituted triarylphosphine against 3σ . The slope of the line of ρ value is -0.70 ± 0.07 .

The three Hammett plots describing the different aspects of the electronic effects of the para substituted triarylphosphine are combined in Figure 15. A very interesting comparison can be made by comparing line 1 and line 2 with line 3 in which a negative ρ value of -0.70 was obtained. This is not surprising since the last step features an electrophilic attack of phosphines on Re(VII) intermediate so that electron donating groups on the para position accelerates the rate while they have the opposite effect in the first ligand exchange step. The overall effect is determined by the first step since the last step occurs after the rate-controlling step. The design of the competition reaction makes it possible to access separately the electronic effect in the last step.

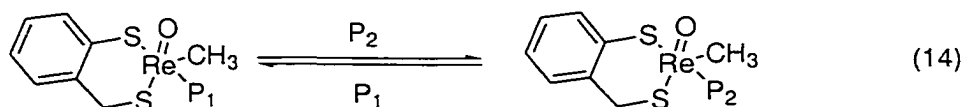
When the identity of the coordinated and the free phosphine are different, further complications arise. Although the original catalyst is $\text{MeReO}(\text{mtp})\text{PPh}_3$, some of it will become $\text{MeReO}(\text{mtp})[(\text{Ar})_3\text{P}]$ through the ligand exchange step in Scheme 2 where $(\text{Ar})_3\text{P}$

stands for the added free phosphine. A Hammett plot was constructed for the reaction between $(4\text{-RC}_5\text{H}_4)_3\text{P}$ and 4-picoline catalyzed by $\text{MeReO}(\text{mtp})(\text{C}_6\text{H}_5)_3\text{P}$. A similar electronic effect is also observed as shown in Figure 15, Line 2 with a smaller ρ value of 0.42 ± 0.09 .

Varying the para substituents on the pyridine N-oxide shows a relatively large electronic effect as one can see from Table 6. Thus, a Hammett plot can also be constructed for the reaction between $4\text{-RC}_5\text{H}_4\text{NO}$ and PPh_3 catalyzed by $\text{MeReO}(\text{mtp})\text{PPh}_3$ (Figure 16). The slope of the line of ρ value is -3.84 ± 0.37 . The reaction rate has a second-order dependence on pyridine N-oxide with one entering in the two equilibrium and in the second prior to the rate-controlling step. In contrast to the case with phosphine, electron-donating substituents accelerate both steps thus resulting a big electronic effect. The reaction also shows a large steric effect due to the formation of 7. With Sterically hindered pyridine N-oxide, for example, 2,6-lutidine N-oxide, the rate is three orders of magnitude less than the $K_1K_2k_3$ value for 4-picoline N-oxide.

Determination of K_1 . Direct determination of the equilibrium constants K_1 for the first ligand exchange step is not available due to the fast steps that follow. From the reaction scheme, K_2 and k_3 represent the steps devoid of phosphine identity. So the ratio of any pair of the $K_1K_2k_3$ values should represent the equilibrium constant of the ligand exchange reactions between P_1 and $\text{MeReO}(\text{mtp})\text{P}_2$ which can be monitored directly (eq 14). The ligand exchange reaction in eq 14 can be obtained by adding free phosphine P_1 to a solution containing $\text{MeReO}(\text{mtp})\text{P}_2$ and measure the concentration of the four species by ^1H NMR allowing enough time for it to reach equilibrium. Thus K_e can be obtained by using

the concentrations at equilibrium in eq 15.²⁰ Table 8 gives two examples of the equilibrium constants K_e obtained by this direct method and by taking the ratios of the $K_1K_2k_3$ values in Table 5. Comparison of these independently obtained data with those determined from kinetic ratios supports the proposed mechanism.



$$K_e = \frac{[\text{MeReO(mtp)P}_2][\text{P}_1]}{[\text{MeReO(mtp)P}_1][\text{P}_2]} \quad (15)$$

Table 8. Equilibrium Constants of eq 11 obtained by two different methods. K_e was obtained by eq 12.

P_1	P_2	K_e	$P_1(K_1K_2k_3)/P_2(K_1K_2k_3)$
$(\text{C}_6\text{H}_5)_3\text{P}$	$(4\text{-CH}_3\text{C}_6\text{H}_5)_3\text{P}$	5.6	5.3
$(\text{C}_6\text{H}_5)_3\text{P}$	$(4\text{-ClC}_6\text{H}_4)_3\text{P}$	0.10	0.15

Re(V) or Re(VII). In the proposed mechanism, compound **5** was formed first where the methyl group is trans to the phenolic sulfur and it then picks up another 4-picoline N-oxide to generate the six-coordinated intermediate **6**. An alternative mechanism was also considered in which the first formed **5** would pick up another 4-picoline N-oxide to form the “normal” compound **8** where the methyl group is cis to the phenolic sulfur again through a turnstile mechanism.²⁰ Noting that in compound **1**, the methyl group is also *cis* to

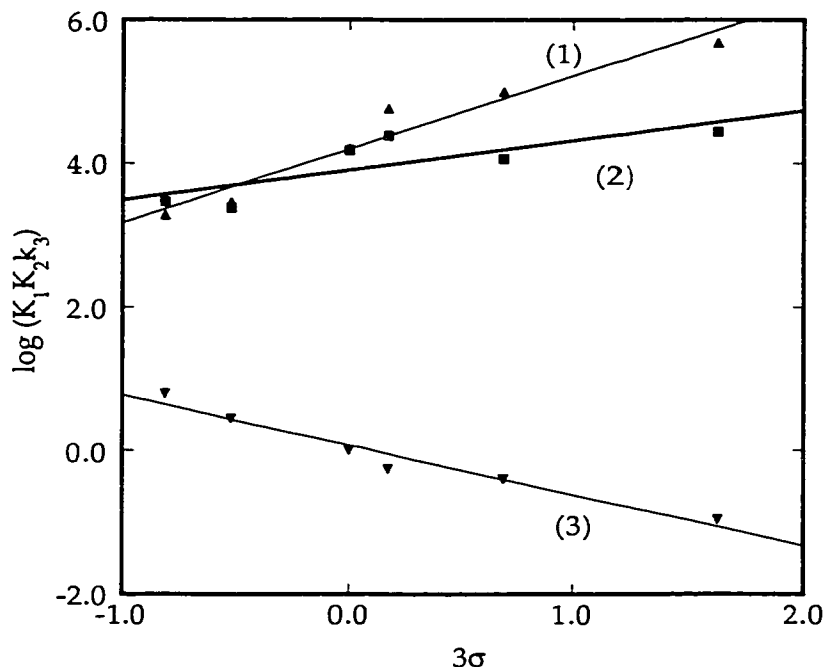


Figure 15. Three Hammett plots showing the electronic effects by varying the para substituents on the phenyl ring of the triarylphosphine in different reaction steps. Line 1 stands for the Hammett plot of $\log(K_1K_2k_3)$ against the substituent constant 3σ when (4- R - C_6H_4) $_3P$ was used in the reaction with 4-picoline N-oxide catalyzed by the corresponding phosphine Re(V) dithiolato complex $MeReO(mtp)[(4-RC_6H_4)_3P]$. Line 2 stands for the Hammett plot of $\log(K_1K_2k_3)$ against the substituent constant 3σ when different 4-substituted phosphines were used in the reaction with 4-picoline N-oxide catalyzed by **1**. All the rate constants were determined in benzene at 25°C. Line 3 is the Hammett plot of $\log(k_4^Y/k_4^H)$ against the substituent constant 3σ when different para substituted triaryl phosphine pairs were used to react with 2-methyl-4-nitropyridine N-oxide catalyzed by $MeReO(mtp)PPh_3$ monitored by 1H or ^{31}P NMR at 25°C in C_6D_6 .

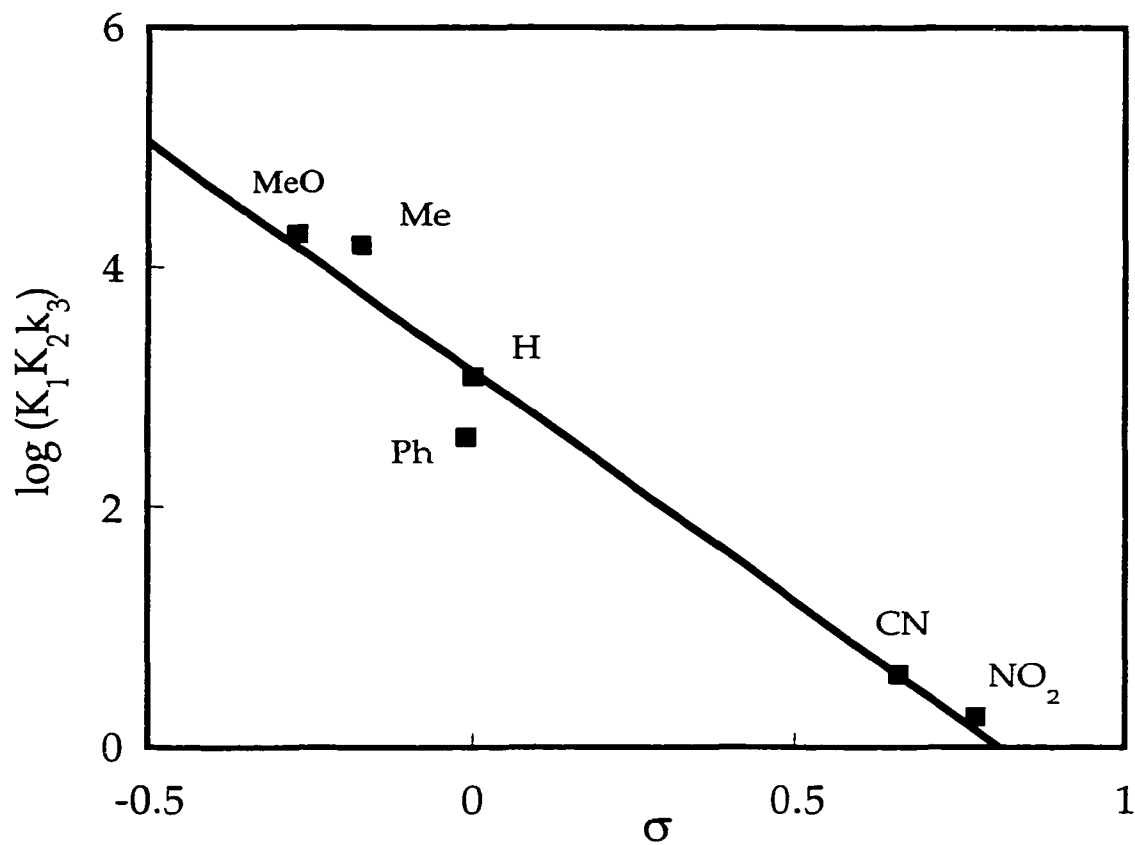
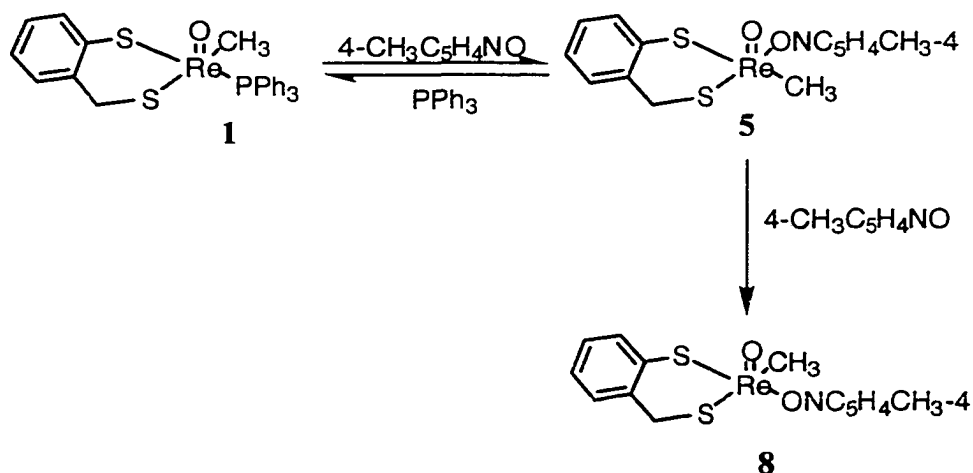
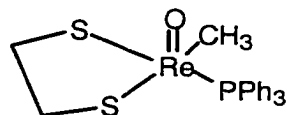


Figure 16. Hammett plot of $\log(K_1K_2K_3)$ (Table 6) against the substituent constant σ when different 4-substituted pyridine N-oxides were used in the reaction with triphenylphosphine and **1**. The slope of the reaction constant (ρ) is -3.84 .

the phenolic sulfur. This alternative mechanism can also explain the second-order dependence on pyridine N-oxides (Scheme 2). Can this “normal” 4-picoline N-oxide monomeric Re(V) compound **8** be the active catalytic form instead of Re(VII) compound **7**? To test this hypothesis, MeReO(SCH₂CH₂S)(PPh₃), abbreviated as MeReO(edt)PPh₃ **9** was used as the catalyst in the kinetic study. Because the symmetry of the edt ligand, the similar isomers doesn't exist. If the reaction goes through the above route, one would expect to see first-order dependence on 4-picoline N-oxide instead of second-order dependence since compound **5** and **8** will become identical with edt as the dithiolate ligand instead of mtp. To the contrary, kinetic study showed the same rate law with second-order dependence on 4-picoline N-oxide at high triphenylphosphine concentration giving a $K_1K_2k_3$ value of $(1.3 \pm 0.2) \times 10^4 \text{ M}^{-1} \text{ s}^{-1}$. This result rules out the formation of the compound **8** as the active catalytic form.

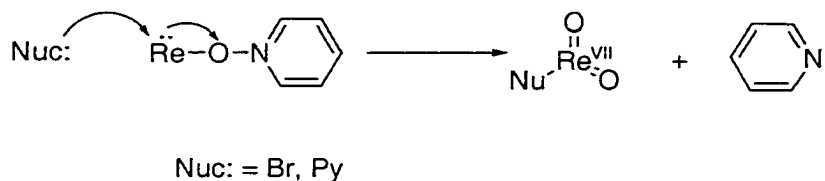
Scheme 4



MeReO(edt)PPh₃

9

Other catalytic systems. Bromide and pyridine accelerate the oxygen atom transfer reactions between picoline N-oxide and triphenylphosphine catalyzed by **1** as seen from Figure 13. It might be that the pyridine and bromide provide the nucleophilic assistance thus accelerating the rate to form the Re(VII) dioxo intermediate. Scheme 5 shows a simplified scheme for such assistance, in that bromide and pyridine will assist the electron donation from the rhenium to the oxygen atom and cleaving the N–O bond.

Scheme 5

The dramatic catalytic effect of the {MeReO(mtp)}₂ **3** is worth noting. Although compound **3** can be monomerized to compound **1** by phosphines, that occurs more slowly. So the active catalytic species should be different from compound **1** catalysis. The active catalytic intermediate might be a half-opened Re(V)-Re(VII) intermediate, which is more

effective than 7. Detailed kinetic studies are needed in order to fully understand this catalytic system.

References

- (1) Holm, R. H. *Chem. Rev.* **1987**, *87*, 1401.
- (2) Holm, R. H.; Berg, J. M. *Acc. Chem. Res.* **1986**, *19*, 363.
- (3) Lippard, S. J.; Berg, J. M. *Principles of Bioinorganic Chemistry*; University Science Books: Mill Valley, CA, 1994; Chapter 11, p 283.
- (4) Li, H.; Palanca, P.; Sanz, V.; Lahoz, L. *Inorg. Chim. Acta.* **1999**, *285*, 25.
- (5) Hille, R. *Chem. Rev.* **1996**, *96*, 2757.
- (6) Caradonna, J. P.; Reday, P. R.; Holm, R. H. *J. Am. Chem. Soc.* **1988**, *110*, 2139.
- (7) Baird, D. M.; Barron, L. S.; Rodrigues, S. A. *Inorg. Chim. Acta.* **1995**, *237*, 117.
- (8) Jacob, J.; Guzei, I. A.; Espenson, J. H. *Inorg. Chem.* **1999**, *38*, 1040.
- (9) Jacob, J.; Lente, G.; Guzei, I. A.; Espenson, J. H. *Inorg. Chem.* **1999**, *38*, 3762.
- (10) Lente, G.; Jacob, J.; Guzei, I. A.; Espenson, J. H. *Inorg. React. Mech.* **2000**, *2*, 169.
- (11) Wang, Y.; Espenson, J. H. *Org. Lett.* **2000**, *2*, 3525.
- (12) Huang, R.; Espenson, J. H. *Inorg. Chem.* **2001**, *40*, 994.
- (13) Ochiai, E. *J. Org. Chem.* **1953**, *18*, 354.
- (14) Rosenau, T.; Potthast, A.; Ebner, G.; Kosma, P. *Synlett* **1999**, *6*, 623.
- (15) Trost, B. M.; Fleming, L. *Comprehensive Organic Synthesis*; Pergamon Press: Oxford, 1991; Vol. 8, p390.

- (16) Ochiai, E. *Aromatic Amine Oxides*; Elsevier Publishing Co.: Amsterdam, 1967; Chapter 5, p184.
- (17) Lu, X.; Sun, J.; Tao, X. *Synthesis* **1982**, 185.
- (18) Hermann, W. A.; Kratzer, R. M.; Fischer, R. W. *Angew. Chem. Int. Ed. Engl.* **1997**, *36*, 2652.
- (19) Jacob, J.; Espenson, J. H. *Chem. Commun.* **1999**, 1003.
- (20) Lahti, W. D.; Espenson, J. H. *J. Am. Chem. Soc.* **2001**, *123*, 6014.
- (21) Lente, G.; Shan, X.; Espenson, J. H. *Inorg. Chem.* **2000**, *39*, 480.
- (22) Lente, G.; Espenson, J. H. *Inorg. Chem.* **2000**, *39*, 1311.
- (23) Espenson, J. H. *Chemical Kinetics and Reaction Mechanisms, 2nd ed.*; McGraw-Hill: New York, 1995.

CHAPTER II. EFFICIENT CATALYTIC CONVERSION OF PYRIDINE N-OXIDES TO PYRIDINES WITH AN OXORHENIUM(V) CATALYST

A paper published in *Organic Letters*

Ying Wang and James H. Espenson*

Abstract

The compound $\text{CH}_3\text{Re}(\text{O})(\text{SR})_2\text{PPh}_3$, where $(\text{SR})_2$ represents the dianion of 2-(mercaptomethyl)thiophenol, catalyzes the rapid and efficient transfer of an oxygen atom from a wide range of ring-substituted pyridine N-oxides to triphenylphosphine, yielding the pyridines in high yields.

Introduction

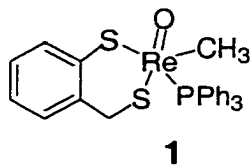
The selective deoxygenation of heteroaromatic-N-oxides has received previous attention, being an important step in the synthesis of heterocycles in many procedures.^{1,2} Various methods have been developed,³⁻⁶ but many are limited by side reactions or reduction of the ring substituents and may require tedious procedures.^{3-5,7,8}

Results and Discussion

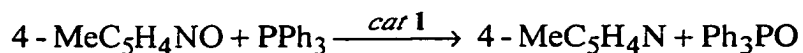
We have found that the rhenium compound 1 catalyzes the transfer of oxygen from numerous pyridine N-oxides to triphenylphosphine. The synthesis of 1 has been reported before;^{9,10} only a small quantity is needed. One group of reactions was carried out in benzene-d₆, where the reactions occur rapidly. Typical conditions are these: 14 mM

Wang, Y.; Espenson, J. H. *Org. Lett.* **2000**, *2*, 3525

4-picoline N-oxide and 14 mM PPh₃, with 42 μM **1** (0.3% mol/mol) in 0.7 mL C₆D₆ in air. The reaction reached completion (100% conversion) within one min. The other compounds in Table 1 also gave quantitative conversions with 0.1–5% **1**, within a few minutes (entries 1-6) or hours (entries 7-15), when studied on this scale. The system is tolerant of nitro and halide substituents, which can cause problems in earlier procedures.^{3,11-13} Even sterically-hindered compounds like 2-picoline N-oxide and 2,6-lutidine N-oxide gave 100% conversion, the latter more slowly; on a larger (1 g) scale, however, 2-picoline was formed in but 67% yield. Other amine oxides undergo this conversion: both 6-methoxyquinoline N-oxide and trimethyl amine N-oxide also gave high yields of product.



As a control, the reagents were mixed without **1**; no reaction was found for >10 h. Molecular oxygen is not involved in the catalysis or stoichiometry, in that the same reaction performed under argon gave virtually the same result. The overall stoichiometry is simply



Benzene was usually used as solvent and in limited tests toluene did as well. THF can be used, but it must be freshly distilled and the reaction run under argon, as a trace of

peroxide destroys the catalyst. Acetone gave adequate results, but the reactions proceeded more slowly and in reduced yield. In chloroform and acetonitrile the reaction stopped at an early stage.

To show the generality of this catalytic system and extend its applicability to reactions carried out on a larger scale, many pyridine oxides were studied on a scale of 1.0 g substrate and 1.0 equiv. phosphine in 60 mL solvent. Since several of the pyridine N-oxides are nearly insoluble in benzene, in some cases 5 mL water and 55 mL benzene were used as a two-phase medium. In such cases 5% of (n-Bu)₄NBr was added to be a phase transfer catalyst. **Table 1** presents 15 examples on this larger scale. Most of the reactions run in ambient-temperature benzene (or benzene-water mixtures) proceeded nearly quantitatively with 0.1–0.5% **1**. At this scale, reaction times were 0.3–7 h, dividing into two groups as with smaller-scale reactions.

As it turns out, (n-Bu)₄NBr may be more than a phase-transfer catalyst. Both it and pyridine are pronounced accelerators (co-catalysts) as shown in **Figure 1**. Their role is likely to be one of promoting ligand substitution reactions of **1**.^{14,15} The mechanism of this interesting transformation remains under investigation, but entry of PyO into the coordination sphere of rhenium will certainly play a role; release of pyridine *may* occur by a process we abbreviate like this: $L_n\text{Re}-\text{OPy} \rightarrow L_n\text{Re}=\text{O} + \text{Py}$.

Table 1. Oxygen transfer from pyridine N-oxides to triphenylphosphine, catalyzed by **1**

Entry	RC ₅ H ₄ NO R =	Scale ^a	Solvent ^b	1	Time/h	Py Yield, % ^c
1	4-Me	1.0 g	AB	0.1%	0.7	100
2	4-Cl	1.0 g	B	0.1%	3	94
3	4-MeO	1.0 g	AB	0.5%	3	93
4	2-Me	1.0 g	AB	0.1%	0.3	67 ^d
5	4-Ph	1.0 g	B	0.1%	0.3	100
6	4-(CH ₂) ₃ Ph	1.0 g	B	0.1%	0.3	100
7	4-NO ₂	1.0 g	B	0.5%	6	100
8	4-CN	1.0 g	AB	0.5%	6	92
9	2,6-Me ₂	1.0 g	B	0.5%	7	100
10	2-Me, 4-NO ₂	1.0 g	B	0.5%	5	100
11	2-OH	1.0 g	AB	0.5%	3	50
12	3-CH ₂ OH	1.0 g	B	0.1%	1	90

Table 1 continued

Entry	RC ₅ H ₄ NO R =	Scale ^a	Solvent ^b	1	Time/h	Py Yield, % ^c
13	3-OH	1.0 g	B	0.5%	7	99
14	3-C(O)NH ₂	0.5 g	THF	0.5%	2	51
15	3-COOH	0.5 g	THF	0.5%	3	57

^a With 1.0 equiv. PPh₃; ^bSolvents are 60 mL benzene (B), 10% water with benzene containing 5% (n-Bu)₄NBr (AB), tetrahydrofuran under argon (THF); ^c The solution was stirred throughout and monitored intermittently by TLC and ³¹P NMR. After the reaction had finished, the water layer was separated, the organic layer was dried over anhydrous magnesium sulfate and evaporated to dryness; the residue was then taken up in C₆D₆ for determination of the Py yield; ^dOn a smaller scale, 100% conversion of 2-picoline N-oxide was obtained.

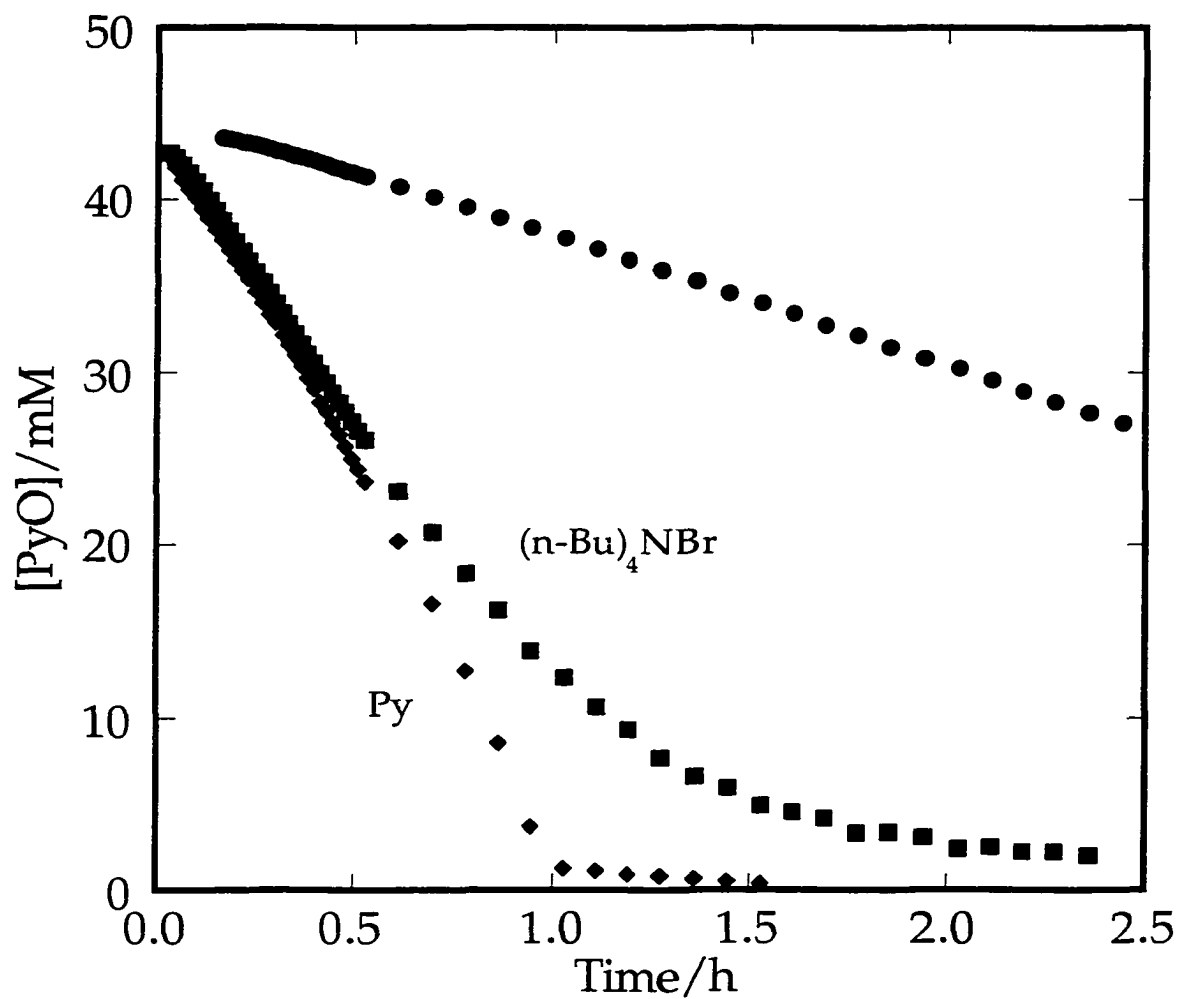


Figure 1. An experiment in benzene with 44.4 mM each of 2-methyl-4-nitropyridine N-oxide and Ph_3P containing 1.0 mM **1**, showing the decrease in the concentration of the pyridine oxide in the catalyzed reaction and the further rate acceleration brought about with 4.4 mM $(\text{n-Bu})_4\text{NBr}$ or 8.8 mM pyridine added.

References

- (1) Ochiai, E. *J. Org. Chem.* **1953**, *18*, 354.
- (2) Rosenau, T.; Potthast, A.; Ebner, G.; Kosma, P. *Synlett* **1999**, *6*, 623.
- (3) Trost, B. M.; Fleming, L. *Comprehensive Organic Synthesis*; Pergamon Press: Oxford, 1991; Vol. 8, 390
- (4) Konwar, D.; Boruah, R. C.; Sandhu, J. S. *Synthesis* **1990**, 337-339.
- (5) Sim, T. B.; Ahn, J. H.; Yoon, N. M. *Synthesis* **1996**, 324-326.
- (6) Nakagawa, H.; Higuchi, T.; Kikuchi, K.; Urano, Y.; Nagano, T. *Chem. Pharm. Bull* **1998**, *46*, 1656-1657.
- (7) Ochiai, E. *Aromatic Amine Oxides*; Elsevier Publishing Co: Amsterdam, 1967, Chapter 5, p 184
- (8) Katritzky, A. R.; Lagowski, J. M. *Chemistry of the Heterocyclic N-Oxides (Organic Chemistry, a Series of Monographs)*; Academic Press: London, New York, 1971, Chapter 3, p 170
- (9) Jacob, J.; Espenson, J. H. *Chem. Commun.* **1999**, 1003-1004.
- (10) Jacob, J.; Guzei, I. A.; Espenson, J. H. *Inorg. Chem.* **1999**, *38*, 1040-1041.
- (11) Balicki, R. *Synthesis* **1989**, 645-646.
- (12) Kagami, H.; Motoki, S. *J. Org. Chem.* **1978**, *43*, 1267-1268.
- (13) Jousseau, B.; Chanson, E. *Synthesis* **1987**, 55-56.
- (14) Jacob, J.; Lente, G.; Guzei, I. A.; Espenson, J. H. *Inorg. Chem.* **1999**, *38*, 3762-3763.
- (15) Lente, G.; Jacob, J.; Guzei, I.; Espenson, J. H. *Inorg. Chem.* **2000**, *39*, 1311.

**CHAPTER III. OXIDATION OF SULFIDES BY *TERT*-BUTYL
HYDROPEROXIDE CATALYZED BY AN OXORHENIUM(V)
DITHIOLATO COMPLEX—A GENERAL AND EFFICIENT
SYNTHESIS OF SULFOXIDES AND SULFONES.**

A paper being prepared for submission to the *Journal of Organic Chemistry*

Ying Wang and James H. Espenson

Abstract

A wide variety of sulfides, RSR' , where R, R' = aryl or alkyl, can be catalytically oxidized to sulfoxides in excellent yields by a stoichiometric quantity of *tert*-butyl hydroperoxide catalyzed with easily-prepared Re(V) dithiolato catalysts. Several catalysts were used, but the one most extensively studied was $\text{MeReO}(\text{mtp})\text{PPh}_3$ **1**, where mtpH_2 is 2-(mercaptomethyl)thiophenol. Both the occurrence of the catalysis and studies of the mechanism are presented here. For all examples of RSR' , the reaction went rapidly (hours) and selectively with 0.05–3 mol% catalyst. Included in the list of sulfide reagents are heavily substituted thiophenes, which can also be converted to their S-oxides in moderate to excellent yields. The reaction scheme features ligand exchange between **1** and *tert*-butyl hydroperoxide. The induction period for sulfoxide built-up observed at the beginning of the reaction can be attributed to the ligand exchange step. The hydroperoxo dithiolato rhenium complex thus formed gives $\text{MeRe}(\text{O})_2(\text{mtp})$, a Re(VII) dioxo species, which was detected at 240 K by its $^1\text{H-NMR}$ spectrum. Inhibition by the sulfide reagents was observed, which can be attributed to the reversible formation of inactive $\text{MeReO}(\text{mtp})(\text{SRR}')$. Kinetic

modeling of a proposed reaction scheme was used to validate the general scheme although detailed rate constant specifics could not be resolved. In the presence of an three equiv. of *tert*-butyl hydroperoxide and 0.3-0.5% **1** at 50 °C, sulfones were obtained quantitatively.

Introduction

Catalytic oxidations and reductions of sulfoxides are particularly interesting from biological, mechanistic and synthetic perspectives.¹ Molybdenum-containing DMSO reductases are known to utilize DMSO and other sulfoxides as oxidizing substrates and have been the subject of intensive study.²⁻⁴ The reverse reaction, the catalytic oxidation of sulfides, is equally important. Oxidation of sulfides is the most widely used method for synthesizing sulfoxides and sulfones, both of which are important intermediates in organic synthesis.^{1,5} A number of successful methods have been developed for such conversions employing various oxidants and catalysts.⁶⁻⁹ In many cases, over-oxidation of sulfoxides to sulfones is unavoidable.^{6,10} In the presence of other functional groups, side oxidation reactions may occur.^{6,7} Therefore, there is still a considerable interest in the development of general and selective methods for such transformations.

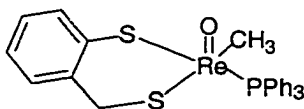
Aside from these fundamentals, one practical matter should be cited. Hydrodesulfurization is the major method for removing the sulfur compounds from fuels.^{11,12} Recently, even lower levels of permitted sulfur in diesel fuels have been legislated.¹³ However, thiophenes, especially heavily substituted ones, are not treated by the existing methods, presenting a challenge.¹⁴ Oxidation of petroleum oil, which has a long history of development, is one of the alternative methods for removal of the thiophenes

from other petroleum components.^{13 15,16} Thus further efforts are needed to devise better methods that forms environmentally benign by-products with good selectivity.

Methyltrioxorhenium, CH_3ReO_3 , abbreviated as MTO, is a good catalyst for the oxidation of organic sulfides and thiophenes by hydrogen peroxide.^{17,18} The active catalytic forms are the peroxy species formed from the reaction between MTO and hydrogen peroxide. The catalytic cycle is formed between MTO, an oxo rhenium(VII) compound and the corresponding peroxy rhenium(VII) species. Rhenium remained in oxidation state VII. Recently, a series of Re(V) complexes were synthesized in our group and we reported that, among them, compound **1**, $\text{MeReO}(o\text{-SC}_6\text{H}_4\text{CH}_2\text{S})(\text{PPh}_3)$, also written as $\text{MeRe}(\text{O})(\text{mtp})\text{PPh}_3$, where mtpH_2 is 2-(mercaptomethyl)thiophenol, is a very efficient catalyst for deoxygenation of pyridine N-oxides by triphenylphosphine.¹⁹ In that case, the catalytic cycle is formed between original Re(V) catalyst and a dioxo Re(VII) intermediate, $\text{MeRe}(\text{O})_2(\text{mtp})(4\text{-CH}_3\text{C}_5\text{H}_4\text{NO})$, which in turn oxidizes PPh_3 to Ph_3PO .

In the course of learning the scope and versatility of this catalytic system, sulfoxidation reactions came into our attention. Recently, the $\text{Re}(\text{VII})=\text{O}$ bond in oxorhenium(VII) oxazoline complexes has been estimated to be ~ 20 kcal/mol²⁰ In light of the SO bond strength of $\text{RS}(\text{O})\text{R}'$ which lies generally in the range of 87-90 kcal/mol, sulfides are good candidates to serve as the oxygen atom acceptor for $\text{Re}(\text{VII})=\text{O}$. Indeed, compound **1**, and related compounds, catalyzes the oxidation of sulfides cleanly to sulfoxides by *tert*-butyl hydroperoxide. With appropriate adjustment, clean oxidation to sulfones can be realized instead. Thus, separate procedures for synthesizing sulfoxides and sulfones have been developed. In the course of this research, concurrently, mechanistic

studies were also carried out to help us understand this catalytic cycle and in turn to optimize catalysis and, especially, selectivity.



MeReO(mtp)PPh₃

1

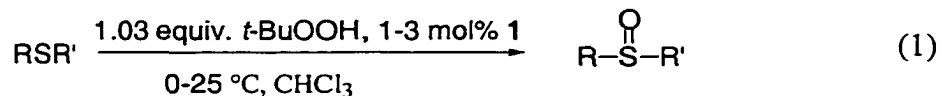
Results and Discussion

Preliminary Considerations. Sulfoxides, and under certain distinct conditions, sulfones, were formed by adding catalyst **1** slowly to a solution containing *t*-BuOOH and sulfide through a syringe pump in usually 1-3 hours. The syringe pump was used to ensure the survival of the catalyst for the maximum catalytic efficiency. This method gave very good product yields. Later it was found that directly introducing all of the catalyst at the beginning of the reaction also gave similarly good product yields as compared to the syringe pump method in the same reaction time.

Without **1**, control reactions showed that < 5% reaction occurred between *tert*-butyl hydroperoxide and sulfides under the conditions used. Chloroform proved to be a better solvent than benzene with which only inferior conversions to sulfoxides were obtained. MTO, one of the decomposition products of the compound **1** by *tert*-butyl hydroperoxide, does not catalyze this reaction.

Synthesis of Sulfoxides at Room Temperature. Sulfoxides can be easily synthesized by syringe pump addition of 1-3 mol % of catalyst **1** over ca. 1-3 h into a

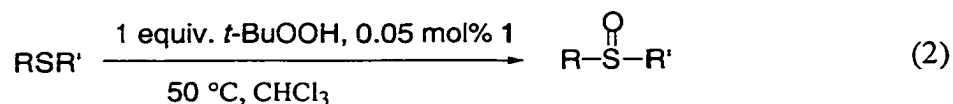
solution containing 2 mmol of the sulfide and 2.05 mmol of *tert*-butyl hydroperoxide at room temperature (eq 1).



As one can see from Table 1, the method is quite general and efficient. It gives excellent yields of sulfoxides from dialkyl, diaryl, alkylaryl and cyclic sulfides. The reaction also tolerates the functional groups, such as NO₂, CN, Br and C=O. In the case of vinyl phenyl sulfide, the only oxidation product is vinyl phenyl sulfoxide. Note that the double bond is untouched whereas it is epoxidized by many of the literature methods.⁶ In the workup, the other product, *tert*-butyl alcohol, evaporates with the solvent, leaving the crude product. The ¹H-NMR spectrum showed only the sulfoxide and small amount of unreacted sulfide (<5%). This makes this synthetic procedure particularly attractive in terms of easy work-up and separation. Moreover, aqueous workups, which are often required when peroxyacids are used as the oxidants, are avoided. This is particularly useful for obtaining the water-soluble sulfoxides.

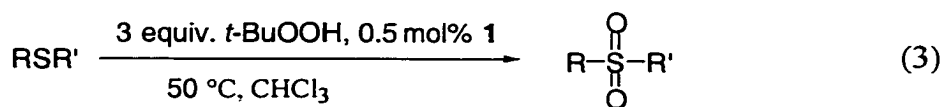
No sulfones were formed at room temperature under the conditions specified in eq 1 and used to obtain the data presented in Table 1. Over-oxidation of sulfoxides to sulfones is a common problem for many of the literature methods especially with diaryl sulfoxides.⁹ Diphenyl sulfide gave no diphenyl sulfone (Table 1, entry 6).

Synthesis of Sulfoxides at 50°C. At 50 °C, one could further lower the concentration of catalyst **1** without sacrificing the excellent yields of sulfoxides (eq 2). Under this condition, it is essential to use only one equiv. *tert*-butyl sulfoxide lest sulfones be formed with excess *tert*-butyl hydroperoxide at 50°C as discussed in the next section. In one experiment, 0.05 mol % of the catalyst was added through a syringe pump to a solution containing 1.0 mmol 4-nitrophenyl methyl sulfide and 1.0 mmol *tert*-butyl hydroperoxide in one hour at 50 °C. From that, 4-nitrophenyl methyl sulfoxide was isolated in 95% yield. A control reaction without catalyst **1** showed that only 2% of 4-nitrophenyl methyl sulfoxide was formed during the same reaction time.



Synthesis of Sulfones. At 50 °C, when 2 equiv. of *t*-BuOOH was used, sulfides were further oxidized to sulfones in 2 h giving excellent yields with only 0.3-0.5 mol% of catalyst **1**. As can be seen from Table 2, it is also a general and efficient method for synthesizing various sulfones. Note again that the double bond in phenyl vinyl sulfide remained unchanged even at 50 °C. When two equiv. of *tert*-butyl hydroperoxide was used, sulfones were formed in yields ranging from 70-85%. Almost quantitative yields were achieved by using three equiv. of *tert*-butyl hydroperoxide (eq. 3). Under these conditions, sulfides have usually disappeared in 15-30 min. Good yields of sulfones were also obtained

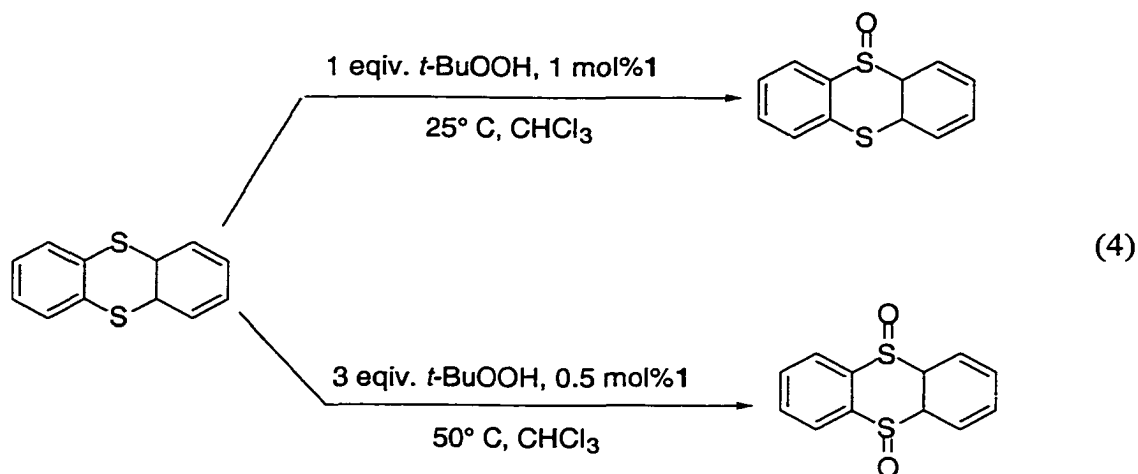
when the catalyst concentration was lowered by a factor of ten, 0.05 mol% (Table 2, entry 1).



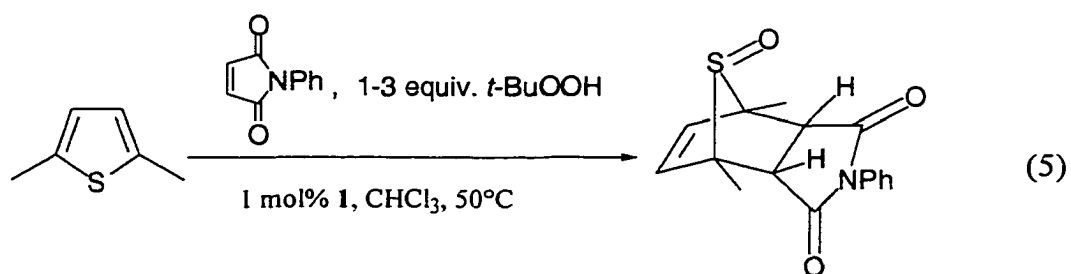
Oxidation of Thianthrene. In principle, several products can be formed from oxidation of thianthrene due to the two “S” sites; the products may be thianthrene 5-oxide (SSO), thianthrene 5,5-dioxide (SSO₂), thianthrene 5,10-dioxide (SOSO), thianthrene 5,5,10-trioxide (SOSO₂) and thianthrene 5,5,10,10-tetraoxide (SO₂SO₂).²¹⁻²³ When the standard procedures for sulfoxide and sulfone synthesis were applied to thianthrene, only thianthrene 5-oxide and thianthrene 5,10-dioxide were obtained, each in excellent yield. No other oxidation products were detected (eq 4).

Oxidation of Thiophenes. Heavily substituted thiophenes were oxidized to thiophene monoxide or dioxide with good yields using this catalytic system. From Table 1, entries 13 and 15 and Table 2, entry 5, one can see that even very bulky thiophenes can be oxidized satisfactorily. This procedure is of interest in the context of the fuel desulfurization procedures other than HDS considering the simplicity of the procedure, the easy separation method, and the efficiency of the catalyst.

The reaction of 4,6-dimethylthiophene with one to three equiv. of *tert*-butyl hydroperoxide in the presence of 1 mol% catalyst at both room temperature and at 50 °C gave < 20% 4,6-dimethyl thiophene 1,1-dioxide; unreacted thiophene and unidentified

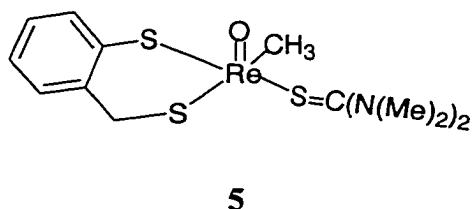
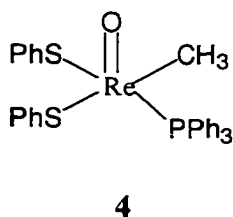
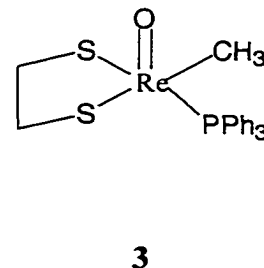
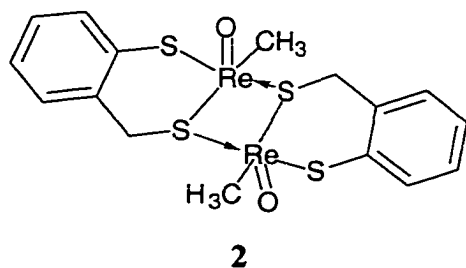


products remained. Addition of more catalyst did not improve the yield. 4,6-Dimethyl thiophene monoxide was not observed under the conditions used here. It is known that thiophene oxides lacking heavily substituted rings are highly reactive species. They can undergo rapid cyclization reactions in the solution.²⁴ Similar observations were also found in other oxidative systems.^{25,26} The thiophene monoxides can be captured by adding dienophiles to the reaction system.²⁷⁻²⁹ Thus, the Diels-Alder adduct between the 2,6-dimethylthiophene monoxide, which acts as a diene and the dienophile, N-phenylphthalimide, was formed and isolated in 78% as described in eq 5.



Other Re(V) Dithiolato Catalysts. A variety of Re(V) compounds **2-5** (Chart 1) were able to catalyze the sulfoxidation reaction with *tert*-butyl hydroperoxide.

Chart 1



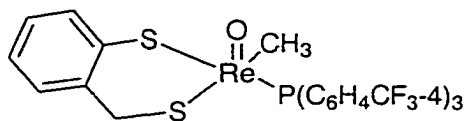
With methyl 4-nitrophenyl sulfide (2 mmol) was used as the substrate, good yields of methyl 4-nitrophenyl sulfoxide were obtained using 1 mol% of **2-5** as catalysts with *t*-BuOOH (2.05 mmol). The reaction becomes much faster when compound **2** was used. Compounds **3** and **5** showed a catalytic effect similar compared to that of **1** giving almost quantitative yields of sulfoxides. With compound **4**, inferior yields of sulfoxides were obtained (Table 3).

Table 1. Oxidation of MTS (2 mmol) by *t*-BuOOH (2.05 mmol) by different Re(V) catalysts at 25°C in CHCl₃. The yields were determined by ¹H NMR spectrums after evaporation.

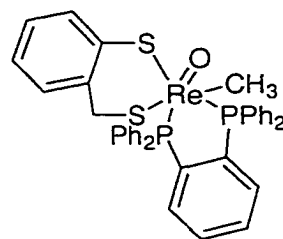
Catalyst (1 mol%)	Time (h)	4-NO ₂ C ₆ H ₄ S(O)CH ₃ Yield (%)
1	1	99
2	2.5	95
3	2.5	95
4	4	75
5	2.5	97

Mechanistic Study. The reaction progress was monitored by following the growth of sulfoxide as a function of time by ¹H-NMR spectroscopy. The oxidation of MTS by *t*-BuOOH with **1** was used as the model reaction. The concentrations of MTS, *t*-BuOOH and **1** were varied to see the effect of the reagents on the reaction rate (Figures 1-3). Oxidations of MTS by *t*-BuOOH catalyzed by **2**, **3**, **6** and **7** occurred at different rates (Figure 4). In the four compounds, the reaction rates are different as seen from Figure 4 with a order of **2** > **6** > **3** > **1**, whereas compound **7** showed no catalytic effect at all. The shapes of the curves are all similar, suggesting that the catalytic systems go through similar steps.

Chart 2



6



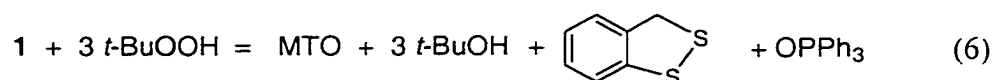
7

The reaction rate increased with increasing concentration of *t*-BuOOH and **1**, from Figures 1 and 2. However, increasing the concentration of MTS slowed the reaction dramatically, Figure 3. An induction period is common to all the curves, the length of which varied with the substrate concentration. Increases in the concentration of the catalyst and *tert*-butyl hydroperoxide have a similar effect—they shorten the induction period and accelerate the rate (Figures 1 and 2). On the contrary, increasing the concentration of MTP and other sulfides caused a longer induction period as well as a longer reaction time. However, ¹H NMR data showed that the reaction still went to completion given enough time.

It is known PPh₃ can be oxidized by *t*-BuOOH catalyzed by **1** faster than the sulfides at the same concentration (Here, however, [MTS] >> [PPh₃]). Compound **1** has a triphenylphosphine ligand attached to it. To probe the role of the PPh₃, yet avoid a change the identity of the main reaction for sulfide oxidation to phosphine oxidation, the oxidation of MTS was also monitored in the presence of a small amount of PPh₃. When 1.0 mM of free phosphine was added to a solution containing 33.9 mM MTS and 83 mM *t*-BuOOH in

the presence of **1**, the induction period became longer and so did the reaction time, Figure 5. The reaction was monitored to 80% conversion of MTS to MTSO. At a longer time, the ^1H NMR spectrum showed 100% conversion.

Detection of the Re(VII) Intermediate in the Absence of RSR'. The direct reaction between *tert*-butyl hydroperoxide and **1** was monitored by ^1H -NMR both at room temperature and 240-260 K. The final decomposition products of **1** are MTO, phosphine oxide and the disulfide oxidation product mtp; they were formed without any intermediate being detected (eq 6).



The dimeric compound **2** also can catalyze the sulfoxidation reaction, as seen from Figure 4. When 8.0 mM *tert*-butyl hydroperoxide was added to a solution containing 2.0 mM **2** in CDCl_3 at 260 K, compound **2** was converted to a red compound **8** almost quantitatively in about 30 min. as detected by ^1H NMR (Figure 6). (^1H NMR of **8**: δ (ppm) 2.71 (s, 3H, Re-CH_3), 4.55 (d, 1H, $J = 8$ Hz), 5.36 (d, 1H, $J = 8$ Hz), 7.1-7.6 (m, 4H)). The structure of the red species is tentatively assigned as the structure of **8**. Because the ^1H NMR spectrum showed *t*-BuOH was also formed, it is reasonable to assume that **2** had been oxidized to Re(VII). Further evidence was obtained by adding 10 mM picoline to a solution of **8** in deuterated toluene. This gave **9**, which had been detected before (Scheme 1).³⁰

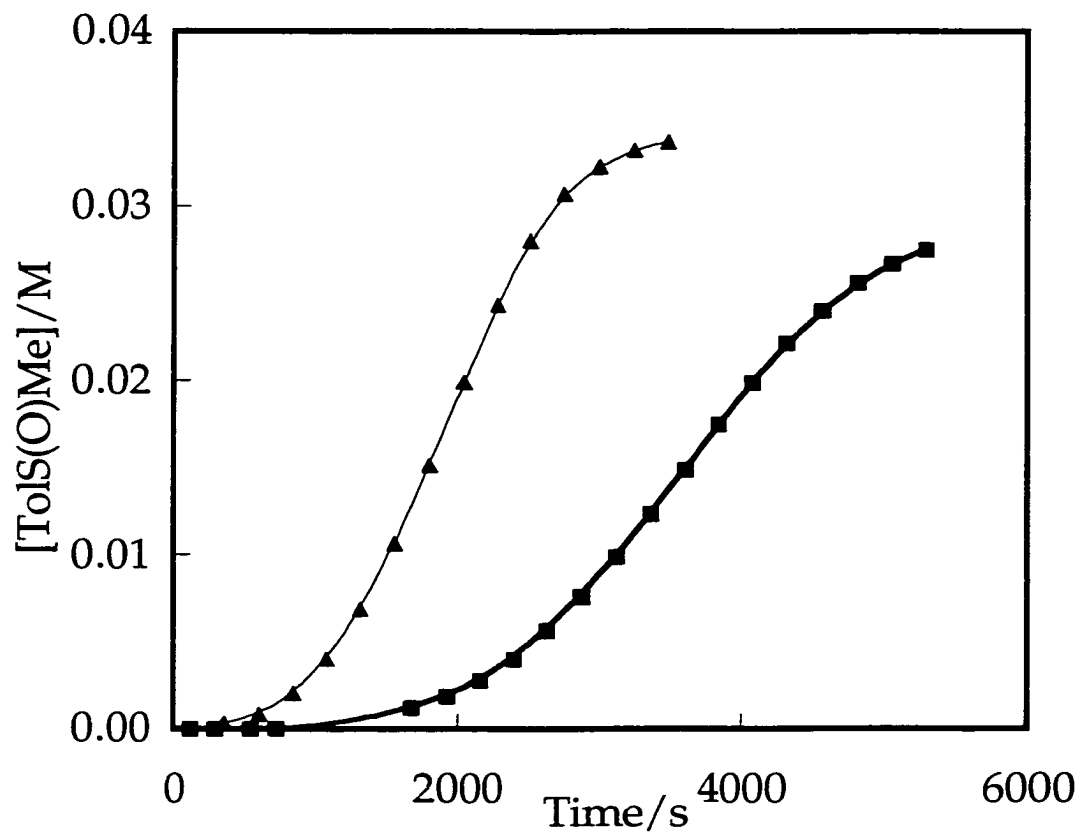


Figure 1. Plots of product buildup as a function of time show the effect of the catalyst **1** by monitoring the growth of methyl tolyl sulfide by ^1H NMR for the reaction between 0.0339 M methyl tolyl sulfide and 0.083 M *t*-BuOOH in CDCl_3 at 25°C . From top to bottom: $[\mathbf{1}] = 0.94$ mM; $[\mathbf{1}] = 0.31$ mM.

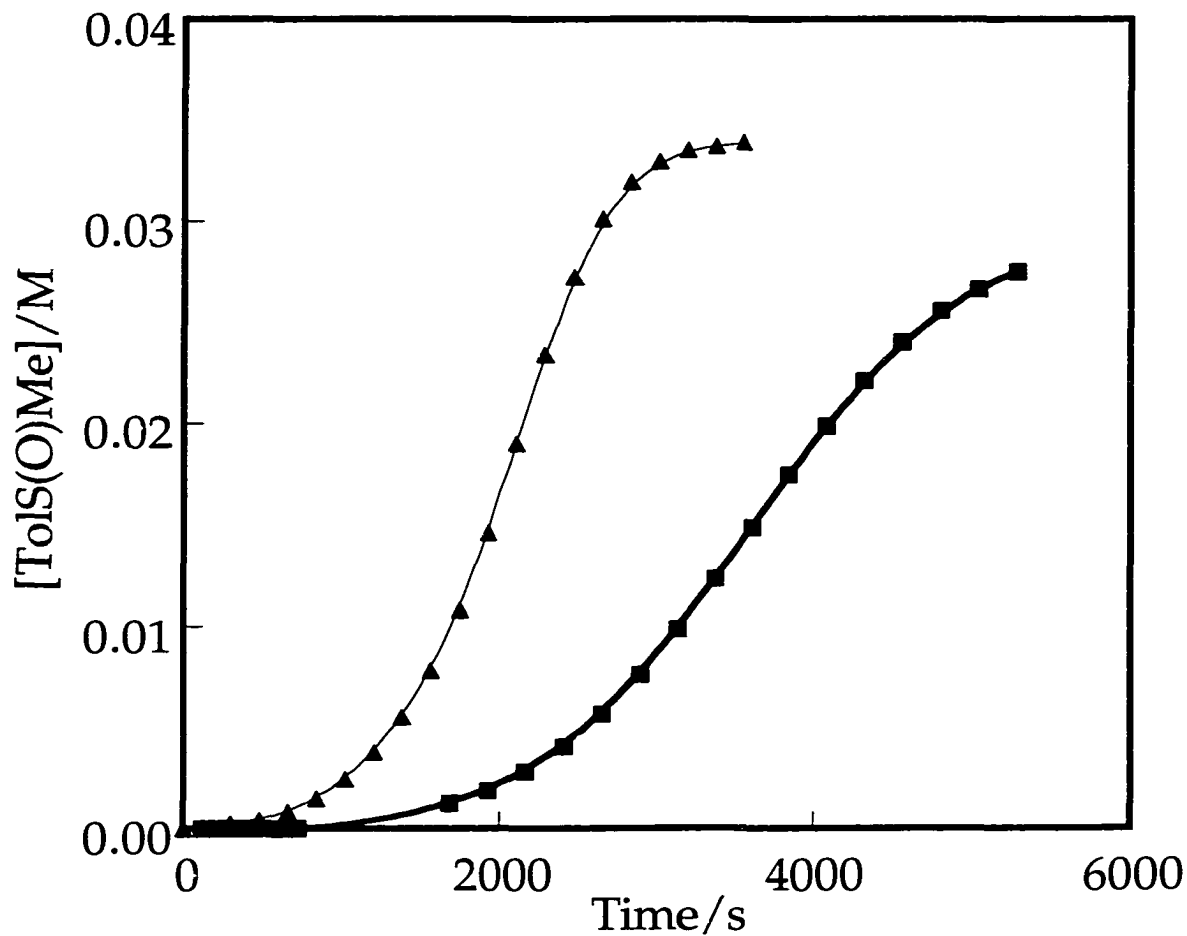


Figure 2. Plots of product buildup as a function of time show the effect of the *t*-BuOOH by monitoring the growth of methyl tolyl sulfoxide by ^1H NMR for the reaction between 0.0339 M methyl tolyl sulfide and 0.31 mM catalyst **1** in CDCl_3 at 25°C . From top to bottom: $[t\text{-BuOOH}] = 0.166\text{ M}$ and 0.083 M .

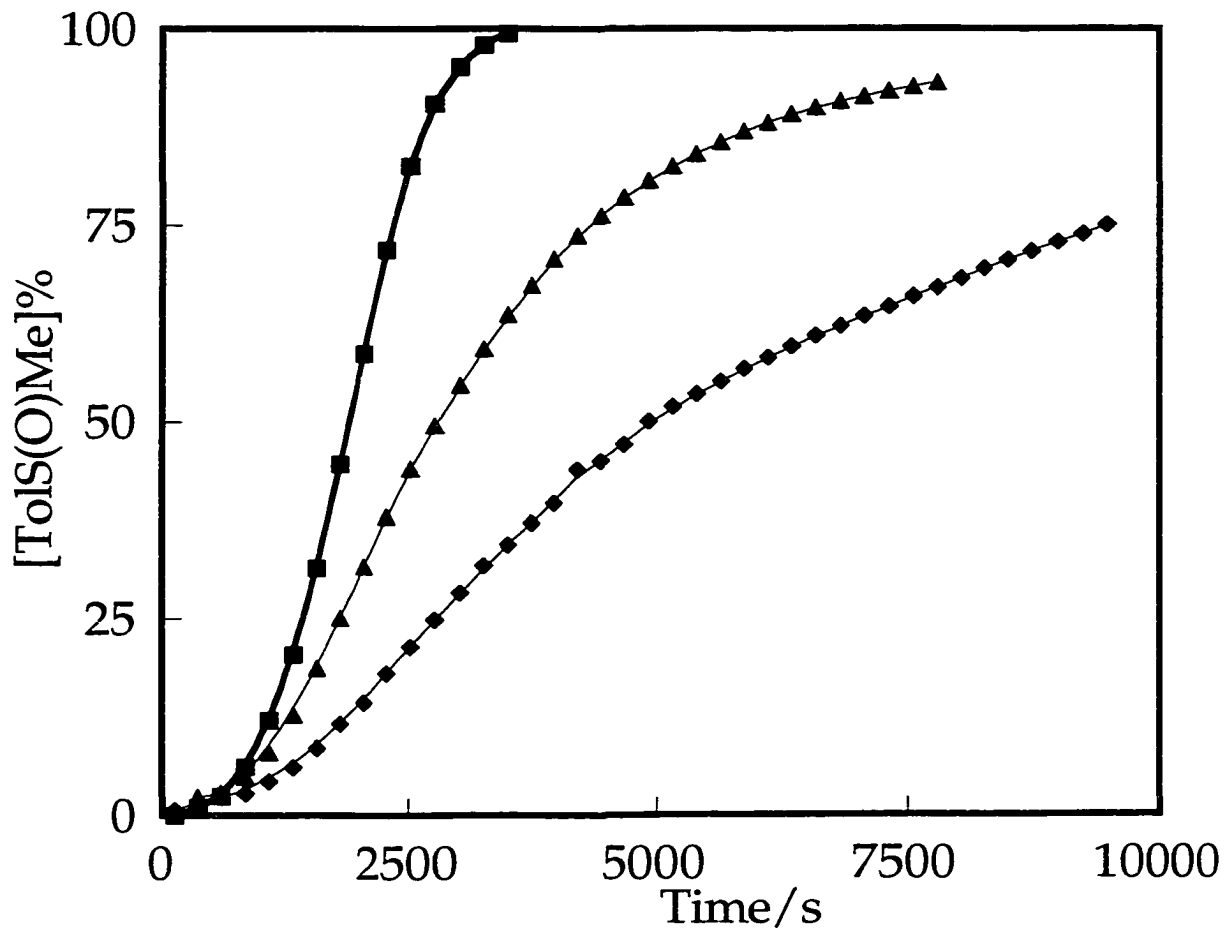


Figure 3. Plots of product buildup as a function of time show the inhibiting effect of methyl tolyl sulfide by monitoring the growth of methyl tolyl sulfoxide by $^1\text{H-NMR}$ for the reaction between 0.166 M *t*-BuOOH and 0.31 mM catalyst **1** in CDCl_3 at 25°C . From top to bottom: $[\text{TolSCH}_3] = 0.0339 \text{ M}$, 0.102 M and 0.316 M.

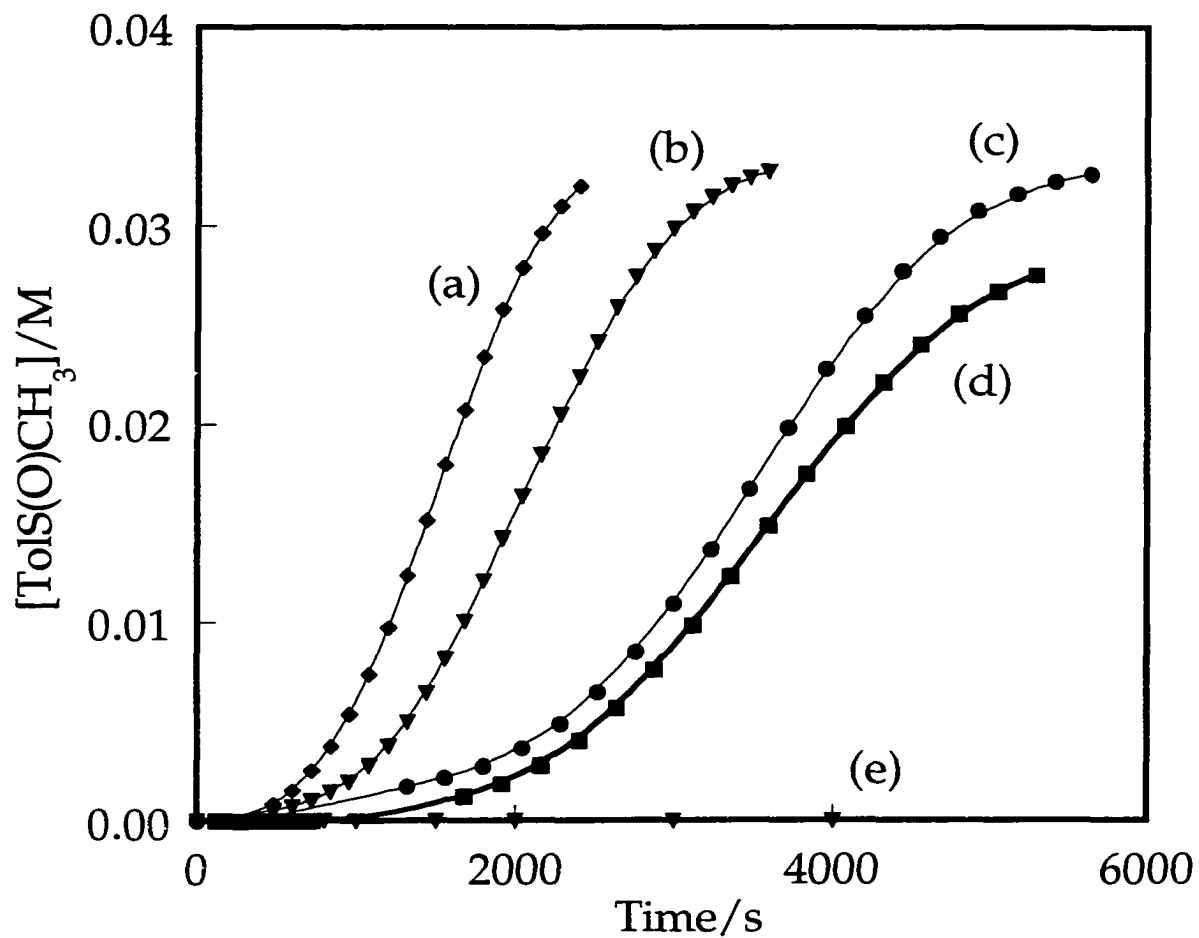


Figure 4. Plots of product buildup as a function of time show the effects of catalysts by monitoring the growth of methyl tolyl sulfoxide by $^1\text{H-NMR}$ for the reaction between 0.083 M *t*-BuOOH and 0.0339 M methyl tolyl sulfide in CDCl_3 at 25°C . (a): $[\mathbf{2}] = 0.157 \text{ mM}$; (b): $[\mathbf{6}] = 0.31 \text{ mM}$; (c) $[\mathbf{3}] = 0.31 \text{ mM}$; (d) $[\mathbf{1}] = 0.31 \text{ mM}$; (e) $[\mathbf{7}] = 0.31 \text{ mM}$.

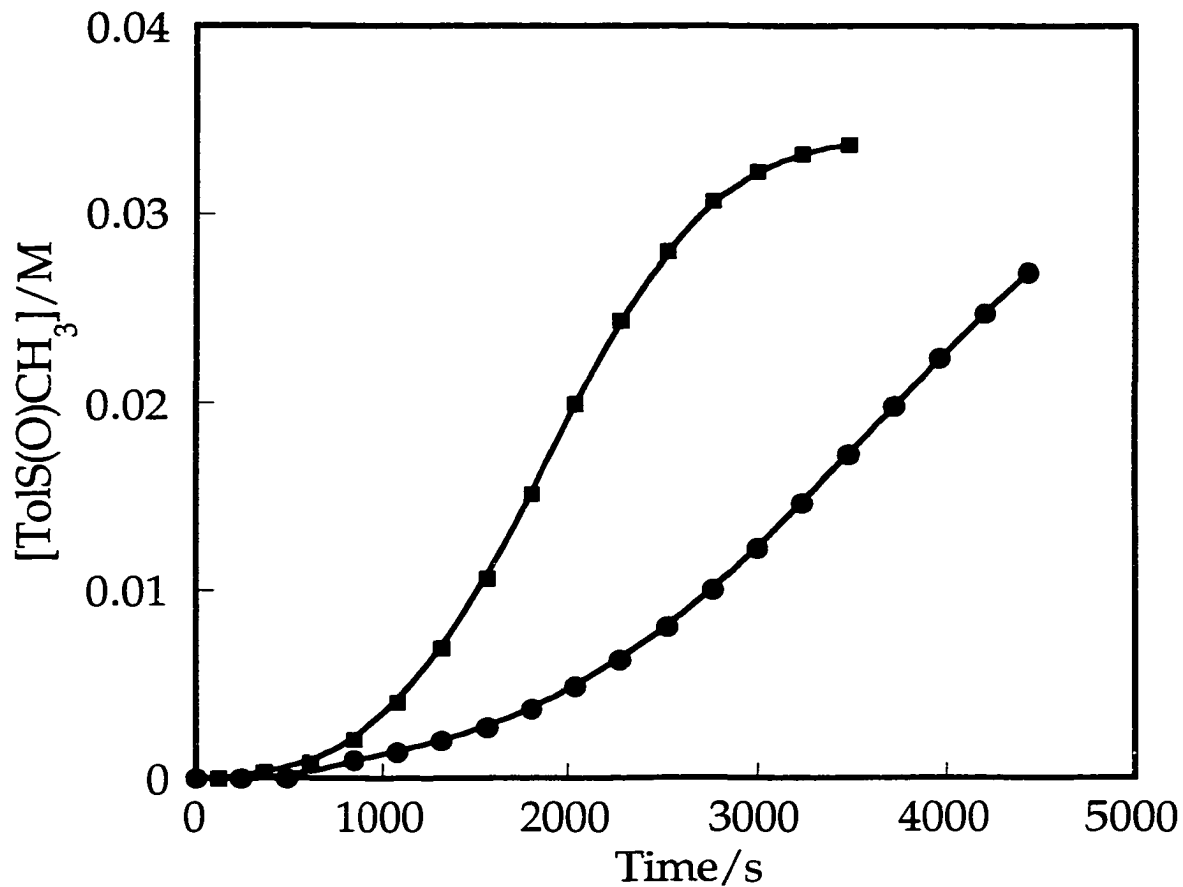
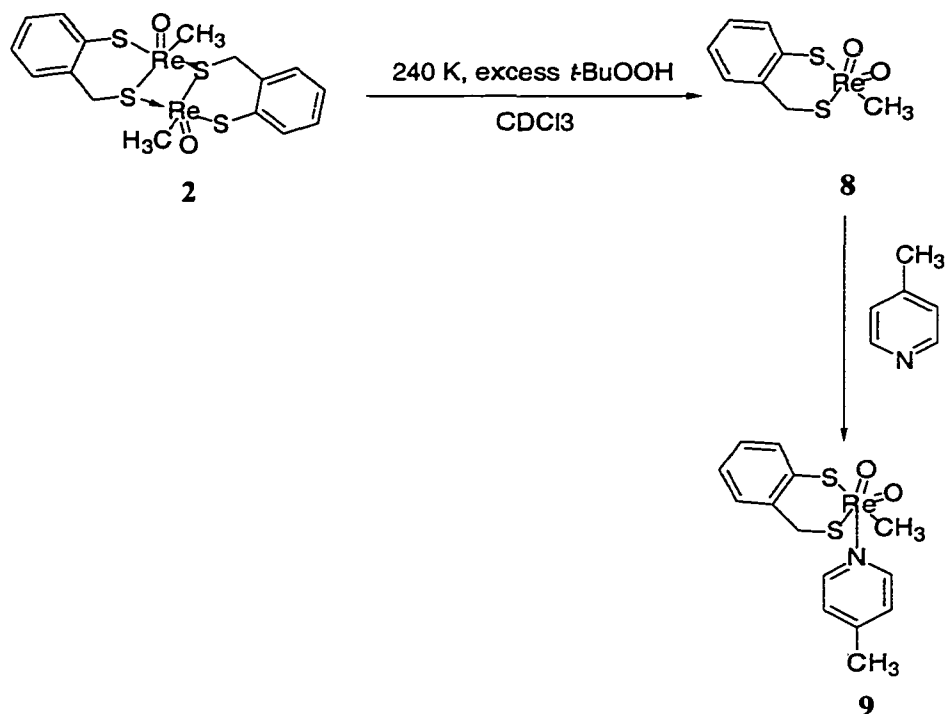


Figure 5. Plot of product buildup as a function of time show the effect of triphenylphosphine by monitoring the growth of methyl tolyl sulfoxide by $^1\text{H-NMR}$ for the reaction between 0.166 M *t*-BuOOH and 0.0339 M methyl tolyl sulfide catalyzed by 0.31 mM **1** in CDCl_3 at 25°C . From top to bottom: $[\text{PPh}_3] = 0 \text{ mM}$; $[\text{PPh}_3] = 1 \text{ mM}$.

Scheme 1



Compound **8** is stable in solution at 260 K for > 1 hour. Efforts tried to obtain it in solid form failed, however, probably due to its reactive nature. When methyl sulfide and triphenylphosphine were added to a solution of **8** at 260 K, dimethyl sulfoxide and triphenylphosphine oxide were formed immediately as monitored by the $^1\text{H-NMR}$ spectra, which suggests the Re(VII) intermediate **8** is the active catalytic intermediate.

Attempted Chiral Induction. We also used compound **10**, which has a chiral phosphine ligand, as the catalyst in the synthesis. The chiral phosphine ligand, (+)-neomenthylidiphenylphosphine, has been successfully used in asymmetric catalysis before.^{31,32} Here **10** was used in the oxidation of MTS by *t*-BuOOH in hopes that the chiral phosphine ligand would be able to introduce chirality into the oxidation product,

MTSO. Good catalytic activity (> 95% yield) was found, but chiral induction was not observed. The e.e. = 0 as determined by use of a chiral GC column.³³

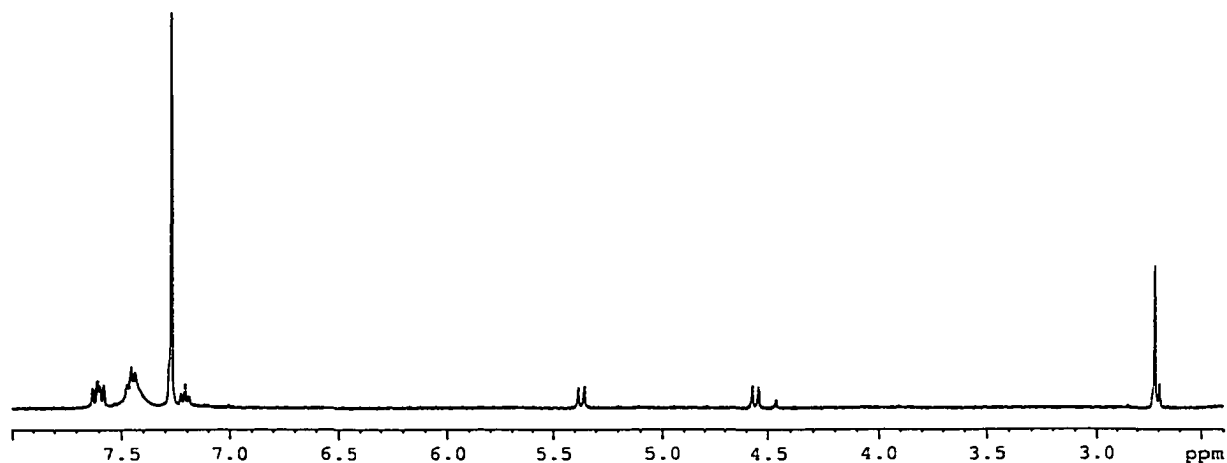
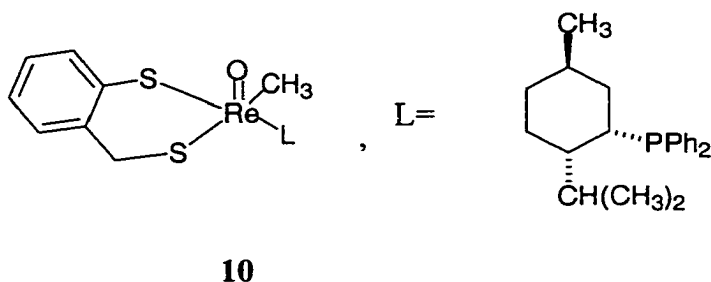


Figure 6. The ¹H NMR spectrum of a solution of **8**, MeRe(O)₂(mtp), taken 30 min after adding 8.0 mM *t*-BuOOH into a solution containing 2.0 mM **2** in CDCl₃ at 260 K. The following resonances belong to **8**: δ (ppm) 2.71 (s, 3H, Re-CH₃) 4.55 (d, 1H, J = 8 Hz), 5.36 (d, 1H, J = 8 Hz), 7.15-7.7 (m, 4H). Small peaks were detected at δ (ppm) 2.68, MTO (Re-CH₃) and at 4.46, (-CH₂-) of mtp, a disulfide, respectively. The residual ¹H NMR peak of CDCl₃ is at δ = 7.26 ppm.

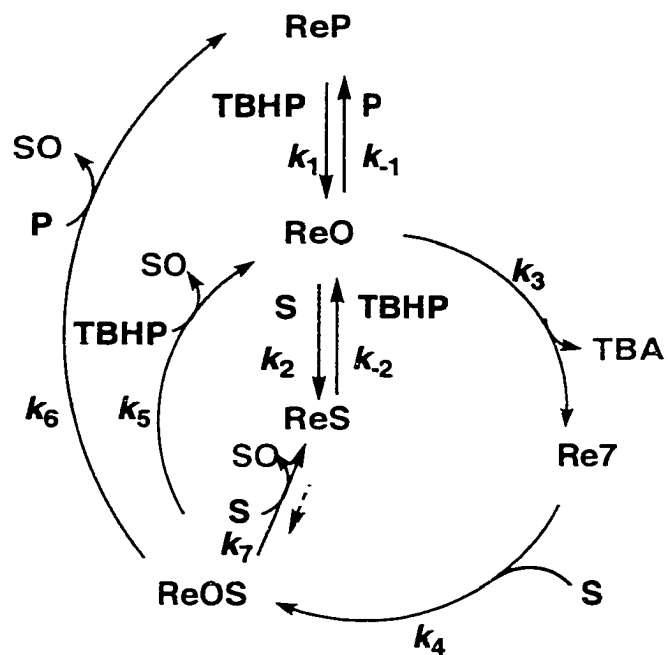
Discussion. Based on the information obtained, the mechanism shown in Scheme 2 was proposed. These are the steps:

- (a) A slow ligand exchange reaction between **1** and *t*-BuOOH reversibly forms the adduct **ReO** and eliminates PPh₃.
- (b) Intermediate **ReO**, in the k_2 pathway, equilibrates with **ReS** through ligand exchange; in the k_3 pathway, it transforms into the Re(VII) intermediate **Re7**, which has been detected and assigned the structure of **8**.
- (c) In turn, **Re7** transfers an oxygen atom to sulfide, releasing sulfoxide.
- (d) The cycle continues through three competing steps that convert the intermediate **ReOS** to **ReO**, **ReP** and **ReS**; these are all further examples of ligand substitution on Re(V).

It is reasonable to assume that triphenylphosphine is released in the first step considering that it is unlikely to form a Re(V) six-coordinated intermediate with two bulky ligands, *tert*-butyl hydroperoxide and triphenylphosphine. Moreover, the addition of free phosphine has been shown to slow down the reaction, Figure 4. This agrees with the proposed mechanism and arises from mass-law retardation of the first step. The oxygen atom transfer reaction from **Re7** to MTS will generate **ReOS** in a fast step. The rhenium intermediate can go back to the catalytic cycle by **ReOS** ligand substitution reaction.

The slowness of the first ligand exchange step accounts for the observed induction period. The rate constant k_1 will be small considering the bulkiness of the *tert*-butyl hydroperoxide and triphenylphosphine, a value of $k_1 \sim 10^{-3} \text{ M}^{-1} \text{ s}^{-1}$ might be estimated from the literature.³⁴

Scheme 2



Red	Re Compounds
Blue	Starting material
Green	Products
ReP	MeReO(mtp)PPh ₃
ReO	MeReO(mtp)(TBHP)
ReS	MeReO(mtp)(SMeTo!)
Re7	Mere(O) ₂ (mtp)
ReOS	MeReO(mtp)(OSMeTo!)

Sulfide can coordinate to the rhenium center in a ligand exchange step with **ReO** to form **ReS**.³⁵ Compound **ReS** is an inactive rhenium species in this catalytic cycle that inhibits the reaction, explaining the retardation by the substrate MTS. The value of K_2 is assumed to be large in order to see the dramatic inhibition by MTS.

Kinetic Simulations. To test this hypothesis, we were able to simulate the kinetic traces under the condition we used for the curves in Figure 1-4 with proposed mechanism by the aid of a kinetics simulation program-KinSim.³⁶ With this program, one enters the reaction scheme as the model, the concentrations and the value or estimate of each rate constant. The KinSim program then displays the calculated product buildup as a function of time, allowing comparison with the experimental data. In this case, since no absolute individual rate constant was determined, the rate constants were chosen by trial and error. Simulated curves that resemble those obtained experiment data, thus supporting the proposed mechanism (Figure 7a and 7b), although a single self-consistent set of values has not yet been obtained

The simulated curves do not match the real experimental data perfectly and the rate constants used in simulations weren't the same from experiment to experiment to obtain a reasonable match. Nevertheless, we are encouraged by the match to the general features: the induction period, τ_i , reaction time and conversion matched the data at least roughly. It was found that the k_1 value must be several orders of magnitude smaller than k_3 to be able to see the an induction period like that observed experimentally. The bulkiness of *t*-BuOOH and weak coordinating ability cause the induction period. Besides, $K_1 \ll 1$ as discussed earlier. K_2 should be > 1 to realize the inhibiting effect of sulfide. Considering the weak coordination ability of *t*-BuOOH, the equilibrium will favor the formation of **ReS** than **ReO**. If the comparison is made between **ReP**, which is compound **1**, and **ReS**, **ReP** is much favorable than **ReS** since phosphine is a much stronger coordinating ligand. Thus, $(1/K_1) > K_2$ was used in all simulations. The value of k_3 was assigned on the order of 10^3 -

10^4 s^{-1} for the sulfoxide buildup rate to agree with the experimental data. The value of k_4 should be high, from the low temperature $^1\text{H NMR}$ experiments. As a result, it occurs after the rate controlling step. Thus, we assign the k_4 value as $10^5 \text{ M}^{-1} \text{ s}^{-1}$. No rate law was obtained due to the complexity of the Scheme. For the ease of handling the simulation, k_{5-7} were not considered in the simulation here.

With catalyst **5**, the first ligand exchange step becomes faster, as shown in Figure 5, due to the electron-withdrawing ability of the CF_3 substituent, which makes it easier for *t*-BuOOH to coordinate to the rhenium center. This shortens the reaction time and the induction period as well. In the case of **2**, since no strong ligand is coordinated to the rhenium center, the rate enhancement is probably caused by faster formation of **8** although a shorter induction period was still observed due to the weak coordination ability of *t*-BuOOH.

Used in place of **1**, compound **7** (Chart 2), a six-coordinated Re(V) dithiolato compound, gave no sulfoxide in > 4 hours. This can be explained by the proposed reaction scheme. Since compound **7** is six-coordinated, *tert*-butyl hydroperoxide is unable to approach the rhenium center, blocking the ligand exchange process and preventing the catalysis.

Conclusions

Rhenium(V) dithiolato compounds, $\text{MeReO}(\text{SR})_2\text{L}$, in general, catalyze the oxidation of sulfides to sulfoxides and sulfones by *tert*-butyl hydroperoxide. This reaction features a simple procedure, high efficiency of easily obtained and convenient catalysts, high generality and selectivity. Chloroform is a suitable solvent and the reaction proceeds

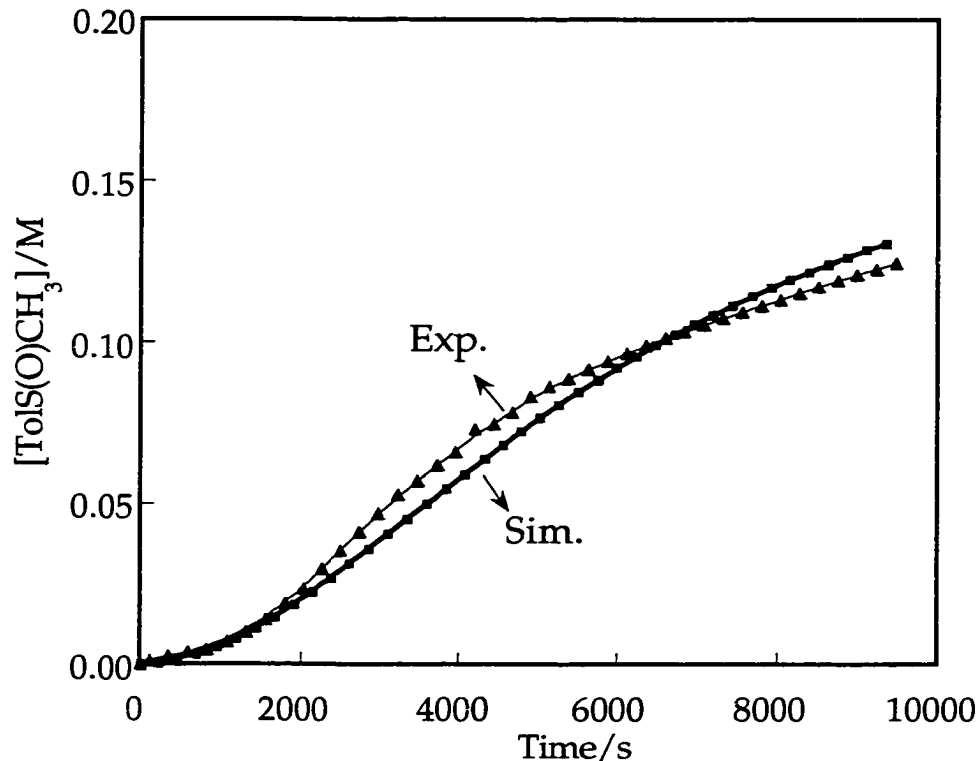


Figure 7a. Plots of product built-up as a function of time show the agreement between experimental data and simulated data by KinSim by monitoring the growth of methyl tolyl sulfoxide by $^1\text{H-NMR}$ for the reaction between 0.166 M *t*-BuOOH and 0.316 M methyl tolyl sulfide catalyzed by 0.31 mM **1** in CDCl_3 at 25°C . The rate constants used for getting the simulated data: $k_1 = 1.23 \times 10^{-3} \text{ M}^{-1} \text{ s}^{-1}$, $k_{-1} = 1 \times 10^3 \text{ M}^{-1} \text{ s}^{-1}$; $k_2 = 1 \times 10^2 \text{ M}^{-1} \text{ s}^{-1}$, $k_{-2} = 0.04 \text{ M}^{-1} \text{ s}^{-1}$; $k_3 = 1 \times 10^3 \text{ s}^{-1}$; $k_4 = 1 \times 10^5 \text{ s}^{-1}$.

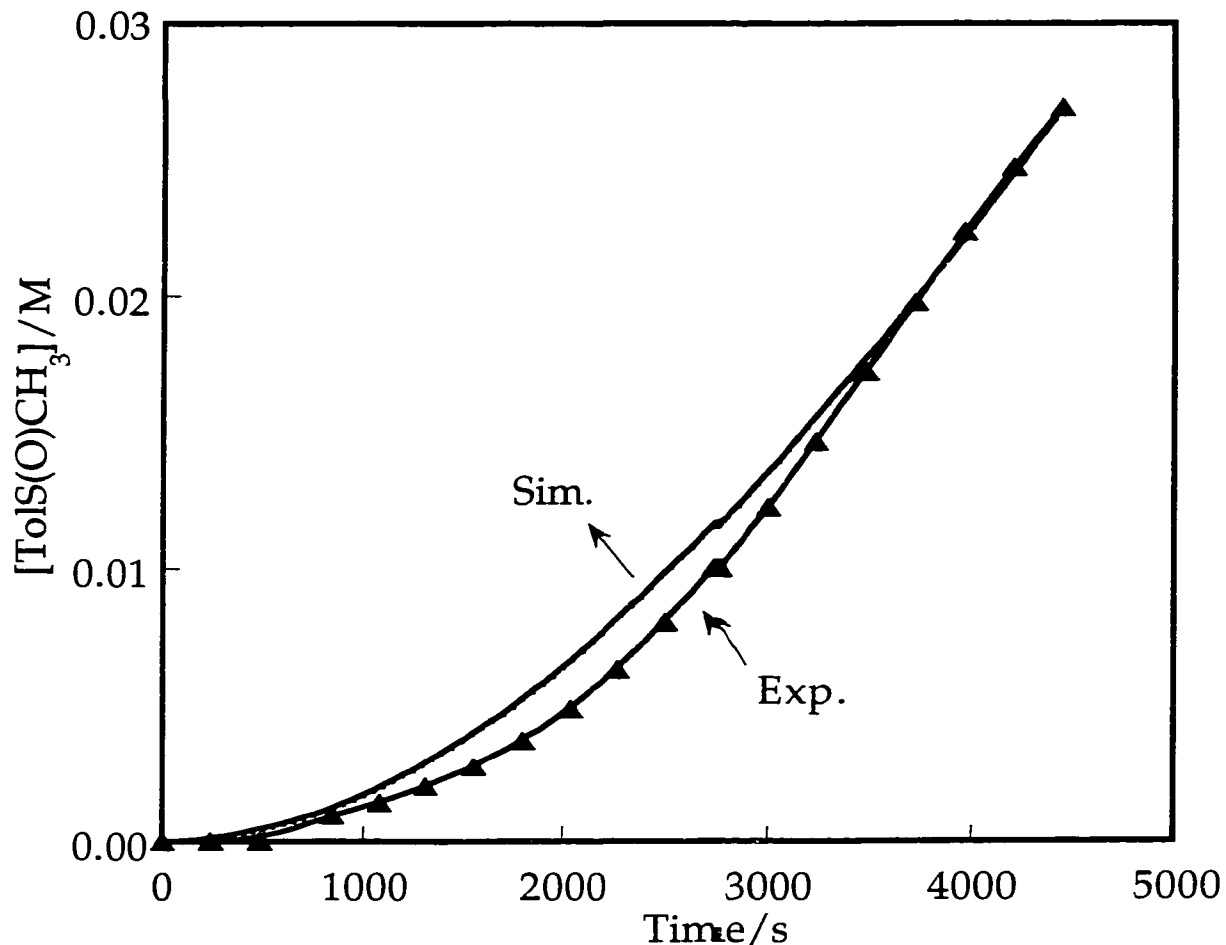


Figure 7b. Plots of product built-up as a function of time show the agreement between experimental data and simulated data by KinSim by monitoring the growth of methyl tolyl sulfoxide by $^1\text{H-NMR}$ for the reaction between 0.166 M *t*-BuOOH and 0.0339 M methyl tolyl sulfide catalyzed by 0.31 mM **1** in the presence of 1 mM PPh_3 in CDCl_3 at 25°C . (a) experimental data; (b) simulated data. The rate constants used for getting the simulated data: $k_1 = 4.8 \times 10^{-4} \text{ M}^{-1} \text{ s}^{-1}$, $k_{-1} = 1 \times 10^3 \text{ M}^{-1} \text{ s}^{-1}$; $k_2 = 1 \times 10^2 \text{ M}^{-1} \text{ s}^{-1}$, $k_{-2} = 0.04 \text{ M}^{-1} \text{ s}^{-1}$; $k_3 = 1 \times 10^3 \text{ s}^{-1}$; $k_4 = 1 \times 10^5 \text{ s}^{-1}$.

without sensitivity to air and humidity. The reaction scheme features an induction period caused by slow ligand exchange steps. The rate was inhibited by the sulfide reagents, which can be explained by its coordination to the rhenium center. The active catalytic dioxorhenium(VII) intermediate was detected by low temperature ^1H NMR experiments.

Experimental Section

Materials. Chloroform was used as the solvent. Sulfides were used as received from commercially available sources without further purification. *tert*-Butyl hydroperoxide (5-6 M in nonane) was purchased (Aldrich). Compound **2** was synthesized from MTO and mtpH_2 as reported earlier.³⁷ Compound **1**, **5** and **6** were prepared by reacting 2.1 equiv. of triphenylphosphine, tetramethylthiourea and tris(4-trifluoromethylphenyl)phosphine with **2**, respectively.^{38,39} Compound **7** was obtained by reacting 6 equiv. of *tert*-butylpyridine with **2** in toluene, then adding 2.1 equiv. of 1,2-bis(diphenylphosphino)benzene. A brown solid was isolated overnight.⁴⁰ Compound **3** and **4** were prepared as reported earlier.⁴¹ Compound **10** was synthesized from **2** and 2.1 equiv. (+)-neomenthylidiphenylphosphine. The ^1H NMR spectrum of this compound is: δ (ppm) 2.45 (d, 3H, Re- CH_3 , $J = 8$ Hz), 2.90 (d, 1H, $J = 12$ Hz), 4.98 (d, 1H, $J = 12$ Hz), 1.23 (d, 3H, $J = 8$ Hz), 0.62 (d, 3H, $J = 8$ Hz), 0.18 (d, 3H, $J = 8$ Hz), 4.23 (m, 1H), 1.60-2.20 (m, 9H), 8.00 (m, 2H), 7.53-7.66 (m, 6H), 7.19-7.32 (m, 6H). The ^{31}P NMR spectrum of **10** (δ (ppm): 28.86). All the ^1H NMR spectra were recorded on a Bruker DRX 400 MHz spectrometer in deuterated chloroform or toluene.

General Procedure for Synthesizing Sulfoxides. 2.05 mmol *t*-BuOOH was added to 2 mL of chloroform containing 2.00 mol of sulfide at room temperature. catalyst 1-3% was dissolved in 1-2 mL of chloroform and either added slowly over a specified time (Table 1) by syringe pump or by direct addition to the solution. The reaction was checked periodically by TLC or ^1H NMR. When reaction had finished, the solvent was evaporated along with the other product, *t*-BuOH. The ^1H -NMR spectra thus obtained were fairly clean (Figure 8) in most cases and sulfoxides were verified by comparing the ^1H and ^{13}C data with literature value.^{42,43} High purity sulfoxides were obtained after flash chromatography using ethyl acetate as eluent.

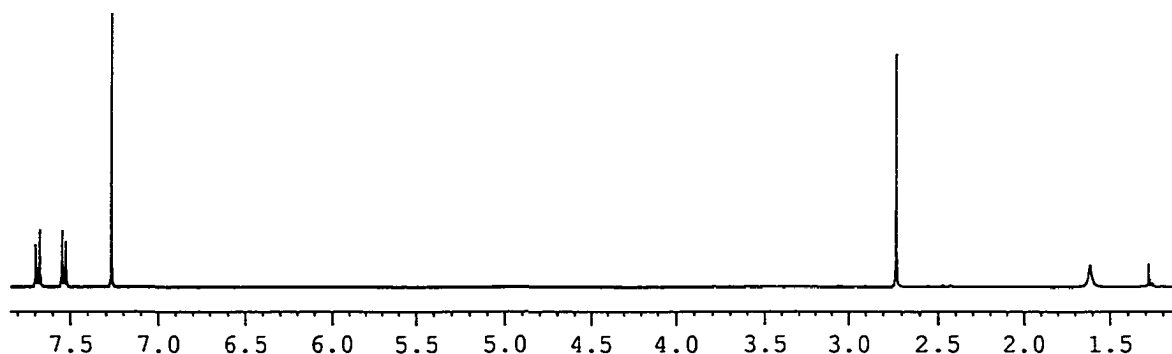


Figure 8. The ^1H NMR spectrum of $4\text{-BrC}_6\text{H}_4\text{S(O)CH}_3$ obtained after evaporation from the reaction between 2.00 mmol of $4\text{-BrC}_6\text{H}_4\text{SCH}_3$ and 2.05 mmol *t*-BuOOH with 1.5 mol% 1 (Table 1, entry 8). ^1H NMR spectrum of $4\text{-BrC}_6\text{H}_4\text{S(O)CH}_3$ is: δ (ppm) 2.73(s, 3H), 7.53(m, 2H), 7.67(m, 2H). The residual ^1H NMR peak of CDCl_3 is at $\delta = 7.26$ ppm.

General Procedure for Synthesizing Sulfones. To 2 mL of chloroform containing 1.0 mmol of sulfide, 3.0 mmol *t*-BuOOH was added. The catalyst **1** 0.3-0.5%, was dissolved in 1 mL of chloroform and added slowly by a syringe pump over 2 h at 50°C, as reaction was monitored by TLC periodically. The sulfones were obtained after evaporation and identified by their ¹H and ¹³C NMR spectra.^{8,9}

Oxidative Cycloaddition of 2,5-Dimethylthiophene with N-Phenylmaleimide. To a solution of 2,5-dimethylthiophene (112 mg, 1.00 mmol) and N-phenylmaleimide (320 mg, 1.85 mmol) in 3 mL chloroform was added 2.00 mmol *t*-BuOOH at 50 °C. Compound **1** (6.3 mg, 1 mol%) was dissolved in 1 mL chloroform and added slowly by syringe pump in 2 hours. The reaction was further stirred for one hour. After evaporation, the product N-phenyl-1,4-dimethyl-7-thiabicyclo[2.2.1]hept-5-ene-2,3-dicarboxamide 7-oxide was separated by flash chromatography using hexane:ethyl acetate 2:1 as eluent. The product obtained (78%) was identified from its ¹H, ¹³C NMR and MS data in comparison with literature values.²⁹ The ¹H NMR of this cycloaddition product is: δ (ppm) 1.82 (s, 6H), 3.85 (s, 2H), 6.23 (s, 2H), 7.15 (m, 2H), 7.35-7.53 (m, 3H).

References

- (1) Oae, S. *Organic Sulfur Chemistry: Structure and Mechanism*; CRC Press: Boca Raton, FL, 1991; pp 203-291.
- (2) Hille, R. *Chem. Rev.* **1996**, *96*, 2757.
- (3) George, G. N.; Hilton, J.; Temple, C.; Prince, R. C.; Rajagopalan, K. V. *J. Am. Chem. Soc.* **1999**, *121*, 1256.

- (4) Lippard, S. J.; Berg, J. M. *Principles of Bioinorganic Chemistry*; University Science Books: Mill Valley, CA, 1994; Chapter 11, p283.
- (5) Trost, B. M.; Fleming, I. *Comprehensive Organic Synthesis*; Pergamon Press: Oxford, 1991; Vol. 7, pp 757-787.
- (6) Madesclaire, M. *Tetrahedron* **1986**, *42*, 5459.
- (7) Breton, G.; Fields, J. D.; Kropp, P. L. *Tetrahedron Lett.* **1995**, *36*, 3825.
- (8) Rozen, S.; Bareket, Y. *J. Org. Chem.* **1997**, *62*, 1457.
- (9) Ali, M. H.; Bohnert, G. J. *Syn. Commun.* **1998**, *28*, 2983.
- (10) Patai, S.; Rappoport, Z. E. *Synthesis of Sulphones, Sulphoxides and Cyclic Sulphides*; John Wiley&Sons, Inc., 1994.
- (11) Zakharov, I. I.; Startsev, A. N.; Zhidomirov, G. M.; Parmon, V. N. *J. Mol. Catal. A* **1999**, *137*, 101.
- (12) Blanchard, P.; Payen, E.; Grimblot, J.; Bihan, L. L.; Poulet, O.; Loutaty, R. *J. Mol. Catal. A* **1998**, *135*, 143.
- (13) Collins, F. M.; Lucy, A. R.; Sharp, C. *J. Mol. Catal. A* **1997**, *117*, 397.
- (14) Galpern, G. D., Gronowitz, S. Ed. *The Chemistry of Heterocyclic Compounds—Thiophene and its Derivatives*; J. Wiley and Sons: New York, 1985; 44.
- (15) Venturello, C.; Alneri, E.; Ricci, M. *J. Org. Chem.* **1983**, *48*, 3831.
- (16) Tam, P. S.; Kittrell, J. R.; Eldridge, J. W. *Ind. Eng. Chem. Res.* **1990**, *29*, 324.
- (17) Vassell, K. A.; Espenson, J. H. *Inorg. Chem.* **1994**, *33*, 5491.
- (18) Brown, K. N.; Espenson, J. H. *Inorg. Chem.* **1996**, *35*, 7211.
- (19) Wang, Y.; Espenson, J. H. *Org. Lett.* **2000**, *2*, 3525.

- (20) Arias, J.; Newlands, C. R.; Abu-Omar, M. M. *Inorg. Chem.* **2001**, *40*, 2185.
- (21) Adam, W.; Golsch, D. *J. Org. Chem.* **1997**, *62*, 115.
- (22) Ballistreri, F. P.; Tomaselli, G. A.; Toscano, R. M.; Conte, V.; Furia, F. D. *J. Am. Chem. Soc.* **1991**, *113*, 6209.
- (23) Adam, W.; Haas, W.; Lohray, B. B. *J. Am. Chem. Soc.* **1991**, *113*, 6202.
- (24) Nakayama, J. *Bull. Chem. Soc. Jpn.* **2000**, *73*, 1.
- (25) Nakayama, J.; Nagasawa, H.; Sugihara, Y.; Ishii, A. *J. Am. Chem. Soc.* **1997**, *119*, 9077.
- (26) Nagasawa, H.; Sugihara, Y.; Ishii, A.; Nakayama, J. *Bull. Chem. Soc. Jpn.* **1999**, *72*, 1919.
- (27) Li, Y.; Matsuda, M.; Thiemann, T.; Sawada, T.; Mataka, S.; Tashiro, M. *Synlett* **1996**, 461.
- (28) Naperstkw, A. M.; Macaulay, J. B.; Newlands, M. J.; Fallis, A. G. *Tetrahedron Lett.* **1989**, *30*, 5077.
- (29) Li, Y.; Thiemann, T.; Sawada, T.; Mataka, S.; Tashiro, M. *J. Org. Chem.* **1997**, *62*, 7926.
- (30) Wang, Y.; Espenson, J. H. *manuscript in preparation* **2001**.
- (31) Zim, D., De Souza, R. F., Dupont, J., Monterio, A. L. *Tetrahedron Lett.* **1998**, *39*, 7071.
- (32) Morrison, J. D., Burnett, R. E., Aguiar, A. M., Morrow, C. J. Phillips, C. *J. Am. Chem. Soc.* **1971**, *93*, 1301.

- (33) *We are grateful for Dr. Daniel W. Armstrong and his students, Jared Anderson and Tom Xiao for determining the e.e. values.*
- (34) Lahti, D. W.; Espenson, J. H. *J. Am. Chem. Soc.* **2001**, *123*, 6014.
- (35) Shan, X.; Espenson, J. H. *unpublished result.*
- (36) Zimmerle, C. T.; Frieden, C. *Biochem. J.* **1989**, *258*, 381.
- (37) Jacob, J.; Espenson, J. H. *Chem. Commun.* **1999**, 1003.
- (38) Jacob, J.; Guzei, I. A.; Espenson, J. H. *Inorg. Chem.* **1999**, *38*, 3762.
- (39) Lente, G.; Espenson, J. H. *Inorg. Chem.* **2000**, *39*, 1311.
- (40) Espenson, J. H., Shan, X.; Lahti, D. W.; Rockey, T. M.; Saha, B.; Ellern, A. *Inorg. Chem. submitted for publication.*
- (41) Lente, G.; Shan, X.; Espenson, J. H. *Inorg. Chem.* **2000**, *39*, 4809.
- (42) Ali, M. H.; Bohnert, G. J. *Synthesis* **1998**, 1238.
- (43) Ali, M. H.; Stevens, W. C. *Synthesis* **1997**, 764.

Table 1. Oxidation of sulfides to sulfoxides by *t*-BuOOH catalyzed by compound **1** at 25°C in CHCl₃.

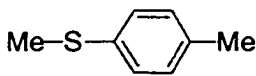
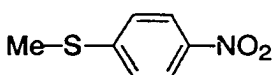
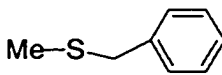
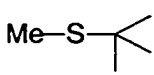
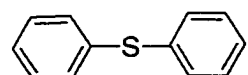
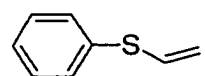
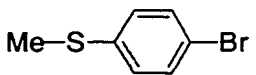
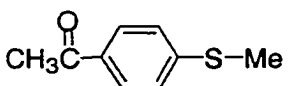
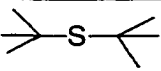
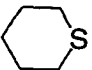
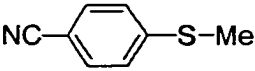
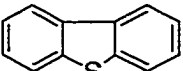
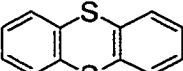
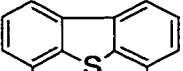
Entry	Compound	Catalyst (mol %)	Temp. (°C)	Time(h)	Yield % ^a
1	Me-S-Me	3	0	0.7	100
2		1	25	1	100
3		1	25	2.5	99(95)
		0.05	50	0.8	98(95) ^b
4		1	25	1.5	100(93)
5		1	25	1.5	100(95)
6		2	25	2.5	100
7		1	25	2	100(92)
8		1.5	25	2	100(97)
9		1.5	25	3	100(95)

Table 1 continued

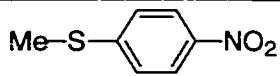
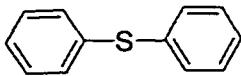
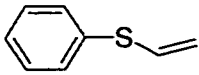
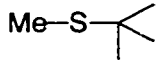
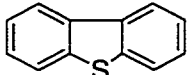
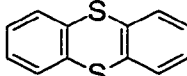
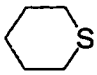
Entry	Compound	Catalyst (mol %)	Temp. (°C)	Time(h)	Yield % ^a
10		1.5	25	2	97(90)
11		1.5	25	2.5	98
12		2	25	2	100(96)
13		3	25	6	89
14		1	25	2	96
15		1	50	4	71 ^c

(a) The yields were determined by taking the ¹H-NMR spectrum of the crude product after evaporation. The number in the parentheses stands for the isolated product yield.

(b) 2 mmol *t*-BuOOH was used.

(c) 1 mmol substrate and 3 mmol *t*-BuOOH were used. The other products is 20% 4,6-dimethylthiophene dioxide after evaporation and 9% 2,6-dimethylthiophene remained.

Table 2. Oxidation of sulfides to sulfones by *t*-BuOOH catalyzed by **1**

Entry	Compound	Catalyst (mol%)	yield (%) ^a
1		0.5	97
		0.05	85
2		0.3	100
3		0.5	100
4		0.5	99
5		0.5	100
6		0.5	98 ^b
7		0.5	97

(a) The yields were determined by taking the ¹H-NMR of the crude product after evaporation. The other product is the corresponding sulfoxide.

(b) The product is 5,10-thianthrene dioxide, not a sulfone.

CHAPTER IV. OXIDATION OF SYMMETRIC DISULFIDES WITH HYDROGEN PEROXIDE CATALYZED BY METHYLTRIOXORHENIUM

A paper published in the *Journal of Organic Chemistry*

Ying Wang and James H. Espenson*

Abstract

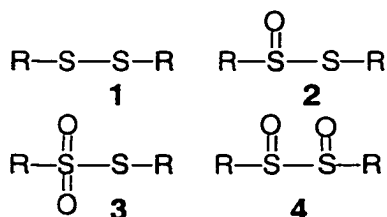
Organic disulfides with both alkyl and aryl substituents are oxidized by hydrogen peroxide when CH_3ReO_3 (MTO) is used as a catalyst. The first step of the reaction is complete usually in about an hour, at which point the thiosulfinate, RS(O)SR , can be detected in nearly quantitative yield. The thiosulfinate is then converted, also by MTO-catalyzed oxidation under these conditions, to the thiosulfonate and, over long periods, to sulfonic acids, RSO_3H . In the absence of excess peroxide, RS(O)SR ($\text{R} = \textit{para}$ -tolyl), underwent disproportionation to $\text{RS(O)}_2\text{SR}$ and RSSR . Kinetics studies of the first oxidation reaction established that two peroxorhenium compounds are the active forms of the catalyst, $\text{CH}_3\text{ReO}_2(\eta^2\text{-O}_2)$ (**A**) and $\text{CH}_3\text{ReO}(\eta^2\text{-O}_2)_2\cdot(\text{OH}_2)$ (**B**). Their reactivities are similar; typical rate constants ($\text{L mol}^{-1} \text{ s}^{-1}$, 25°C , aq. acetonitrile) are: $k_{\text{A}} = 22$, $k_{\text{B}} = 150$ (Bu_2S_2) and $k_{\text{A}} = 1.4$, $k_{\text{B}} = 11$ (Tol_2S_2). An analysis of the data for $(\textit{para}\text{-XC}_6\text{H}_4)_2\text{S}_2$ by a plot of $\log k_{\text{B}}$ against the Hammett σ constant gave $\rho = -1.89$, supporting a mechanism in which the electron-rich sulfur attacks a peroxo oxygen of intermediates **A** and **B**.

Wang, Y.; Espenson, J. H. *J. Org. Chem.* **2000**, *65*, 104

Introduction

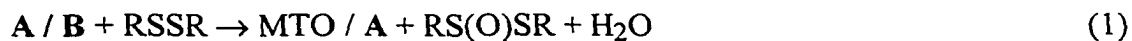
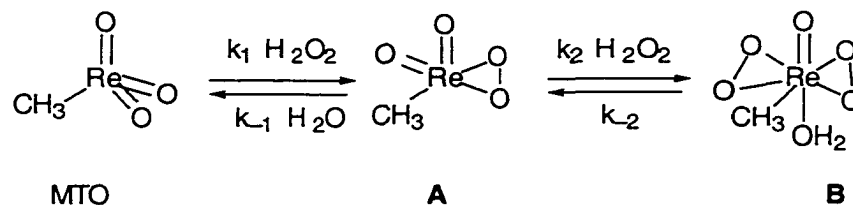
Oxidation of the disulfide functional group (Chart 1) has been studied quite extensively because of its important role in metabolism, via a variety of mechanistic paths.¹ With the use of different oxidants and well-controlled situations, various intermediate compounds have been obtained.²⁻⁶ Among these are thiosulfinates, **2**, which can provide a sulfinyl group that acts as a removable source of diastereoselectivity in asymmetric syntheses.⁷ Similarly, such reactions can produce thiosulfonates, **3**, which are powerful sulfonylating agents useful for the temporary blocking of mercapto groups in protein chemistry.⁸

Chart 1. Disulfide and oxidation products; R = alkyl, aryl



Peracids are the reagents most commonly used to oxidize disulfides, although hydrogen peroxide in acetic acid also finds application. The hydrogen peroxide reactions, in the absence of a catalyst, often require a large excess and a higher temperature.^{1,3} Oxometal complexes are catalysts for the oxidation; molybdates and tungstates are effective, especially under phase-transfer conditions.⁹⁻¹¹

Methyltrioxorhenium, CH_3ReO_3 or MTO, has been widely used as a catalyst for reactions that use hydrogen peroxide as a stoichiometric oxidant.¹²⁻¹⁵ One can anticipate that either or both of the peroxorhenium species that exist in an equilibrium or a steady-state relation with MTO, as shown in **Scheme 1**, will be the active form of the catalyst. Since a sequence of oxidation steps will occur, the experiments were carried out. The principal objective of this research is the study of the reaction kinetics, of the first stage in particular, as written in eq 1. The first reaction proved to be faster than the subsequent oxidations. This allowed, when hydrogen peroxide was taken in only 1:1 ratio to the disulfide, the detection of the thiosulfonates, otherwise difficult to realize owing to their transient nature. We also report, qualitatively, on the formation of thiosulfonates and sulfonic acids.

Scheme 1

Experimental Section

Reagents. Aqueous acetonitrile was used as the reaction solvent, the water being purified by a Millipore-Q water purification system. The disulfides were used as received

from Aldrich, save for *para*-chlorophenyl disulfide which was prepared by the literature method¹⁶ and purified by recrystallization from ethanol-water, and for *tert*-butyl disulfide, which was vacuum distilled.

Kinetics. Both UV/visible and ¹H-NMR methods were used. Quantitative measurements were made at 25 °C in 4:1 v/v acetonitrile-water at pH 1 (to stabilize MTO in peroxide-containing media)¹⁷ maintained by trifluoromethanesulfonic acid. Owing to the large molar absorptivities of the diaryl disulfides, it was often necessary to use cuvettes of 0.01–0.05 cm optical path. One or more wavelengths were chosen for each compound to allow quantitative monitoring of the reaction progress. The conditions and wavelengths selected were such that the loss of ArSSAr was followed, although at other wavelengths, not used for kinetics, a rise in absorbance accompanying the buildup of **2** could be seen. Under the conditions of the spectrophotometric determinations, principally that [ArSSAr] was quite low and [H₂O₂] effectively constant, the reactions followed pseudo-first-order kinetics. The absorbance-time data from each experiment were analyzed according to eq 2, from which a value of k_{ψ} was obtained by nonlinear least-squares fitting.

$$\text{Abs}_t = \text{Abs}_{\infty} + (\text{Abs}_0 - \text{Abs}_{\infty}) \cdot \exp^{-k_{\psi} \cdot t} \quad (2)$$

In the case of dialkyl disulfides, where there are no useful UV absorptions, the reaction kinetics was evaluated from NMR intensities. These values were converted to concentrations based on the total intensity of the starting material using a computer program to do so.¹⁸ Certain data sets were analyzed by first-order kinetics according to eq 3,

$$C_t = C_0 \cdot e^{-k_{\psi}t} \quad (3)$$

That was allowable at high concentrations of hydrogen peroxide, where (see later) the rate becomes peroxide-independent. On the other hand, at lower peroxide concentrations the data conform to the Michaelis-Menten form for catalytic reactions, and the data cannot be analyzed by an integrated rate law. In these circumstances the method of initial rates was used. To determine the value of the initial rate, v_i , the concentration was expressed as a polynomial function, eq 4, by least-squares fitting

$$C_t = C_0 - a_1 \cdot t - a_2 \cdot t^2 - a_3 \cdot t^3 - \dots \quad (4)$$

from which it can be seen that $v_i = a_1$. For one compound, with R = *para*-tolyl, it was confirmed that both UV and NMR methods gave the same ultimate parameter value.

Products. The procedure used to identify the reaction products was based on chromatography and spectroscopy. A solution containing MTO (2.5 μ mol) and hydrogen peroxide (1 mmol) was slowly added to 1 mmol *para*-ditolyl disulfide (for example) in 5.0 mL acetonitrile. The reaction was allowed to run for 2 h, during which time its progress was monitored periodically by TLC. When this test showed that the reaction progress had nearly stopped, the mixture was separated by preparative TLC, using cyclohexane–ethyl acetate (95:5) as the eluting agent. This gave *p*-tolyl *p*-toluenethiosulfinate, **2**, as the major product along with a barely detectable amount of *p*-tolyl *p*-toluenethiosulfonate, **3**. These products were identified either by $^1\text{H-NMR}$ and GC-MS techniques, in comparison with the values of the authentic compounds or literature values.^{7,19-21} Adding excess hydrogen peroxide into the above solution eventually afforded the final product, *para*-toluenesulfonic

acid. The reaction was also monitored by ^1H NMR, during which both the thiosulfinate **2** and thiosulfonate **3** were detected. No α,α' -disulfonate **4** was detected for any of the substrates used in this study.

Results

Preliminary experiments. No significant interaction was found between the disulfides and MTO based on ^1H -NMR results. This finding implies that the reaction does not proceed by way of a prior complex between these two. The result further suggests that the reaction, when it does occur as hydrogen peroxide is added, does not feature attack of the sulfur at the rhenium center, for there is no reason to believe that this interaction would occur then, when it did not do so on its own. All six substrates (see **Table 1**) were initially examined in the absence of a catalyst. Without MTO, there was no evidence for a reaction, even with excess hydrogen peroxide, as indicated either by a UV spectrum that remained nearly unchanged for several hours or by the absence of new peaks growing in the NMR spectrum.

Once MTO had been added, however, the spectra immediately began to show the buildup of the product. These determinations were also performed with equal initial concentrations of the disulfide and hydrogen peroxide. A certain small amount of the thiosulfonate was detected along with the major thiosulfinate for R = Ph, *para*-tolyl, and *para*-chlorophenyl. With three of the compounds, those with R = Me, *tert*-Bu and *para*-nitrophenyl, the thiosulfinate was very nearly the only product. Isosbestic points were

maintained during these reactions, even with a small excess of hydrogen peroxide. Such a series of repetitive scans is shown in **Figure 1**.

For this second group of disulfides, the further steps of oxidation beyond the thiosulfinate are a great deal slower, and for all of the disulfides studied there is a considerable rate advantage found in the first stage of oxidation. This information was used to plan the quantitative studies of the kinetics, so that only the first oxidation stage was important during the data acquisition time.

Kinetics studies. The first part of understanding the reaction scheme lies in the two kinetic steps shown in **Scheme 1**. In this solvent system, these are the relevant parameters at 298 K: $k_1 = 15.5 \text{ L mol}^{-1} \text{ s}^{-1}$, $k_{-1} = 0.17 \text{ s}^{-1}$, $K_1 = 91 \text{ L mol}^{-1}$, $K_2 = 347 \text{ L mol}^{-1}$.²² It is useful to differentiate studies at "low" and "high" concentrations of hydrogen peroxide, by which we mean experiments at <7 mM and >0.5 M, respectively. We start by presuming that **A** and **B** are separate participants in the oxidation, and denote their respective rate constants as k_3 and k_4 . We further presumed, and later confirmed for two compounds, that k_3 and k_4 are of the same order of magnitude. If so, then the term in the rate law for the reaction of **B** with disulfide makes $\leq 10\%$ contribution in experiments with "low" concentrations of hydrogen peroxide. Under those conditions, the reaction proceeds largely with the **A** form of the catalyst and its velocity is given by

$$v = \frac{k_1 k_3 [\text{Re}]_T \cdot [\text{R}_2\text{S}_2] \cdot [\text{H}_2\text{O}_2]}{k_{-1} + k_3 [\text{R}_2\text{S}_2] + k_1 [\text{H}_2\text{O}_2]} \quad (5)$$

For purposes of data analysis, the values of k_1 and k_{-1} were set at their known values.²² With that, the only unknown in eq 5 is k_3 . Its value could be determined for each

experiment, no matter whether the data are in the form of v_i or k_ψ . Under those conditions the variation in the initial rate with hydrogen peroxide concentration, at fixed concentrations of the disulfide and MTO, defines a rectangular hyperbola. Data from experiments with Me_2S_2 are presented in **Figure 2**. A second method for data analysis, based on the same chemical mechanism, was used for di-*tert*-butyl disulfide. The concentration-time data for all the experiments with Bu^t_2S_2 were fit globally with the use of the program FitSim.²³

At "high" hydrogen peroxide, when $[\text{B}] \gg [\text{A}]$, the absorbance-time (UV-Vis) or concentration-time (NMR) data fit first-order kinetics. Because $[\text{B}] \cong [\text{Re}]_T$, the rate law under this condition becomes:

$$v = k_4[\text{Re}]_T \cdot [\text{R}_2\text{S}_2] = k_\psi [\text{R}_2\text{S}_2] \quad (6)$$

For these determinations, a series of experiments was carried out with constant $[\text{H}_2\text{O}_2]$ and $[\text{R}_2\text{S}_2]$ in which $[\text{Re}]_T$ was varied, typically 0.1–0.5 mM. The plot of k_ψ against $[\text{Re}]_T$ was linear, as depicted for three compounds in **Figure 3**. The values of k_4 given by the slopes of these lines are summarized in **Table 1**.

It should be noted that the various aspects of the data analysis presented are all different components of the same reaction scheme. The differences arise from the different ranges of concentration chosen for different sets of experiments and also because the relative rate constants are different from one disulfide to the next.

Fate of the thiosulfinates. Compounds of the formula RS(O)SR tend to be unstable, and usually cannot be isolated. Careful NMR measurements were made during the reaction between 20 mM di(*para*-tolyl) disulfide and a limited (10 mM) concentration of

hydrogen peroxide. Once the thiosulfinate had been formed, it slowly decomposed with the formation of the thiosulfonate, $\text{RS(O)}_2\text{SR}$, and partial regeneration of the disulfide. This is compatible with a disproportionation process:



A companion experiment with di(*tert*-butyl) disulfide gave a thiosulfinate that seemed stable for a much longer period, suggesting that disproportionation is sterically impeded by the bulky R group.

Discussion

To assess the extent to which electronic factors play a role in the transition state, the rate constants for the diaryl disulfides were examined by the Hammett correlation. The plot of $\log(k_4)$ vs. σ , the Hammett substituent constant, was constructed. The four points define a reasonable straight line; its slope is the reaction constant, $\rho = -1.89$ (correlation coefficient 0.997). The negative value of ρ implies that the reaction center (the sulfur atom) shows a buildup of positive charge relative to that in the free molecule. This effect, although in the same direction as that found for RSAr ($\rho = -0.98$),²⁴ is considerably larger. We argue that the enhanced ρ value arises principally from the conjugative effect caused by the *para*-conjugated phenylmercapto group. In this case, the electronic effect of this group seems comparable to that of a phenyl group. The electronic effect of the *para* substituent on the sulfur atom that is not being oxidized appears muted.

When these results are combined with the information already available about organic sulfides²⁴ and thioketones,²² comparisons can be made to gain an understanding of these results. The disulfides are some 10^3 – 10^4 less reactive than either of those families of compounds. This comparison does not require a precise one-to-one match of substituents, since the rate effects are quite large. This is one series that constitutes a reasonable one for comparison: Et₂S, thiocamphor, Me₂S₂; values of $k_3/L \text{ mol}^{-1} \text{ s}^{-1}$ are 2×10^4 , 3×10^3 , and 6.4. This large difference can be ascribed to the substitution of an SR group for an R group. Despite the electron-releasing conjugative effect, the –SMe group is electron withdrawing; its Hammett σ value is +0.07 and the Taft σ_1 value is +0.23. This effect may lower the nucleophilicity of the sulfur atom to which it is bound in the disulfide, thus lowering, relative to the sulfides and thioketones, the rate at which it attacks the peroxorhenium compound.

The reactivity of **B** as compared to **A** is given by the ratio k_4/k_3 . With but the one exception of allyl alcohols,²⁵ clearly a special case, the reactivity of these two are comparable and often in favor of **A**. In the two cases examined here (and, by extrapolation, likely all six) **B** is somewhat more reactive than **A** by a factor of ca. 7.

From the results obtained here, and the general pattern set by other reagents with the MTO-H₂O₂ system, we propose a transition state in which one sulfur atom of the substrate nucleophilically attacks the peroxy group of **A** or **B**. Probing more closely, we note that certain reactions show virtually no steric effect, such as observed for R₂S₂: the values of $k_3/L \text{ mol}^{-1} \text{ s}^{-1}$ are 6.4 (R = Me) and 5.6 (R = *tert*-Bu). This insensitivity of rate to steric

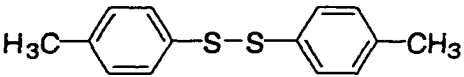
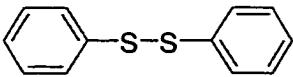
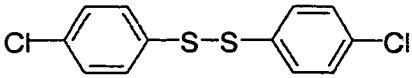
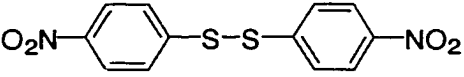
bulk is in accord with values for PAR_3 ,²⁶ R_2S ,²⁴ and Br^- .²⁷ In contrast, the epoxidation of olefins show an important steric effect.²⁸ Oxidation of MeSSBu^t by peracetic acid forms MeS(O)SBu^t and MeSS(O)Bu^t in 1:2 yield,²⁹ showing that these reactions, too, have small steric effects.

References

- (1) *Organic Sulfur Chemistry: Structure and Mechanism*; Oae, S., Ed.; CRC Press: Boca Raton, 1991; Vol. 1, p 213-216.
- (2) Bhattacharya, A. K.; Hortman, A. G. *J. Org. Chem.* **1978**, *43*, 2728.
- (3) Allen, P., Jr; Brook, J. W. *J. Org. Chem.* **1962**, *27*, 1019.
- (4) Gu, D.; Harpp, D. N. *Tetrahedron Lett.* **1993**, *34*, 67.
- (5) Folkins, P. L.; Harpp, D. N. *J. Am. Chem. Soc.* **1993**, *115*, 3066.
- (6) Freeman, F. *Chem. Rev.* **1984**, *84*, 117-135.
- (7) Cogan, D. A.; Liu, G.; Kim, K.; Backes, B. J.; Ellman, J. A. *J. Am. Chem. Soc.* **1998**, *120*, 8011.
- (8) Trost, B. M. *Chem. Rev.* **1978**, 78.
- (9) Anisimov, A. V.; Mokhammad, R.; Akhmad, S. A.; Borisenkova, A. V.; Tarakanova, S. V.; Barkhanova, S. V.; Dergacheva, V. M.; Negrimovskii, V. M.; Kaliya, O. L.; Luk'yanets, E. A. *Neftekhimiya* **1994**, *34*, 358.
- (10) Anisimov, A. V.; Mokhammad, R. A.; Tarakanova, A. V.; Borisenkova, S. A. *Neftekhimiya* **1994**, *34*, 421.
- (11) Singh, P. K.; Field, L. J. *J. Org. Chem.* **1988**, *53*, 2608.
- (12) Espenson, J. H.; Abu-Omar, M. M. *Adv. Chem. Ser.* **1997**, *253*, 99-134.

- (13) Gable, K. P. *Adv. Organomet. Chem.* **1997**, *41*, 127-161.
- (14) Herrmann, W. A.; Kühn, F. E. *Acc. Chem. Res.* **1997**, *30*, 169-180.
- (15) Espenson, J. H. *J. Chem. Soc., Chem. Commun.* **1999**, 479-488.
- (16) Overman, L. E.; Matzinger, D.; O'Connor, E. M.; Overman, J. D. *J. Am. Chem. Soc.* **1974**, *96*, 6089.
- (17) Abu-Omar, M.; Hansen, P. J.; Espenson, J. H. *J. Am. Chem. Soc.* **1996**, *118*, 4966-4974.
- (18) We are grateful to Dr M. Englehardt of Bruker Corp. for supplying this program.
- (19) Kozzuka, S.; Takahashi, H.; Oae, S. *Bull. Chem. Soc. Jpn* **1970**, *43*, 129, and references therein.
- (20) Chemla, F. *Synlett* **1998**, 894.
- (21) Sas, W. *J. Chem. Research* **1993**, 160.
- (22) Huang, R.; Espenson, J. H. *J. Org. Chem.* **1999**, *64*, 6374.
- (23) Zimmerle, C. T.; Frieden, C. *Biochem. J.* **1989**, *258*, 381-387.
- (24) Vassell, K. A.; Espenson, J. H. *Inorg. Chem.* **1994**, *33*, 5491.
- (25) Tetzlaff, H. A. R.; Espenson, J. H. *Inorg. Chem.* **1999**, *38*, 881-885.
- (26) Abu-Omar, M. M.; Espenson, J. H. *J. Am. Chem. Soc.* **1995**, *117*, 272.
- (27) Espenson, J. H.; Pestovsky, O.; Huston, P.; Staudt, S. *J. Am. Chem. Soc.* **1994**, *116*, 2869.
- (28) Al-Ajlouni, A.; Espenson, J. H. *J. Org. Chem.* **1996**, *61*, 3969-3976.
- (29) Block, E.; O'Connor, J. J. *J. Am. Chem. Soc.* **1974**, *96*, 3921.

Table 1. Rate constants at 298 K for the oxidation of disulfides by peroxorhenium complexes **A** (k_3) and **B** (k_4) in aq. acetonitrile ^{a-c} containing 0.100 M CF₃SO₃H

Substrate	$k_3/\text{L mol}^{-1} \text{s}^{-1}$	$k_4/\text{L mol}^{-1} \text{s}^{-1}$
$\text{Bu}^t\text{-S-S-Bu}^t$	22.08 ± 0.812^a 6.44 ± 0.25^b	$\sim 150^a$
$\text{H}_3\text{C-S-S-CH}_3$	5.57 ± 0.16^b	
	1.43 ± 0.20^b	10.1 ± 0.03^c 12.7 ± 0.01^b
		8.57 ± 0.00^c
		2.66 ± 0.01^c
		0.27 ± 0.00^c

^a CD₃CN/H₂O (1:1 v/v), by NMR; ^b CD₃CN/H₂O (4:1 v/v) by NMR; ^c CD₃CN/H₂O (4:1 v/v) by UV.

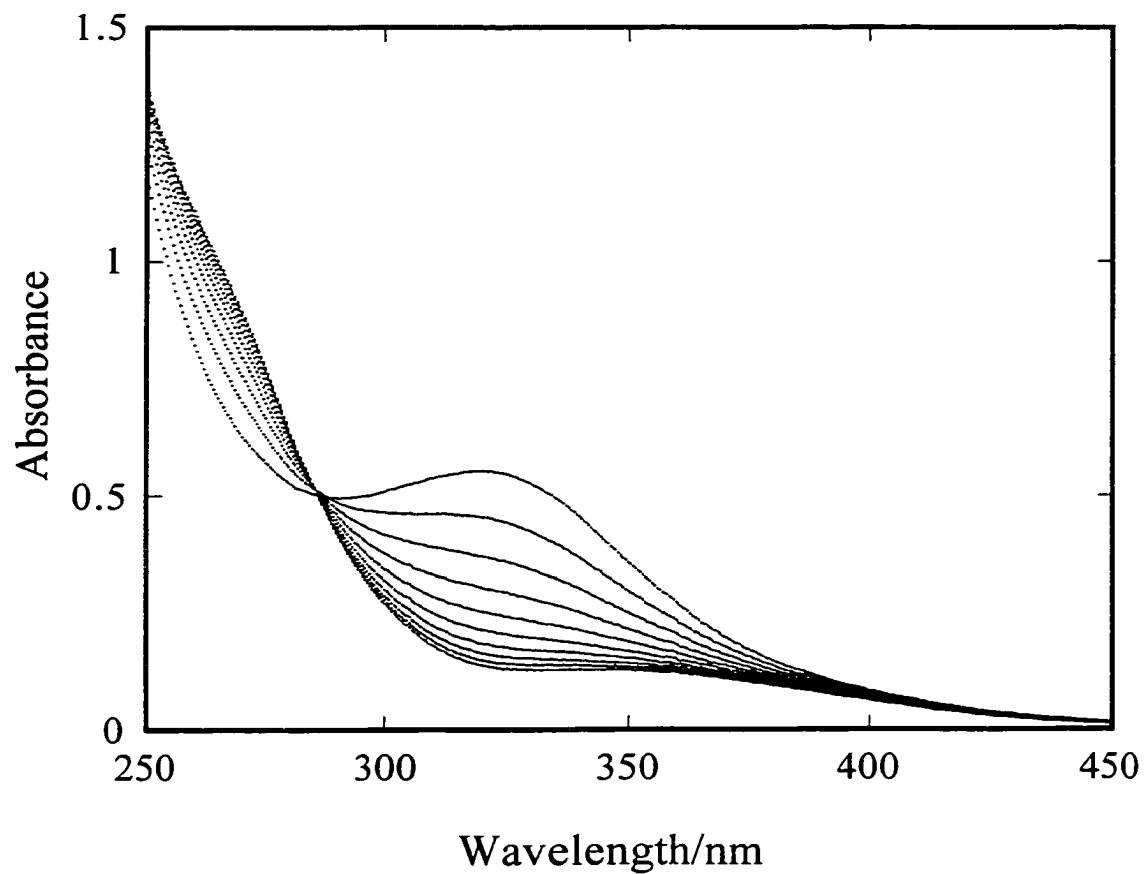


Figure 1. Spectral changes at 5.0 min intervals for the oxidation of *para*-nitrophenyl disulfide (0.5 mM) with H_2O_2 (0.65 M) in the presence of 0.1 mM MTO at pH 1 in 4:1 $\text{CH}_3\text{CN-H}_2\text{O}$.

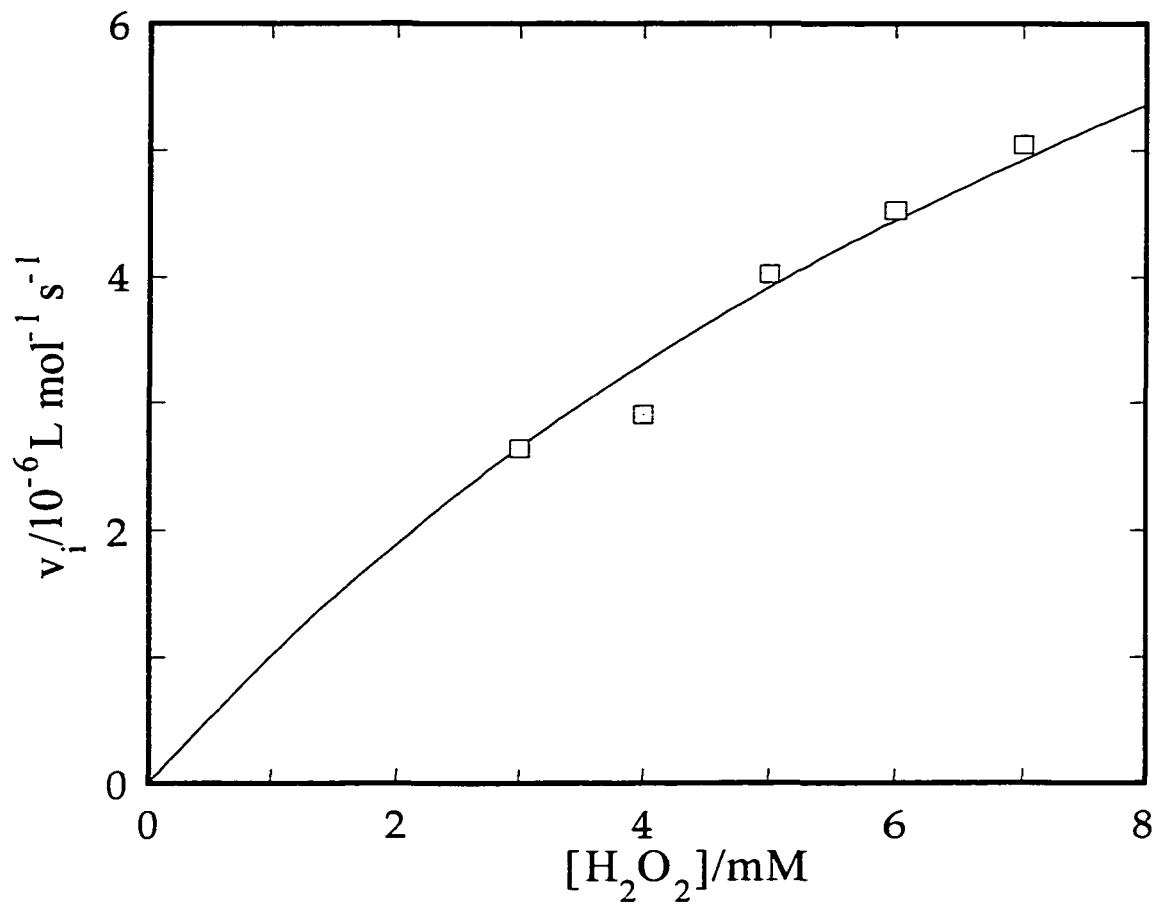


Figure 2. Variation of initial rate of reaction of dimethyl disulfide with the concentration of hydrogen peroxide. The curve is a fit to eq 5. This is applicable when $[\text{B}]$ is negligible compared to $[\text{A}]$. The values of k_1 and k_{-1} (Scheme 1) were fixed at $15.5 \text{ L mol}^{-1} \text{ s}^{-1}$ and 0.17 s^{-1} . Conditions used: 0.5 mM MTO, 5 mM Me_2S_2 in 4:1 $\text{CH}_3\text{CN-H}_2\text{O}$ at $25.0 \text{ }^\circ\text{C}$ and pH

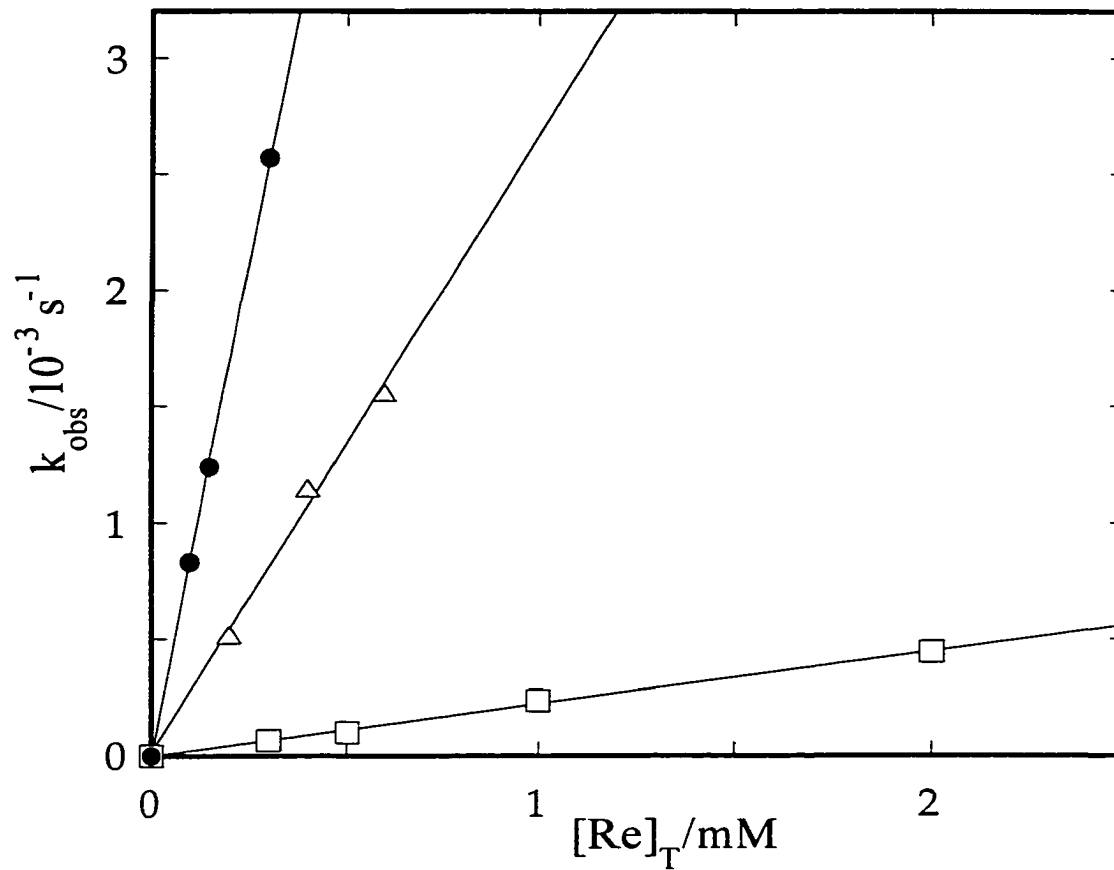


Figure 3. The pseudo-first-order rate constants (4:1 CH₃CN-H₂O at 25.0 °C and pH 1) for the oxidation of diaryl disulfides (0.5 mM) by H₂O₂ (0.65 M) vary linearly with the total catalyst concentration, as shown in order of increasing slope for these para substituents: NO₂, Cl and H. The slope of this line affords the values of k_4 .

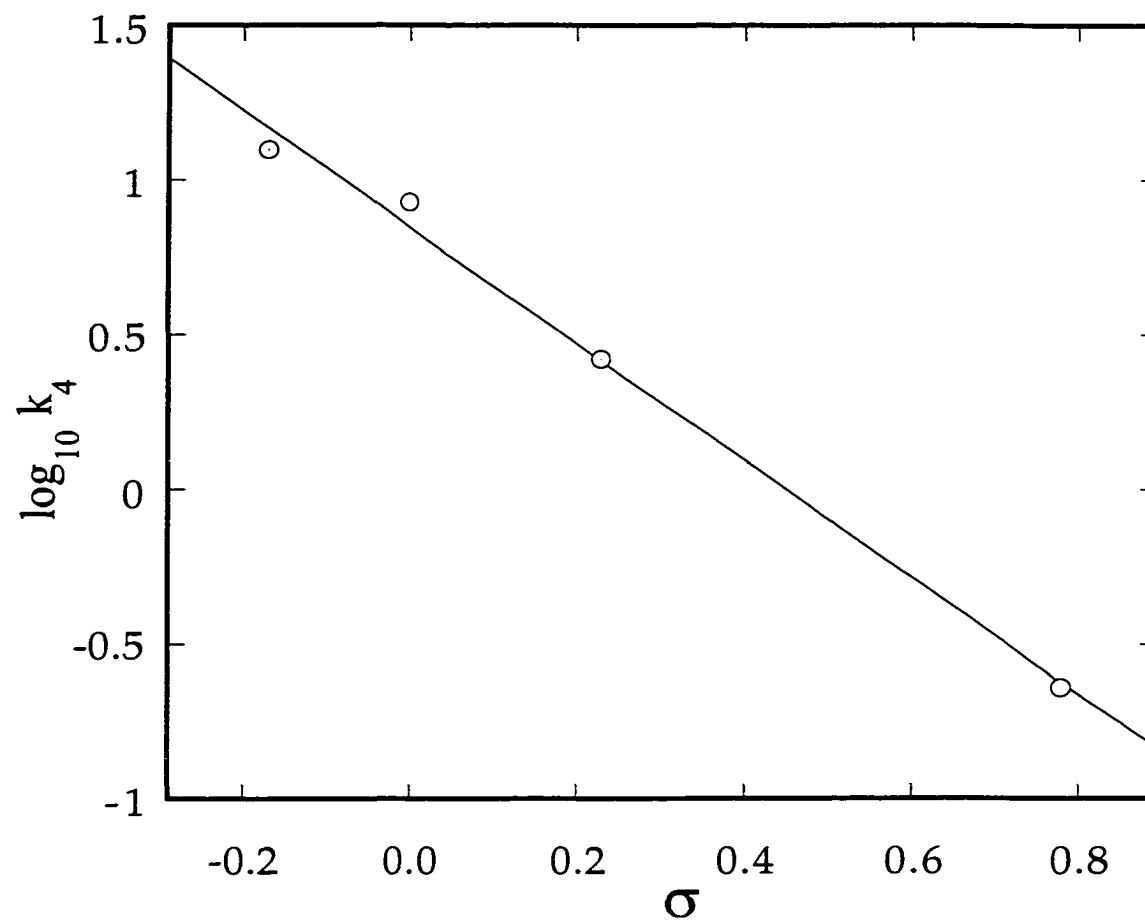


Figure 4. Hammett plot for the oxidation of substituted phenyl disulfides by the peroxorhenium compound **B**. The slope of the line gives $\rho = -1.89$.

GENERAL CONCLUSIONS

A series of Re(V) dithiolato compounds with general formulas $\text{MeReO}(\text{SR})_2\text{L}$ was found to be reactive catalysts for oxygen atom transfer reactions between phosphines and pyridine N-oxides. This reaction succeeds for a wide range of ring-substituted pyridine N-oxides, giving high yields of the corresponding pyridines on one-gram scale. The advantages of this reaction are the mild reaction condition, high catalytic efficiency and good selectivity. Pyridine and bromide are found to be good cocatalysts. The most intriguing catalyst is $\{\text{MeReO}(o\text{-SC}_6\text{H}_4\text{CH}_2\text{S})\}_2$ which catalyzes the above reaction more than 90 times faster than $\text{MeReO}(o\text{-SC}_6\text{H}_4\text{CH}_2\text{S})\text{PPh}_3$. Studies of the kinetics and mechanisms were carried out. Phosphines were found to inhibit the reaction while the rate shows a second-order dependence with respect to the concentration of the pyridine N-oxide. A reaction scheme was proposed and rate constants were obtained to account for the observations. A dioxorhenium(VII) species was detected by low temperature ^1H -nmr experiments. Its reacting with phosphine plays a critical role in closing the catalytic cycle.

These Re(V) dithiolates were also found to be good catalysts for oxidizing sulfides to sulfoxides and sulfones with *tert*-butyl hydroperoxide, affording a general and efficient route to various sulfoxides and sulfones including thiophene oxides. The ease of separation and work-up makes this method particularly attractive. The kinetics of this catalytic oxidation features an induction period and inhibition by the sulfide. A reaction scheme is proposed in which a slow ligand exchange step accounts for the induction period and coordination of the sulfide to the rhenium center causes the inhibition. The similar

dioxorhenium(VII) intermediate was observed at low temperature, and it again plays a key role in catalysis.

Methyltrioxorhenium (MTO) catalyzes the oxidation of symmetrical disulfides with hydrogen peroxide. Thiosulfinate, thiosulfonate and sulfonic acid are the only oxidized compounds observed in this catalytic system. The formation of the thiosulfinate is much faster than the following oxidation steps which allows its separation in almost quantitative yield. It also permits the kinetic studies of this step. The reaction utilizes two peroxorhenium intermediate, $\text{MeRe}(\text{O})_2(\kappa\text{-O}_2)$ and $\text{MeReO}_2(\kappa\text{-O}_2)_2(\text{H}_2\text{O})$, which have similar reactivities in this reaction. A Hammett plot was constructed. A transition state shows nucleophilic attack of one sulfur atom of the substrate on an oxygen atom of peroxo group coordinated rhenium(VII).

ACKNOWLEDGMENTS

I would like to thank Professor James H. Espenson for his guidance, encouragement and being one of the best mentors for me whose inspiration and devotion to science have always motivated me.

I would also like to thank previous and present group members, especially Weidong Wang and Ruili Huang for insightful scientific discussions.

Help discussions with Professor William S. Jenks are greatly acknowledged.

My appreciation also goes to Dr. Daniel W. Armstrong and his students Jared Anderson and Tom Xiao for determining e.e. values.

I am also thankful for Dr. Dave Scott and Dr. Shu Xu for assistance in NMR spectroscopy.

My special thanks go to my husband, parents and sister, for their love, understanding, patience and support in every aspect of my life.